2018

Organic nitrogen uptake by marine algae: consequences for marine ecosystem functioning and biodiversity

Raccagni, Monica

COPYRIGHT STATEMENT

UNIVERSITY OF
PLYMOUTH

ORGANIC NITROGEN UPTAKE BY MARINE ALGAE: CONSEQUENCES FOR MARINE ECOSYSTEM FUNCTIONING AND BIODIVERSITY

By

MONICA RACCAGNI

A thesis submitted to the University of Plymouth
in partial fulfilment for the degree of

MASTER OF PHILOSOPHY

School of Geography, Earth and Environmental Sciences

In collaboration with Station Biologique de Roscoff (Université Pierre et Marie Curie, France)

October 2018

ACKNOWLEDGEMENTS

The biggest acknowledgement goes to my director of studies, Dr Mark Fitzsimons, for his support and advice throughout this project and for setting up collaborations prior to my arrival. From the very first day at Plymouth University till the last draft reading he has been very positive and of great patience.

Thanks to my supervisors Professor Maeve Lohan for her important feedback and support, and Dr Ian Probert and all the other scientists from the Station Biologique de Roscoff for their help during the period undertaken abroad. Along with Dr Agnese Marchini for her distance support.

Acknowledgments to the EU commission for funding the study through the MARES programme.

Big thanks also go to all colleagues in the Biogeochemistry Research Centre and the Petroleum Environmental Geochemistry group for their constant constructive feedbacks and encouragement throughout my time at Plymouth. They have all welcome me in the best way and I am grateful for their patience; I would have not got through this year abroad without you.

Finally, I must express my very profound gratitude to my parents and close friends for providing me with unfailing support and continuous encouragement throughout the process of researching and writing this thesis. This accomplishment would not have been possible without them. Thank you.

AUTHOR'S DECLARATION

At no time during the registration for the degree of Master of Philosophy has the author been registered for any other University award without prior agreement of the Doctoral College Quality Sub-Committee.

Work submitted for this research degree at the University of Plymouth has not formed part of any other degree either at the University of Plymouth or at another establishment. The work in this thesis was primarily the work of the author unless acknowledged otherwise.

This research has been conducted under a formal agreement with Station Biologique de Roscoff (Université Pierre et Marie Curie, France), for which a joint award will be awarded. This study was financed with the aid of a studentship from the MARES programme and carried out in collaboration with Station Biologique de Roscoff (Université Pierre et Marie Curie, France).

A programme of advanced study was undertaken, which included the MARES Expert Training Course "An introduction to generalised linear models using R" held at University of Bologna (June 2014) and counts for 4 ETCS credits.

Relevant scientific seminars were attended at which work was presented, which included the Annual Biogeochemistry Centre Conference at University of Plymouth (December 2014) and the Fourth MARES Annual Meeting in Ispra, Italy from February 2-6th February 2015, organised in close cooperation with Pavia University.

Word count of main body of thesis: 30,609

Signed..Monica Ruocco.....

Date: October 2018

ORGANIC NITROGEN UPTAKE BY MARINE ALGAE: CONSEQUENCES FOR MARINE ECOSYSTEM FUNCTIONING AND BIODIVERSITY

by

Monica Raccagni

ABSTRACT

Dissolved organic nitrogen (DON) represents a major pool of fixed, reactive nitrogen in marine systems. It is now recognized that this pool can support primary production and the ability of some algal species to exploit DON compounds as sources of Nitrogen (N) may indicate that specific DON components can exert selective pressure on the composition of the phytoplankton community.

In this study the ability of monocultures of ecologically-relevant algal species from the English Channel (*Emiliania huxleyi*, *Micromonas pusilla*, *Alexandrium minutum* and *Chaetoceros peruvianus*) to grow with DON as the only N source was examined using different artificial media. Among the two tested artificial seawater recipes, Aquil* was preferred as it contained lower micronutrient concentrations, and gave better growth results for all used species.

In order to constrain the DON uptake to algae alone, a method for bacterial removal was tested using antibiotic additions. Both Slocombe antibiotic mixture (Cefotaxime-Carbenicillin-Kanamycin-AugmentinTM) and Penicillin-Streptomycin-Neomycin used were effective and not toxic to the algae. Incubation with the antibiotic up to 48 hours and a transfer period into antibiotic-free medium after 72 hours proved to be effective. However, the treatment removed bacteria in *A. minutum* cultures only; further treatment would be required for the other species to be cultured axenically.

The ability to use DON was tested for the above mentioned species using the amino acid L-Arginine (ARG) as the sole N source, and growth was compared with nitrate-containing cultures of the same species. All the selected species grew in both NO_3^- and in ARG, reaching lower final densities when incubated with ARG, although these

were not significant. This study has shown that *E. huxleyi*, *A. minutum*, *M. pusilla* and *C. peruvianus* can grow on organic N, either by direct or indirect uptake, and develop comparable biomasses to species using inorganic N. Both *C. peruvianus* and *M. pusilla* cultures contained dissolved ammonium at the end of the experimental period, indicating potential indirect use by the algae of organic N converted to inorganic N by bacteria. *A. minutum* grew in the presence of ARG along with the cosmopolitan *E. huxleyi*; N-demand estimates, based on the molar concentration of N-ARG consumed, correlated with the final cell density, indicating that the species did not develop on inorganic N produced from ARG mineralisation, but directly on the ON substrate. Since *A. minimum* has been linked to harmful algal blooms, and *E. huxleyi* contributes significantly to oceanic $CaCO_3$ deposition, their ability to utilise DON has environmental consequences in addition to the oceanic N-budget.

Climate change scenarios predict both episodic conditions of elevated rainfall and extended periods of dry conditions leading to variable riverine inputs to coastal areas, altered nitrogen to phosphorus (N:P) ratios, and changes in the inorganic to organic balance of the nutrient pools. Organic N can constitute up to 69 % of the total N pools, respectively, making it crucial, to understand the cycling of this fraction in coastal waters, and how changes in the composition of nutrient pools could impact on marine ecosystem function and health.

TABLE OF CONTENTS

AKNOWLEDGEMENTS..……v
AUTHOR'S DECLARATION……...……..vii
ABSTRACT……...……...ix
TABLE OF CONTENTS……...……xi
LIST OF FIGURES……..……xiii
LIST OF TABLES ……..……..…xv
LIST OF COMMON ABBREVIATIONS……..……..…….xviii

1. Introduction

1.1. NITROGEN BIOGEOCHEMISTRY 1
1.2. DON IN SEAWATER 4
1.3. THE CHEMICAL COMPOSITION OF THE DON POOL 7
1.4. IMPORTANCE OF PHYTOPLANKTON TO MARINE ECOSYSTEM FUNCTIONING 9
1.4.1. Phylum Haptophyta – Emiliania huxleyi 10
1.4.2. Phylum Heterokontophyta – Chaetoceros peruvianus.....13
1.4.3. Phylum Dinophyta – Alexandrium minutum.....16
1.4.4. Phylum Chlorophyta – Micromonas pusilla 18
1.5. DON UPTAKE BY PHYTOPLANKTON 19

2. This study.....25

2.1. AIM AND OBJECTIVES 25
2.2. EXPERIMENTAL DESIGN 26
2.2.1. Algal strains selection.....26
2.2.2. Experiments I, II and III – Testing artificial media 27
2.2.3. Experiments IV – Preparation of axenic cultures.....27
2.2.4. Experiments V – Growth comparison on Amino acid and Nitrate ..28

3. Methodology 31

3.1. CHEMICALS.....31
3.2. GENERAL LABORATORY PREPARATION 32
3.3. ANALYSES OF ARGININE.....33
3.3.1. Preparation of calibration solutions.....33
3.3.2. Derivatisation.....33
3.3.3. HPLC 34
3.4. PHYTOPLANKTON BATCH CULTURES 35
3.5. PREPARATION OF CULTURE MEDIUM 38
3.5.1. Natural seawater culture medium.....38

3.5.1.1. Culture medium 0 – modified k/2 38
3.5.2. Artificial seawater culture medium 39
3.5.2.1. Culture medium 1 – ESAW 40
3.5.2.2. Culture medium 2 – Aquil* 41
3.6. ANTIBIOTIC TREATMENTS – BACTERIAL REMOVAL 43
3.6.1. Antibiotic treatment of microphytoplankton – A. minutum and C. peruvianus 43
3.6.2. Antibiotic treatment of nano- and picophytoplankton – E. huxleyi and M. pusilla. 45
3.7. DETERMINATION OF ALGAL GROWTH 46
3.7.1. Cell counting with light microscope 47
3.7.2. Enumerating cells by flow cytometry 48
3.8. NUTRIENTS AND BIOMASS QUANTIFICATION 49
3.8.1. Dissolved inorganic nutrients 49
3.8.2. Biovolume estimation 50
3.8.3. Particulate organic carbon and nitrogen analysis 50
3.9. CHLOROPHYLL A 51
4. Results 55
4.1. PHYTOPLANKTON GROWTH IN ARTIFICIAL MEDIUM 55
4.2. AXENIC CULTURING 63
4.3. PHYTOPLANKTON GROWTH WITH ARGININE AS SOLE N SOURCE 65
4.3.1. Emiliania huxleyi 65
4.3.2. Micromonas pusilla 71
4.3.3. Alexandrium minutum 77
4.3.4. Chaetoceros peruvianus 82
5. Discussion 89
5.1. TESTING ARTIFICIAL MEDIA 89
5.2. AXENIC CULTURE PREPARATION 92
5.3. PHYTOPLANKTON GROWTH COMPARISON WITH ARG AND NO_3^- AS SOLE N SOURCE 93
6. Conclusions 97
7. Appendix I. Experiments list and details 98
8. References 99

LIST OF FIGURES

Figure 1: the average concentration of DON observed in different aquatic environments from riverine to deep ocean (adapted from Bronk, 2002).....5

Figure 2: *E. huxleyi* cell image captured using a Phenom scanning electron microscope at Station Biologique de Roscoff (France).....11

Figure 3: live *C. peruvianus* image captured with by optic microscope.....14

Figure 4: live *A. minutum* cell image captured by optic microscope.....16

Figure 5: live *M. pusilla* cell image captured by optic microscope.....18

Figure 6: Schematic diagram of antibiotic treatments used to test removal of bacteria from selected phytoplankton strains grown in CM 0 (k/2). A = antibiotic. Black lines indicate period of time until next antibiotic addition. Red arrows indicate last transfer to fresh medium, different depending on the species.....28

Figure 7: Calibration for L-Arginine measurements by HPLC. Linear regression revealed no significance difference between SW and HPW measurements (e.g. n = 3).....35

Figure 8: Algal growth curve expected under *batch* conditions.....46

Figure 9: An example of a Sedgewick-Rafter Counting slide. The cover glass must be placed diagonally and the chamber filled in the left open space with 1 mL of sample. The cover glass slides into position to seal the chamber.....47

Figure 10: *E. huxleyi* (within the red box) enumeration plot example, defined by Chlorophyll *a* fluorescence (FL3-A) and side scatter (SSC-A). Other dots representing debris and prokaryotes.....48

Figure 11: ESAW growth test using selected algal species. Red arrow indicating the second inoculum for *Synechococcus sp.*.....55

Figure 12: growth comparison of monoalgal strains in a number of culture media.....57

Figure 13: Growth comparison of *E. huxleyi* strains monoalgal cultures with different tested media.....59

Figure 14: *E. huxleyi* A) RCC 1220 strain with no coccoliths and B) CCMP 1516 strain surrounded by coccoliths, cultured with CM1.....60

Figure 15: Growth comparison of monoalgal cultures in A) CM3 (Aquil*) B) CM4 (10% k/2, 90% Aquil*); ×, *M. pusilla*; ◊, *A. minutum*; ▲, *E. huxleyi* CCMP 1516; ■, *C. peruvianus*.....61

Figure 16: deformation of *A. minutum* and auxosporilation of *C. peruvianus* cultured with artificial media. 62

Figure 17: Flow cytometric distributions of bacterial cells during antibiotic treatment with: A) higher concentration; 7.5 % for *A. minutum* and *C. peruvianus*, and 1 % for *E. huxleyi* and *M. pusilla* and B) lower concentration of antibiotic; 5 % for *A. minutum* and *C. peruvianus*, and 0.5 % for *E. huxleyi* and *M. pusilla* concentrations for four phytoplankton species. Samples were stained with SYBR® Green I and visualized on FL3-A vs FL1-A density plots on the BD Accuri C6. A standard gate (P1) was applied to each sample to exclude debris and background. 63

Figure 18: flow cytometric distributions of bacterial cells during antibiotic treatment with A) higher antibiotic concentrations; 7.5% for *A. minutum* and *C. peruvianus*, and 1 % for *E. huxleyi* and *M. pusilla* and B) control cultures with no antibiotic added and sub-cultured in the same way as the treated ones. Samples were stained with SYBR® Green I and visualized on FL3-A vs FL1-A density plots on the BD Accuri C6. A standard gate (P1) was applied to each sample to exclude debris and background. 64

Figure 19: growth of *E. huxleyi* cultures containing NO_3^- (Δ) and Arg (■), and bacteria enumeration. with NO_3^- (○) and ARG (×). Note that the data points represent the average of duplicate samples counted in triplicate (n=6). 65

Figure 20: Concentrations of dissolved nutrients measured on Days 0 and 7 of in cultures of *E. huxleyi* containing A) NO_3^- and B) ARG as the sole nitrogen source. NO_3^- and ARG were analysed at the beginning and end of the incubation, while NH_4^+ was quantified on last day only. Values represent the average of duplicate samples counted in duplicate (n=4). 67

Figure 21. Growth of *M. pusilla* in cultures containing NO_3^- (Δ) and ARG (■), and bacterial enumeration: NO_3^- (○) and ARG (×). The data points represent the average of duplicate samples counted in triplicate (n=6). 71

Figure 22: Dissolved nutrient concentrations on day 0 and 14 of *M. pusilla* incubations with A) NO_3^- and B) ARG. NO_3^- and ARG were analysed at the beginning and end of the incubation, while NH_4^+ was quantified on last day only. Values represent the average of duplicate samples counted in duplicate (n=4). 73

Figure 23: growth of *A. minutum* cultures with NO_3^- (Δ) and Arg (■), and bacteria enumeration. with NO_3^- (○) and Arg (×). The data points represent the average of duplicate samples counted in triplicate (n=6). 77

Figure 24: dissolved nutrients concentration on day 0 and 11 of *A. minutum* experiments with A) NO_3^- and B) ARG. NO_3^- and ARG were analysed at the beginning and end of the incubation, while NH_4^+ was quantified on last day only. Values represent the average of duplicate samples counted in duplicate (n=4). 79

Figure 25: Growth of *C. peruvianus* cultures containing NO_3^- (Δ) and Arg (□), and bacteria enumeration in NO_3^- (○) and Arg (×) cultures. The data points represent the average of duplicate samples counted in triplicate (n=6). Max variation on day 12 was approximately 2000 cells between replicates. 82

Figure 26: Dissolved concentrations of nitrogen substrates in *C. peruvianus* experiments: A) NO_3^- on Days 0 and 8; B) ARG on Days 0 and 12. Note that for ARG cultures, average NH_4^+ concentrations in culture replicates A and B is presented with standard deviation revealing the high differences between the two replicates. 84

LIST OF TABLES

Table 1: Oceanic Inventory, Turnover Rates, and Residence Times for the Major Fixed Nitrogen Species in the Ocean, adapted from Gruber (2008) 2

Table 2: Annual and seasonal net primary production (NPP) of the major units of the biosphere. Values are in petagrams of carbon (1 Pg = 1015 g). Adapted from Geider et al. (2001) 9

Table 3: Postulated transport mechanisms for uptake of nitrogen by phytoplankton. Adapted from Wheeler (1983) 19

Table 4: An amino acid utilization ranking for various marine algal species, including *E. huxleyi*. The ranking system is explained in the text; adapted from Flynn (1990). 29

Table 5: reagents used for this study, including components of culture media and measurement of arginine concentrations. 31

Table 6: Gradient elution program used for amino acid HPLC analysis 34

Table 7: Carbonate concentration of both the artificial medium and natural SW, and percentage of C per liter not to be exceeded with phytoplankton biomass. 37

Table 8: Target cell densities for each cultured species based on reference and measured biovolume values. The maximum number of cells achievable is highlighted and estimated from g C L^{-1} so as not to exceed a 10 % decrease in the carbonate concentration (see Table 7) of both the artificial medium and natural SW 37

Table 9: culture media list and details 38

Table 10: k/2 medium composition used in Exp. II and III. Trace metals and vitamin concentrations were based on k/2 recipe diluted half strength and modified by Ian Probert (Houdan, Probert, Zatylny, Véron, & Villard, 2006), ... 39

Table 11: composition of ESAW medium used for Exp. I and II. Nutrient concentrations were adjusted for the experiment, while vitamins and trace metal amount were used according to the original recipe. 41

Table 12: Composition of Aquil* "basal seawater used for Exp. III 42

Table 13: Dilution series for antibiotic treatment of *A. minutum* and *C. peruvianus* 44

Table 14: dilution series for PNS treatment of *E. huxleyi* and *M. pusilla* 45

Table 15: Growth rate (day^{-1}) estimations for Experiment 2. These were calculated only where possible according to Equation 1. 58

Table 16: growth rates of *E. huxleyi* strains tested in CM0, CM1 and the mixed media CM2 (see Appendix for details). Calculation of growth rate was not possible in all cases. 60

Table 17: growth rates comparison of selected species between mixed CM4, CM3 and CM0. 62

Table 18: *E. huxleyi* and bacteria growth parameters; μ = growth rate, t_d = doubling time, k = number of divisions per day. Calculations were based on Andersen (2005). 66

Table 19: N-NO_3^- demand estimation for *E. huxleyi* cultures enriched with ARG. The theoretical density is calculated by adding the density of the culture on Day 0. 68

Table 20: ARG demand estimation for *E. huxleyi* cultures enriched with Arg. Calculation were made based on reference N and C quota and using the total density difference between the final day and day 0 of the experiment ($\Delta n = n_{end} - n_{start}$) 69

Table 21: PON and POC quantified on harvesting day and related to biomass estimation by biovolume 70

Table 22: *M. pusilla* and bacteria growth parameters; μ - growth rate, t_d = doubling time, k = number of divisions per day. For calculation details see Andersen (2005). 72

Table 23: N- NO_3^- demand estimation for *M. pusilla* cultures enriched with ARG. The theoretical density is calculated by adding the density of the culture on Day 0. 74

Table 24: ARG demand estimation for *M. pusilla* cultures enriched with ARG. Calculation were made based on reference N and C quota and using the total density difference between the final day and day 0 of the experiment ($\Delta n = n_{end} - n_{start}$). 74

Table 25: PON and POC quantified on harvesting day of *M. pusilla* cultures and related to biomass estimation by biovolume 75

Table 26: *A. minutum* and bacteria growth parameters; μ - growth rate, t_d - doubling time, k - number of divisions per day. For calculation details see reference Andersen (2005). 78

Table 27: N- NO_3^- demand estimation for *A. minutum* cultures enriched with ARG. The theoretical density is calculated by adding the density of the culture on Day 0. 79

Table 28: ARG demand estimation for *A. minutum* cultures enriched with ARG. Calculation were made based on reference N and C quota and using the total density difference between the final day and day 0 of the experiment ($\Delta n = n_{end} - n_{start}$). 80

Table 29: PON and POC quantified on harvesting day of *M. pusilla* cultures and related to biomass estimation by biovolume. 81

Table 30: *C. peruvianus* and bacteria growth parameters of cultures during exponential phase; μ - growth rate, t_d - doubling time, k - number of divisions per day. For calculation details see Andersen (2005). 83

Table 31: N-NO_3^- demand estimation for *C. peruvianus* cultures enriched with ARG. The theoretical density is calculated by adding the density of the culture on Day 0. 85

Table 32: ARG demand estimation for *A. minutum* cultures enriched with ARG. Calculation were made based on reference N and C quota and using the total density difference between the final day and day 0 of the experiment ($\Delta n = n_{end} - n_{start}$). 85

Table 33: PON and POC quantified on harvesting day of *M. pusilla* cultures and related to biomass estimation by biovolume. 86

Table 34: list of culture media (CM) used in Exp. I, II and III 90

LIST OF COMMON ABREVIATIONS

2-ME- *2-mercaptoethanol*

AA(s) – amino acid(s)

AcOH - Acetic acid

C – carbon

S - Sulphur

Chl *a* - Chlorophyll *a*

CM – culture media

DMS - dimethylsulfide

DOM - dissolved organic matter

DON - dissolved organic nitrogen

ESAW - Enriched Artificial Seawater

HPW - high purity water

IAc - 2-Iodoacetic acid

LM – light microscopy

N - nitrogen

NaAc - Sodium Acetate

NaTB - Disodium Tetraborate

NH_4^+ - ammonia

NO_2^- - nitrite

NO_3^- - nitrate

ON – organic nitrogen

OPA - *o-phthaldialdehyde*

P- phosphorous

Pheo *a* – pheopigments

PNS - Penicillin- Neomycin-Streptomycin

POC - particulate organic carbon

PON - particulate organic nitrogen

PTC - particulate total carbon

SBR - Station Biologique de Roscoff

SD – standard deviation

Si – silice

THF -Tetrahydrofuran

CM 0 – modified k/2, SW heated at 100°C and filtered nutrient stocks

CM 1 – ESAW, autoclaved AW and autoclaved nutrient stocks

CM 2 – 50%ESAW and 50% k/2

CM 3 – Aquil*, autoclaved AW and autoclaved nutrient stocks

CM 4 – 10% k/2 and 90% Aquil*

CM 5 – Aquil*, SW heated to 100°C and filtered nutrient stocks

1. Introduction

1.1. Nitrogen biogeochemistry

As a limiting element for biological productivity, nitrogen (N) occupies a central role in ocean biogeochemistry, exerting a significant influence on the cycles of many other elements, particularly carbon (C) and phosphorus (P). Unlike C and P, N has 5 relatively stable oxidation states in the marine environment and exists in more chemical forms than most other elements. For example, P, which has the same number of valence electrons, exists in the marine environment almost exclusively as ortho-phosphate (PO_4^{3-}), which may be bound to an organic molecule, (Monbet, McKelvie, & Worsfold, 2007; Svara, Weferling, & Hofmann, 2002) while silicon (Si) also exists in the ocean primarily in the +IV oxidation state, as $Si(OH)_4$ or SiO_2 (opal). In contrast, N is routinely measured in the marine environment as nitrate, NO_3^-, with an oxidation state of +5, nitrite, NO_2^-(+3), nitrous oxide, N_2O (+1) dinitrogen, N_2 (0), and ammonia, NH_4^+ (-3) (Gruber, 2008). The existence of several, stable oxidation states for N is the result of its having five valence electrons, while its small size means that the bonding electron orbitals may rearrange themselves. Phosphorus shares many of the same characteristics as N, but because it has 10 more electrons, which occupy the lower energy orbitals, the energy to break many covalent bonds is much higher (Gruber 2008).

A myriad of chemical transformations are unique to N, almost all of these are undertaken by marine organisms as part of their metabolism, either to obtain N to synthesize structural components, or to gain energy for growth.

By far the largest reservoir of N in the ocean (~ 1×10^7 Tg N; 94 %) is unavailable N_2. The majority of the remaining 'fixed' N occurs as NO_3^- (~ 88 %), followed by dissolved organic N (DON), which makes up nearly all of the remaining 12 %. The other forms,

particulate ON (PON), NO_2^-, NH_4^+, and N_2O have similar oceanic inventories, but together represent less than 0.3 % of the total fixed N pool, as shown in Table 1 (Gruber 2008).

Table 1: Oceanic Inventory, Turnover Rates, and Residence Times for the Major Fixed Nitrogen Species in the Ocean, adapted from Gruber (2008)

Species	**Mean conc. euphotic zone (mmol m^{-3})**	**Mean conc. aphotic zone (mmol m^{-3})**	**Oceanic inventory (Tg N)**	**Turnover rates (Tg N yr^{-1})**	**Turnover time (years)**
NO_3^-	7	31	5.8×10^5	1,570	370
NO_2^-	0.1	0.006	160		
NH_4^+	0.3	0.01	340	7,000	0.05
DON	6	4	7.7×10^4	3,400	20
PON	0.4	0.01	400	8,580	0.05
N_2O	0.01	0.04	750	6	125
N_2	450	575	1×10^7	200	54,000

The abundance of N_2 in the ocean is entirely due to its inertness, as the thermodynamically most stable form of N for aerobic environments is NO_3^-. The much lower mean concentrations of nitrate, nitrite and ammonium reflect their status as intermediary N species which are rapidly produced and consumed throughout the water column. Concentrations of DON are high, which may be partly due to certain constituents of this pool being very refractory; this is discussed further in Chapter 2.

The conversion of NO_3^- or NH_4^+ to organic N by marine phytoplankton is the process that quantitatively dominates the marine N cycle. As NH_4^+ is thought to be a preferred source of fixed nitrogen for phytoplankton, its assimilation does not involve a redox reaction and therefore requires little energy (Mitamura et al., 2013; Zehr & Ward, 2002). By contrast, the assimilation of NO_3^- involves the reduction of nitrogen, requiring the investment of a substantial amount of energy. Since NO_3^- is generally much more abundant that NH_4^+ in the ocean, most phytoplankton species contain the *Nitrate reductase* enzyme needed for this reduction.

Most of the fixed organic nitrogen in the ocean is returned back to nitrate by remineralization processes. This occurs in two distinct steps: ammonification and nitrification. The first step is undertaken by heterotrophic bacteria, which convert organic carbon to CO_2 to obtain energy, and release N as NH_4^+. Nitrification, which requires the presence of O_2 and tends to be inhibited by light, is most often performed by two distinct groups of organisms: ammonium and nitrate oxidizers; the best known are *Nitrosomonas* spp, an ammonium oxidizer, and *Nitrobacter* spp, a nitrite oxidizer.

Interest in the marine N cycle has greatly increased in the last decade, influenced by several factors. First is the growing recognition that the massive acceleration of the production of artificial nitrogen fertilizers and its subsequent application to agricultural soils (Galloway et al., 2004) has had an environmental effect. While the increased availability of fixed nitrogen has enabled humankind to greatly increase food production, it has also led to a host of environmental problems, ranging from eutrophication of terrestrial and aquatic systems to global acidification (Beman, Arrigo, & Matson, 2005; Gruber & Galloway, 2008).

Many national and international research programmes have already focused on the anthropogenic N problem and possible mitigation strategies. Less emphasis has been placed on understanding the interactions of N with the other major biogeochemical cycles, and how these cycles interact within a climate system that is more and more affected by human intervention (P. Falkowski et al., 2000). The perturbations of the global N and C cycles caused by human activity are linked, in part, because industrially-produced N is deposited in a form that is readily available to plants, thereby stimulating productivity and enhancing the uptake of CO_2 from the atmosphere (negative feedback), and thus mitigating climate change effects. However, at the same time, changes to the global N cycle may also have a positive feedback enforcing climate change effects, by reducing the ability of the Earth system to absorb anthropogenic CO_2. This is because the

magnitude of this fertilization-induced uptake amounts, in the next 100 years, to several hundred petagrams of carbon, an amount of reactive nitrogen (several thousand teragrams), clearly not available in the Earth system. Thus, N limitation is bound to substantially determine the ability of the terrestrial biosphere to act as a CO_2 sink in the future. (Gruber and Galloway, 2008).

Several examples of coastal eutrophication occurring in direct response to the input of anthropogenically derived nitrogen (mainly by rivers), have been reported. Nitrogen-rich agricultural runoff has stimulated large (54–577 km^2) phytoplankton blooms in the Gulf of California (Pegau, Boss, & Martinez, 2002; Riley, Ortiz-Monasterio, & Matson, 2001). Runoff exerts a strong and consistent influence on biological processes, stimulating blooms within days of fertilization and irrigation of agricultural fields during summer periods in 80% of cases (Beman *et al*., 2005). Moreover Beman *et al*. projected that, by the year 2050, 27–59 % of all nitrogen fertilizer would be applied in developing regions located upstream of nitrogen-deficient marine ecosystems, so future vulnerability of these ecosystems to agricultural runoff may be substantial. The impact of ecosystem changes can be multi-faceted, ranging from loss of habitat for fish due to reduced oxygen concentrations to the increased occurrence of harmful algal blooms (Gruber and Galloway, 2008).

These impacts indicate that the nitrogen cycle can regulate biogeochemical process and ecosystem resilience.

1.2. DON in seawater

The role and distribution of inorganic forms of nitrogen has been the focus of many studies because of their demonstrated participation in marine primary production and on biological controls on species distribution. Nevertheless, a considerable proportion of the total reactive nitrogen (TN) pool (i.e. the pool of nitrogen excluding gaseous N_2) in many freshwater and marine environments is frequently associated with the DON fraction. This

fraction frequently exceeds DIN in abundance (Bates & Hansell, 1999; Cavender-Bares, Karl, & Chisholm, 2001; Wong, Yu, Waser, Whitney, & Johnson, 2002), and is operationally defined and differentiated from its particulate counterpart as the fraction of marine organic N passing through a filter of 0.7 μm pore size (typically glass fiber) or 0.2 μm (polycarbonate, polysulfone, or aluminum filters) (Aluwihare & Meador, 2008).

DON is a subset of marine dissolved organic matter (DOM), and can comprise up to 69 % of the total dissolved nitrogen pool, excepting the deep-ocean and excluding molecular nitrogen (Bronk, 2002). Indeed, in open ocean surface environments, DON can comprise up to 83 % of the TN pool, while the mean total of NH_4^+, NO_3^-, and NO_2^-counts for only 10 %. In estuarine and coastal environments DON composes an average of 13 and 18 % of the TN pool (Bronk, 2002).

In general, reported data suggest that DON abundance is progressively higher in ocean, coastal, then estuarine and river waters, as shown in Figure 1.

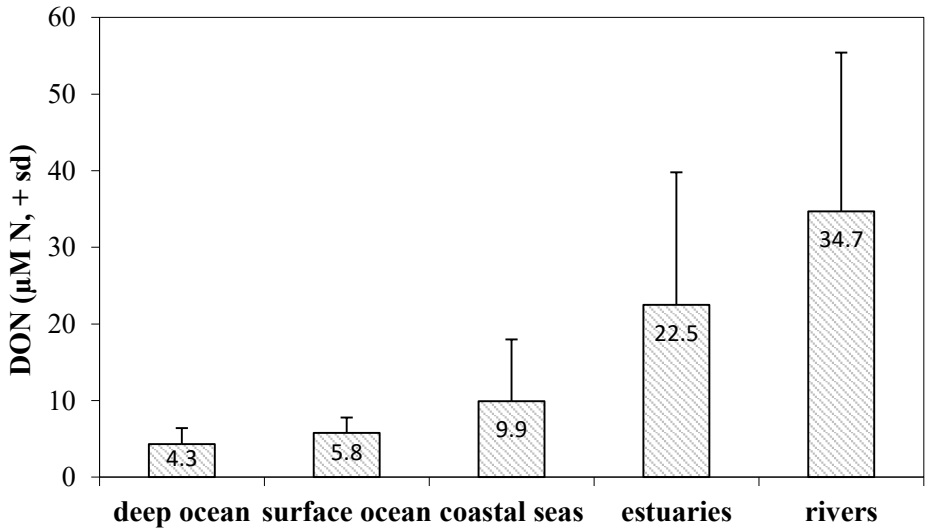

Figure 1: the average concentration of DON observed in different aquatic environments from riverine to deep ocean (adapted from Bronk, 2002)

For surface oceans, the DON concentration range is 0.8 – 13.0 μM with a mean of 5.8 ± 2.0 μM, while in the deep ocean the mean concentration is 3.9 ±1.8. From a global

perspective, it appears that the lowest concentrations of total organic nitrogen occurs at the equator and are higher just to the north and the south. There is increased biological production of DON near the equator fuelled by primary production resulting from upwelled NO_3^-. The released DON is then exported north or south via meridional Ekman transport to nitrogen-depleted subtropical waters (Bronk, 2002). Vertical profiles of DON generally show surface enrichment, export to depth and subsequent ammonification and nitrification which is estimated to supply between 10-25 % of remineralized NO_3^- in various parts of the ocean (Hopkinson et al., 1998).

In general, oligotrophic environments have not been shown to exhibit seasonality in DON, but this might be expected given the lack of long term datasets, which are of clear importance in defining this type of pattern (Bronk, 2002). Butler *et al*. (1979) documented a steady increase in DON from January through to August and then a steady decline from August to December in the English Channel over 11 years. Moschonas *et al*. (2015) studied DON seasonal concentrations in the Irish Sea and found increase in spring or early summer, during or following the drawdown of DIN by phytoplankton production, and its subsequently decreases over the course of several weeks or months.

Sources of DON can be both allochthonous and autochthonous. The former includes terrestrial runoff, leaching from plant detritus and soils into streams and rivers, sediments, and atmospheric deposition; autochthonous inputs comprise release by exudation from phytoplankton, macrophytes and bacteria, from cell death or viral lysis, or from micro- and macrozooplankton grazing and excretion.

In the open ocean, autochthonous sources of DON dominate, especially for the more labile constituents of the pool. DON is excreted by living algae and, although the actual amounts of DON released are still disputed, in the open bay of Monterey DON release resulting from NH_4^+ and NO_3^- uptake were approximately equal, and >90% of the NO_3^- taken up at the base of the euphotic zone resulted in DON production (0-1.1 µg-at N L^{-1}

d^{-1}) (Bronk & Ward, 2000). DON is also released when algae lyse, due to viral infection (Bratbak, Jacobsen, & Heldal, 1998) or by natural cell death (apoptosis), when grazers feed 'sloppily' (Jumars, Penry, Baross, Perry, & Frost, 1989), or during zooplankton excretion (Lampert, 1978).

The four main sinks for DON are bacterial uptake, phytoplankton uptake, photochemical decomposition and abiotic adsorption. Degradation resulting from bacterial activity probably accounts for the major flux of N out of the DON pool in aquatic systems. The components of the DON pool vary in terms of their lability. Many of the intermediate compounds formed (e.g. amino acids from hydrolysis of proteins and peptides, urea from purine breakdown) could theoretically be taken up and utilized directly by bacteria and phytoplankton (Gruber, 2008; Margaret R Mulholland et al., 1998; P. Wheeler, North, Littler, & Stephens, 1977). Further breakdown generates NH_4^+, which is either assimilated directly by the microbiota or nitrified to NO_3^-. Berman and Chava (1999) showed that NH_4^+ and urea were released from indigenous DON compounds in unamended, filtered (1.0 μm) marine- and freshwaters over several days, presumably as the result of bacterial metabolism.

1.3. The chemical composition of the DON pool

DON is a heterogeneous mixture of biologically labile and refractory components, with approximate turnover times on the order of days or weeks, and months to hundreds of years, respectively (Bronk, 2002). The refractory components are more abundant (40-60 % of the TDN pool), but the smaller, more labile compounds (5-20 % of the TDN pool) are increasingly recognised as a potentially-rich source of nutrients for microorganisms (Bronk, 2002). Within the DON pool, a number of compounds has been identified; the smaller low molecular weight (LMW; < 1 kDa) fraction is poorly characterised but could be key for sustaining life in nutrient-depleted open ocean surface layers. Components of

this LMW fraction include urea, dissolved free amino acids (DFAA), dissolved combined amino acids (DCAA), amino sugars, purines, pyrimidines, pteridines, amides and methylamines (Curtis-Jackson, Massé, Gledhill, & Fitzsimons, 2009). The high molecular weight (HMW) pool is believed to be dominated by amide compounds, originating from bacteria (Tanoue, 1995).

Urea is an LMW organic compound originating mainly from its excretion by bacteria and marine organisms (Cho, Park, Shim, & Azam, 1996; Therkildsen, Isaksen, & Lomstein, 1997), or via organic matter degradation in the water column and release from sediments (Thomsen & Jähmlich, 1998). A recent study suggests that urea in runoff can represent a significant proportion of the total DON pool, and an important form of nitrogenous export from fertilised agricultural land (Davis, Tink, Rohde, & Brodie, 2016). Although the contribution of urea in runoff to coastal eutrophication has been perceived as negligible, even small concentrations of urea may trigger an algal bloom (Kibet et al., 2016). Urea is a potential N source for marine microorganisms but its uptake into cells requires an energy-expensive, active transport system to be utilised (Price & Harrison, 1988), and a *urease* to hydrolyse the molecule (Berman & Bronk, 2003).

DFAA concentrations tend to be lower than those of DCAA, due to the close coupling between assimilation and release (Fuhrman, 1990), although no consistent pattern have been noted during algal blooms, which occur according to season, depth, location and time of day (Sellner & Nealley, 1997). Amino sugars (including peptidoglycans) are microbial in origin and are a catabolic product of chitin polymers (Benner & Kaiser, 2003). Pteridines are a large and structurally varied group of compounds involved in the biosynthetic pathways of co-factors and vitamins (Antia, Harrison, & Oliveira, 1991). Methylamines are degradation products of alkyl and quaternary amines that control cellular osmo-regulation (Gibb, Mantoura, Liss, & Barlow, 1999).

1.4. Importance of phytoplankton to marine ecosystem functioning

As photoautotrophs planktonic algae are important primary producers, they obtain energy and nutrients by harnessing sunlight through photosynthesis to make organic substances from inorganic ones. They play a crucial role in global carbon fixation and oxygen production accounting for a little less than half (48 Pg C yr^{-1}) of the global net primary production of 105 Pg C yr^{-1} (Table 2).

Table 2: Annual and seasonal net primary production (NPP) of the major units of the biosphere. Values are in petagrams of carbon (1 Pg = 1015 g). Adapted from Geider et al. (2001)

Marine	NPP	Terrestrial	NPP
Trade Winds Domain (tropical and subtropical)	13	Tropical rainforests	17.8
Westerly Winds Domain (temperate)	16.3	Broadleaf deciduous forests	1.5
Polar Domain	6.4	Mixed Broadleaf and needleleaf forests	3.1
Coastal Domain	10.7	Needleleaf evergreen forests	3.1
Salt marshes, estuaries and macrophytes	1.2	Needleleaf deciduous forest	1.4
Coral Reefs	0.7	Savannas	16.8
		Perennial grasslands	2.4
		Broadleaf shrubs with bare soil	1.0
		Tundra	0.8
		Desert	0.5
		Cultivation	8.0
TOTAL	48.3		56.4

Phytoplankton consist of a wide variety of genres with different capacities to exploit the availability of light and nutrients, while at the same time being able to develop different adaptations in response to environmental variants. Changes in environmental conditions may favour some species which can adapt better than others (Smayda, 1958). Under certain conditions, for example, species which are normally a minor biomass contributor could dominate a bloom, such as toxic algal species. In this regard, understanding the structural variations and/or dynamics that may occur, as a result of environmental changes, is of fundamental importance not only in order to understand coastal marine ecosystem functioning, but also involvement in important ecological phenomena. Some

of the ecological implications for algal blooms are production of mucilage (Reynolds, 2007), extracellular organic matter production of phytoplanktonic origin, or the formation of red-tides which can negatively impact on tourism. Moreover, production of phytotoxins (Hallegraeff, Anderson, Cembella, Enevoldsen, & Commission, 2003) from various algal species under specific conditions can have an impact on human health through the consumption of bivalve molluscs, crustaceans or tropical fish which have accumulated algal toxin by filtering seawater, or through seawater aerosol inhalation containing toxic species leading to respiratory problems or a skin allergic irritations.

1.4.1. *Phylum Haptophyta – Emiliania huxleyi*

Haptophytes (or Primnesiophytes) are primarily marine unicellular biflagellates that have had a major impact on global biogeochemistry for at least 150 million years (Graham, Graham, & Wilcox, 2009). The greatest long-term impact has been on carbon and sulphur cycling and, hence, global climate. Most haptophyte are characterized by the intracellular production of elaborate calcite platelets (coccoliths), arranged extracellularly to form a coccosphere (Taylor et al., 2017). Sedimented coccoliths are the major contributors to ocean floor limestone accumulation, and represent the largest long-term sink of inorganic carbon on earth. In addition, sinking coccoliths ballast particulate organic matter, enabling the transfer of organic carbon to depth (Ziveri et al., 2007). Consequently, coccolithophores are crucial contributors to ocean biogeochemical cycles, estimated to be responsible for up to 10% of global carbon fixation (Poulton et al., 2007). The function of coccoliths have been speculated upon as accelerating photosynthesis with carbon concentrating mechanism and enhanced light uptake via scattering of scarce photons for deep-dwelling species, protection from photodamage from ultraviolet (UV) light and photosynthetic active radiation (PAR) and energy dissipation under high-light conditions, armor protection against viral/bacterial infections and grazing (Monteiro et al., 2016).Most of the 200 species of Haptophytes are globally abundant in most surface

waters, ranging from highly productive eutrophic waters in temperate and subpolar regions to the permanently oligotrophic waters of the subtropical gyres (Monteiro et al., 2016). Another environmental implication is the production of large amounts of dimethylsulfide (DMS), a volatile sulfur-containing molecule that increases acid rain (Arnold, Kerrison, & Steinke, 2013) during extensive ocean blooms of *Emiliania huxleyi* (Figure 2) .

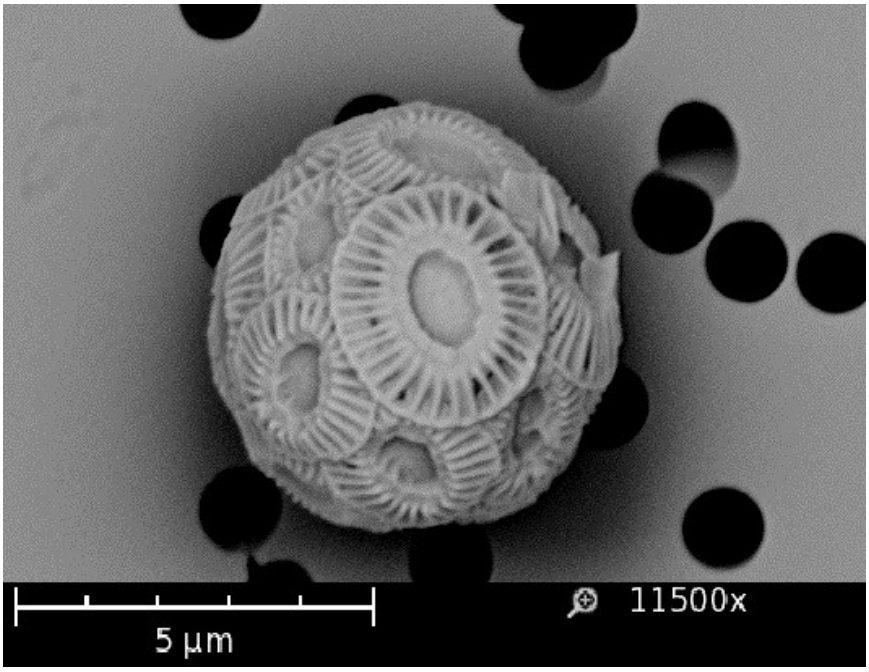

Figure 2: *E. huxleyi* cell image captured using a Phenom scanning electron microscope at Station Biologique de Roscoff (France).

Coccolithophores produce a secondary algal metabolite dimethylsulfoniopropionate (DMSP), whose enzymatic breakdown originates the trace gas Dimethyl sulfide (DMS). DMS emissions from the ocean contribute 17–34 Tg S yr^{-1} to the atmosphere, where it affects cloud formation and climate, which corresponds to 90% of the biogenic sulfur emissions from the oceans and almost 50% of the global biogenic sulfur emissions (Holligan et al., 1993, Lana et al., 2011).

The vast majority of Haptophytes are unicellular biflagellates, though some species also have amoeboid, coccoid, palmelloid or filamentous stages. The chloroplasts are

golden or yellow-brown in colour, because the green Chlorophyll is masked by accessory pigments, of which the most important is fucoxanthin. Plastids of all Haptophytes contain chlorophylls a, c1 and c2, as well as β-carotene, and diatoxanthin (Graham, Graham and Wilcox, 2009).

Among coccolith-producing Haptophytes, *Emiliania huxleyi* is one of the most studied algal species. It is an extremely cosmopolitan phytoplankton species and is present in all oceans, except polar oceans. It can tolerate a wide temperature range (1 – 30 ˚C), and is widely known for bloom formation, contributing to 40% of primary production and phytoplankton biomass in subpolar, temperate, and tropical environments (Poulton et al., 2013). These blooms have significant environmental impacts, via increased water albedo (reflectance), DMS production, large fluxes of $CaCO_3$ out of the surface waters and changes in the oceanic uptake of CO_2 (Westbroek et al., 1993). In a modelling study of the NE Atlantic Ocean by Tyrrel and Taylor (1996), it was concluded that *E. huxleyi* is a fast-growing species with an advantage in conditions conducive to rapid growth (i.e. it is r-selected). Therefore, *E. huxleyi* blooms in eutrophic and upwelling regions but not in large numbers in nutrient-starved, oligotrophic waters; moreover it has a particular advantage at high light (1000 or 1500 μEin m^{-2} s^{-1}) and low phosphate levels (Nanninga & Tyrrell, 1996). A dependence on high light intensity is compatible with the r-selected status (up to 2.8 cell divisions day^{-1} (L E Brand & Guillard, 1981) of *E. huxleyi,* since this condition will favour species with rapid growth rates, if some nutrients are still available. A link with low phosphate concentrations (in conjunction with non-limiting nitrate) could explain why *E. huxleyi* tends to be most abundant towards the end of a bloom sequence, when nutrients start to become depleted. This could also explain why *E. huxleyi* does not usually feature as part of the bloom succession in most of the world's oceans, since oceanic waters are usually nitrate-limited and grazing is the major factor in bloom termination (Toby Tyrrell & Merico, 2004).

Culture experiments have revealed the existence of three cell types, all about 5-7 µm in diameter: coccolith-bearing cells which are non-motile; naked non-motile cells which seem to be mutants rather than part of the regular life cycle; haploids, which are motile flagellate cells that have organic body scales but no coccoliths. In addition, there is a naked, motile amoeboid cell form lacking flagella (Braarud, 1963; Klaveness, 1972); as these are seen very rarely in senescent cultures of coccolith-bearing and naked cells, they are most likely a laboratory artefact.

1.4.2. *Phylum Heterokontophyta – Chaetoceros peruvianus*

Diatoms are the most species-rich algal group on earth and accounting for approximately 25 % of the world's entire net primary production. This is comparable to primary production by pines in temperate and boreal forests and by grasses in savannahs, grasslands and cultivated areas (Werner, 1977). Their wide-spread occurrence, importance as a food-resource for the entire food-web and their multipurpose use in applied science and technology make them a group which has received considerable attention (Willén, 1991). Planktonic diatoms have been studied in many experiments to clarify their competitive ability, particularly during turbulence (Amato et al., 2017) or the onset of stratification at low light (Fisher & Halsey, 2016; Happey, 1970), nutrient and temperature levels (Pancic, Hanse, Tammilehto, & Lundholm, 2015).

Taxonomically, diatoms belong to the Bacillariophyceae class, within which all species are unicellular or colonial coccoid algae. Each cell is encased by a unique siliceous cell wall which takes in the form of a box (termed a frustule), and that cause them to sink rapidly when they die, carrying fixed OC to the deep ocean, influencing the biological pump and shaping the C cycle (Amin et al., 2012). Silica is inert to enzymatic attack, and thus diatoms may have advantages through being less vulnerable to microbial attack or digestion within the guts of herbivores (Pickett-Heaps, Schmid, & Edgar, 1990). In

addition, silica is often plentiful in natural waters and is an energetically inexpensive source of material for cell walls.

The *Chaetoceros* genus is one of the largest marine planktonic diatoms with approximately 400 species described, (Hasle, Syvertsen, Steidinger, Tangen, & Tomas, 1996). Cells are typically more or less rectangular in girdle view, and elliptical to almost circular in valve view. *Chaetoceros* species possess characteristic long hollow outgrowth of valve projecting outside from each angle of the valve margin, with different structure from the valve, called *setae*. Setae are thick, often very long, and armed with spines (Graham, Graham and Wilcox, 2009).

The species *C. peruvianus* (Figure 3) is a centric diatom (order Centrales) which is mostly oceanic and normally found in short chains or solitary cells, all with heterovalvae; the upper valve is rounded and lower valve flat and it has an apical axis of 10-32 µm (Hasle *et al.*, 1996).

Figure 3: live *C. peruvianus* image captured with by optic microscope

Chloroplasts are numerous, small granules throughout the whole cell, setae included. They are usually golden-brown because chlorophyll is masked by the accessory pigment fucoxanthin. Like all Heterokontophytes, *C. peruvianus* possesses chlorophylls *a* and c_2.

Vegetative cells of diatoms are diploid, and gamete production involves meiosis. Thus, like few other algal groups and animals, they have a gametic life cycle. Centric diatoms are oogamous, gamete fusion results in formation of a zygote that develops into a large auxospore, that can be completely free of the parental frustule, attached to one of the parental thecae or enclosed by both parental thecae. Maturing auxospores eventually produce a new two-part silica wall, and under favourable conditions they germinate by a series of divisions that ultimately produces cells with the typical frustule morphology and maximal size (Werner, 1977).

Relatively little is known regarding the environmental cues that induce diatom sexual reproduction; however, increases in temperature or irradiance or changes in nutrient availability are known triggers (Montresor, Vitale, D'Alelio, & Ferrante, 2016). Spores and resting cells allow diatoms to survive during periods unsuitable for growth and then germinate when conditions improve.

1.4.3. *Phylum Dinophyta – Alexandrium minutum*

In aquatic environments dinoflagellates are found in both pelagic (open-water) and benthic habitats. Ecological constraints they can face in such habitats, include sensitivity to turbulence and their relatively large size and consequent low surface area-to-volume (S/V) ratio, which limits their ability to obtain nutrients. When taking up inorganic nutrients at the cell surface, dinoflagellates can be at a competitive disadvantage in comparison to nanophytoplankton, which have higher S/V ratios and thus relatively high nutrient uptake capacities. Many dinoflagellates are known to be photosynthetic, but a large fraction are mixotrophic, combining photosynthesis with prey ingestion (phagotrophy). The high frequency of mixotrophyindicates that photosynthesis does not completely provide the energetic needs of many plastid-bearing species (Graneli & Carlsson, 1998). Dinoflagellates may reach bloom abundances of 10^7-10^8 cells L^{-1}, in conditions of calm waters or along boundary fronts formed at the junction of stratified

open-ocean waters and coastal mixed zones (Spector, 2012). Being flagellates, together with phototactic capacity, confers much greater ability to migrate vertically and harvest organic particles and/or inorganic nutrients from much of the water column, further explained by the fact that about half of the known dinoflagellates species lack plastids and are therefore obligatory heterotrophic (Jones, 1994).

Most dinoflagellates are unicellular flagellates with two distinctive flagella that confer characteristic rotatory swimming motions, achieving rates of 200-500 μm s^{-1} (Graham, Graham and Wilcox, 2009). They are further characterized by cell-covering components that lie beneath the cell membrane, consisting of a single layer of several to many closely adjacent, flattened vesicles (the entire array is known as "amphiesma"). In many species each thecal vesicle contains a thecal plate of cellulose (called thecate); others are called non-thecate.

About 60 species are known to produce water- or lipid-soluble toxins; the majority of toxic species are photosynthetic and capable of producing resting cysts.

The genus *Alexandrium* is widespread globally and was formally established with the description of its type species *A. minutum* Halim (Halim, 1960) (Figure 4), a small-sized dinoflagellate that produced a 'red tide' in the harbour of Alexandria in Egypt.

Figure 4: live *A. minutum* cell image captured by optic microscope

This genus now includes 31 species and is one of the major HAB genera with respect to the diversity, magnitude and consequences of blooms. The ability of *Alexandrium* to colonize multiple habitats and to persist over large regions through time is testimony to the adaptability and resilience of this group of species (Anderson et al., 2012).

A. minutum was first detected on the French coast in 1985, and recurrently formed toxic blooms in the Northern part of Brittany until 1988 (LeDoux, Fremy, Nezan, & Erard, 1989). Over a 15-year period (1992–2007), weekly water samples were collected from a time-series station in the Western English Channel and phytoplankton abundance analysis revealed that dinoflagellate abundance was higher during the summer months (Widdicombe, Eloire, Harbour, Harris, & Somerfield, 2010).

1.4.4. *Phylum Chlorophyta – Micromonas pusilla*

The importance of Green algae is widely known as they participate in a variety of important biotic associations and some can produce nuisance blooms under conditions of nutrient pollution (Carr & Whitton, 1973). Moreover, they are known to be sources of food for aquatic microbes and animals and are grown industrially to produce commercial food supplements (Paerl & Tucker, 1995).

Micromonas pusilla belongs to the Green Algae group, named because the abundant chlorophylls *a* and *b* are not concealed by large amounts of differently coloured accessory pigments. Among green algae *M. pusilla* belongs to the separate clade of Prasinophyceans which are all unicellular.

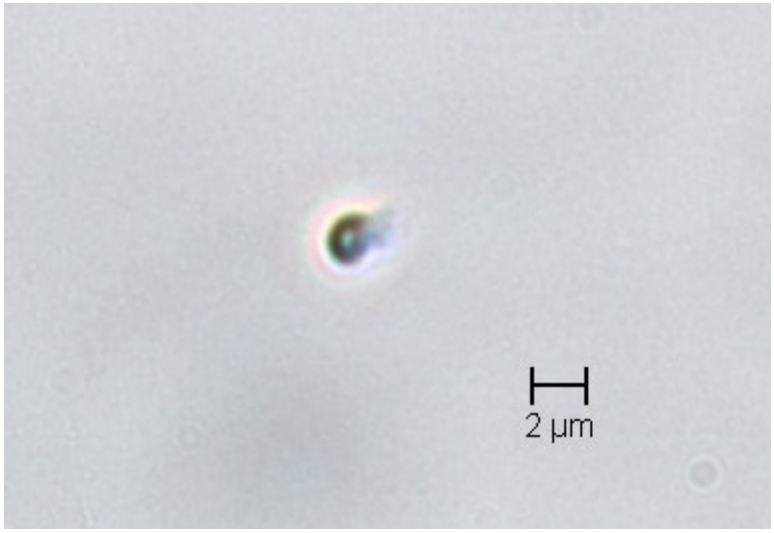

Figure 5: live *M. pusilla* cell image captured by optic microscope

The flagella of the flagellate species typically emerge from an apical depression, and the flagella apparatus can differ widely at an ultrastructure level from species to species (Graham, Graham and Wilcox, 2009). Members are known to be common in temperate and cold regions and can occur as prominent constituents of marine picoplankton (Throndsen, 1976).

Several studies have demonstrated the importance of eukaryotic picoplankton (cell size 0.2 to 3 µm) in terms of biomass and productivity in the euphotic zone of oceanic oligotrophic waters as well as coastal waters. During seasonal sampling off Roscoff (France) at the ASTAN station (48°46' N, 3°57' W) in the Western English Channel, *Micromonas pusilla* was found to be the dominant species and accounted for 45 % of picoplanktonic eukaryotes, with maximum abundance (~ 10 times the winter abundances) in midsummer (Not et al., 2004). *Micromonas* may have a broad ability to respond to light and nutrient variations and thus, because of this large environmental spectrum, may be little affected by changes in the environment.

1.5. DON uptake by phytoplankton

It has been long assumed that in most aquatic environments there is a flux of N from the DON pool to microorganisms and lately there have been suggestions that increased levels

of DON may be responsible for incidences of toxic and blooming phytoplankton in many locations (Cochlan, Herndon, & Kudela, 2008; Graneli, Edler, Gedziorowska, & Nyman, 1985; Margaret R Mulholland et al., 1998; Wetz et al., 2017; Zhang, Shengkang, Xiaoyong, & Xiurong, 2015). In theory, any nitrogenous compound which passes the plasma membrane and enters a biochemical pathway could be considered a nitrogen source. However, the processes of entering the cell, and of incorporation, must proceed rapidly if they are to contribute significantly to growth (Flynn & Butler, 1986).

The individual reaction involved in phytoplankton nitrogen metabolism can be grouped into four major processes; membrane transport, assimilation (metabolic conversion of inorganic nitrogen to small organic metabolites), incorporation (synthesis of macromolecules from small metabolites) and catabolism (breakdown of macromolecules into small metabolites).

Any nitrogenous source can enter a cell by different transport mechanisms, mainly diffusion, which is a non-specific entry and is driven by electrochemical gradients, primary active transport that requires a direct input of energy, or secondary active transport driven by ion gradients. The postulated means of entry of the major nitrogen sources for phytoplankton are listed in Table 3.

Table 3: Postulated transport mechanisms for uptake of nitrogen by phytoplankton. Adapted from Wheeler (1983)

N source	Transport mechanism
NH_4^+,NH_3^-	Diffusion, mediated diffusion or secondary
Urea	Diffusion and secondary active transport
Amino acids	Secondary active transport
NO_3^-	Primary active transport

Significant uptake of nitrogenous nutrients by diffusion is feasible only for NH_3 and urea, since these two compounds are very soluble in the lipid phase of membranes (Raven, 1981). The small amount of data available suggests that NH_4^+, urea and amino acids may enter marine phytoplankton by secondary active transport driven by an Na^+ gradient. Transport of NO_3^- and NO_2^-, on the other hand, may be driven directly by a Cl^- -stimulated ATPase (P. G. Falkowski, 1975). Considering the negative electrochemical gradient across the cell membrane, the anions are probably the most costly nitrogen sources taken up by phytoplankton.

The pathway for the assimilation of NH_4^+ is also that used during the assimilation of nitrate, nitrite, urea and purines because the initial stages of the incorporation of these compounds leads to the intracellular production of ammonium, which is then incorporated into amino acids using the products of CO_2 fixation. On the other hand, when an amino acid is used as an N-source for growth, it is likely to be incorporated directly into protein.

Historically, DON was believed to be composed mainly of refractory compounds resistant to biological degradation and generally unavailable as a source of N nutrition for phytoplankton or bacteria. It now appears that, in many situations, DON can be an important source of phytoplankton N nutrition in the natural environment (Flynn & Butler, 1986; M R Mulholland & Lee, 2009). In the recent study conducted in the Scottish fjord of Loch Creran by Moschonas *et al.* (2017) the N sources that correlated with the multivariate pattern in phytoplankton community composition and abundance were, in order of statistical importance: urea, DFAA, DON, and DIN. They also found that during the spring bloom urea uptake rates can be highest relative to other N sources, up to 44% of the total N uptake. The measured drawdown of DON during the spring bloom could have contributed up to 37 % compared to 63 % from NO_3^-, respectively of the total measured dissolved N drawdown, clearly showing the importance of DON for phytoplankton N nutrition. Indeed in the smaller phytoplankton size fraction considered

(>10 μm), NO_3^- contributed only for 28% during spring and summer but generally much lower, while NH_4^+ (up to 55%), urea (up to 59%), and DFAA (up to 38%) did considerably during spring and summer when regenerated N uptake rates were highest. At different latitudes DON experiments proved to be essential for autotrophs' nutrition. Benner *et al*. (1997) estimated that 30 to 50 % of daily phytoplankton N demand in the equatorial North Pacific could be supplied by remineralization of the DON pool. Interestingly, brown tides off Long Island, USA, usually occur in drought years when NO_3^- inputs are reduced and DON concentrations are high relative to DIN (LaRoche et al., 1997). Moreover in a Chinese river estuary and adjacent shelf Zhang *et al*. (2015) found a decrease in DON and a co-occurred decrease in DFAA and DCAA during the succession from a diatom to dinoflagellate bloom. Variable dynamics of biological indicators used in the study, including the DOC/DON, the amino acid yields, and the degradation index, showed that DON provided a significant portion of the total N demand throughout the duration of the large-scale dinoflagellate bloom under conditions of low DIN availability. DON was also found to be the major source of N for phytoplankton in the Gulf of Riga, Baltic Sea, and may be an important contributing factor to the eutrophication of these waters (Berg, Glibert, Jørgensen, Balode, & Purina, 2001).

Mulholland *et al*. (2009) reported a massive bloom of *Cochlodinium polykrikoides* Margalef (> 10^4 cells mL^{-1}) during August and September 2007, in the lower Chesapeake Bay and its tributaries. Combined with the observed higher turnover times for peptide hydrolysis, organic N was likely to have contributed substantially to supporting the bloom, consistent with the low levels of DIN (< 2 μM), relative to DON, which averaged > 16 μM.

Over the past 11 years an invasion of *Prorocentrum minimum* into the Baltic Sea has been hypothesised by Pertola *et al*. (2005), to be enhanced by DON enrichment, based

on the multiple regression and multivariate statistical analysis, which were negatively-related to inorganic N.

Several studies, both in natural and cultured samples, found evidence of DON utilisation by local phytoplankton. Townsend & Thomas (2002) presented data suggesting that DON provided some of the N requirement at the start of the winter-spring phytoplankton bloom on Georges Bank, while in the freshwater of Lake Kinneret, a bloom of the cyanobacterium *Aphanizomenon ovalisporum* used the DON pool as its major source of N (Berman, 1997). Seitzinger and Sanders (1999) also noted that the community composition of phytoplankton differed in growth experiments using estuarine water enriched with rainwater DON (diatom- and or dinoflagellate-dominated) or with NH_4^+.

There is evidence that inputs of DON to estuarine and coastal waters have stimulated the development of brown tide blooms of *Aureococcus anophagefferens* (Gobler & Sañudo-Wilhelmy, 2001). Additionally, axenic cultures of *A. anophagefferens* were able to hydrolyze a variety of DON compounds (peptides, chitobiose, acetamide and urea) indicating the organism's ability to adapt to different substrates (Berg, Repeta, & Laroche, 2002).

The investigation with xenic cultures of *Entomoneis paludo*sa by Jauffrais *et al*. (2016) revealed the importance of microphytobenthos in N flux mediation by assimilating amino acids, such as Glycine, Glutamine and Arginine, with the latter being the N source which supported biomasses and cell divisions similar to inorganic N, and the first one producing the highest efficiency of photosynthetic light-capture.From axenic culture experiments of 15 different species Flynn (1990) reported that, after addition of a mixture of 20 L-amino acids to N-depleted cells, there was a preference for basic amino acids (arginine, lysine, ornithine, but not histidine), and amidic amino acids (asparagine and glutamine). Of particular note is that glycine did not appear to be a very good choice of

substrate as a 'typical' amino acid, although it has been used as a proxy in studies of algal utilization of amino acids in nature (Schell, 1974; P. Wheeler et al., 1977). Experiments by Flynn and Wright (1986) showed also how the diatom *Phaeodactylum tricornutum* grown in the presence of Arginine (ARG) used 20-25 % less NH_4^+ and contained 10 % less Chl *a* than those grown on NH_4^+ alone. Other studies have reported similar results, such as Admiraal *et al*. (1986) who showed that the available discharged traces of amino acids down to the detection limit of the method (20-30 nmol $\cdot L^{-1}$) indicated that the uptake of ambient amino acids (l-100 nmol $\cdot L^{-1}$) was possible even in a large-celled *Coscinodiscus granii* with its unfavourably low surface to volume ratio.

Hu et al. (2014) compared growth kinetics of *Prorocentrum donghaiense* cultures on different N compounds; while *P. donghaiense* had higher maximum growth rates when supplied with urea or glutamic acid as sole source of N, cells had a higher affinity for cyanate, NO_3^-, and NH_4^+ relative to urea, glutamic acid, and dialanine suggesting that the former compounds might be important sources N when nutrient concentrations are submicro-molar. Because peptides and cyanate are degradation products of decaying cells they are likely available to *P. donghaiense* during bloom maintenance when NO_3^- concentrations are exhausted and recycling processes are important for maintaining cell biomass and turnover.

2. This study

2.1. Aim and objectives

As DON is abundant in seawater, the question arises as to its importance to the marine food web? In order to investigate this question one can start from the very first level of the trophic chain represented by phytoplankton and primary production. A key question is what form of the DON pool might support primary production when concentrations of inorganic N are very low (i.e. summer). In summer, concentrations of organic nutrients are higher than in winter (Butler et al., 1979), so if components of DON are systematically used by all species of phytoplankton, it may help explain why natural populations of phytoplankton do not always show the symptoms of N-limitation expected from the low quantities of inorganic N in their surroundings (Goldman, McCarthy, & Peavey, 1979; M R Mulholland & Lee, 2009; Margaret R Mulholland et al., 1998, 2009).

The experiments described were intended to clarify whether a labile component of DON, like amino acids, may be important in determining not only the amounts, but also the species composition, of the developing phytoplankton assemblage in the Western English Channel.

The hypothesis that form the basis of the experiments is that algal species that can directly access oligopeptides gain an advantage over competitors at low levels of DIN.

To assess the ability of algal species to utilize DON, in the form of amino acid, the first objective was to constrain sources of N within culture media (i.e. seawater). Two different artificial media were initially tested for suitability to the algal species studied.

The second objective was to monitor actual N uptake by the sole phytoplankton, and a method for bacteria removal was developed and tested.

The last objectives were to (i) examine the ability of monocultures of relevant algal species to grow in culture with amino acid as the only N source and (ii) to compare growth

rates in monocultures containing nitrate alone. A final experiment was run to assess both objectives using natural seawater and non-axenic cultures as a preliminary test.

2.2. Experimental design

2.2.1. *Algal strains selection*

The following 4 algal species were selected from the Roscoff Culture Collection (http://www.sb-roscoff.fr/phyto/RCC) according to their importance both in terms of abundance in the Western English Channel ecosystem and potential to form harmful algal blooms:

- *Emiliania huxleyi* CCMP 1516 (Haptophyta, Cocolithophores) is one of the most studied algal species, extremely cosmopolitan and widely known for bloom formation. This strain of *E. huxleyi* was chosen during Experiment II when testing different artificial media.
- *Chaetoceros peruvianus* RCC 2023 (Heterokontophyta, diatoms) was chosen based on the reference list for micro-phytoplankton for the permanent mixed waters of the Western English Channel during the years 2000-2010 (Guilloux et al., 2013), where it was identified with the potential to become dominating (above 500 cells L^{-1} on average for all samples examined).
- *Alexandrium minutum* RCC 1490 (Dinophyta) was selected as it is ecologically relevant and may be a toxin producer,
- *Synecococcus* sp. RCC 744 (Cyanophyta), was initially selected among picophytoplankton in order to investigate the importance of ON to cyanobacteria and the implications with phytoplankton and bacteria interactions. During Exp. I this algae proven to be difficult to be cultured with artificial medium and so was replaced by *Micromonas pusilla*,

- *Micromonas pusilla* RCC 834 (Chlorophyta), was selected for this study as it is an important member of the picophytoplankton community in the Western English Channel (Not et al., 2004), and of a similar biomass to bacteria.

2.2.2. *Experiments I, II and III – Testing artificial media*

Three main experiments were planned;

I. The first experiment was intended to test growth of the selected species in the artificial medium "ES Enriched Artificial Seawater" – ESAW (Harrison, Waters, & Taylor, 1980).

II. A second experiment was run to detect relevant growth differences (rates, biomass, nutrients uptake) compared with that on original medium (based on natural seawater), as shown in Figure 6. Comparison was achieved by monitoring growth in three different media (CM 0, CM 1, and CM 2, see Appendix for details) concurently for all species.

III. For the last artificial medium experiment the Aquil* recipe (Morel, Rueter, Anderson, & Guillard, 1979) was tested. The idea was to proceed with a more gradual acclimation; cells growing in the mixed CM 2 of Exp. 2, were spiked firstly into both a mixture of 10% k/2 and 90% Aquil* (CM 4), to reduce the amount of artificial medium, and 100% Aquil* (CM 3) to see if the new recipe was preferred in terms of growth.

2.2.3. *Experiments IV – Preparation of axenic cultures*

A fourth experiment was run to prepare axenic cultures of selected phytoplankton species and is described by Figure 6. Two antibiotic mixtures were tested for bacteria removal, at

a series of incubation times. After addition of of antibiotic, cells were incubated for 24-48 hours and then 5-10% of each culture was transferred to fresh medium and left for 3 days before further addition of antibiotic.

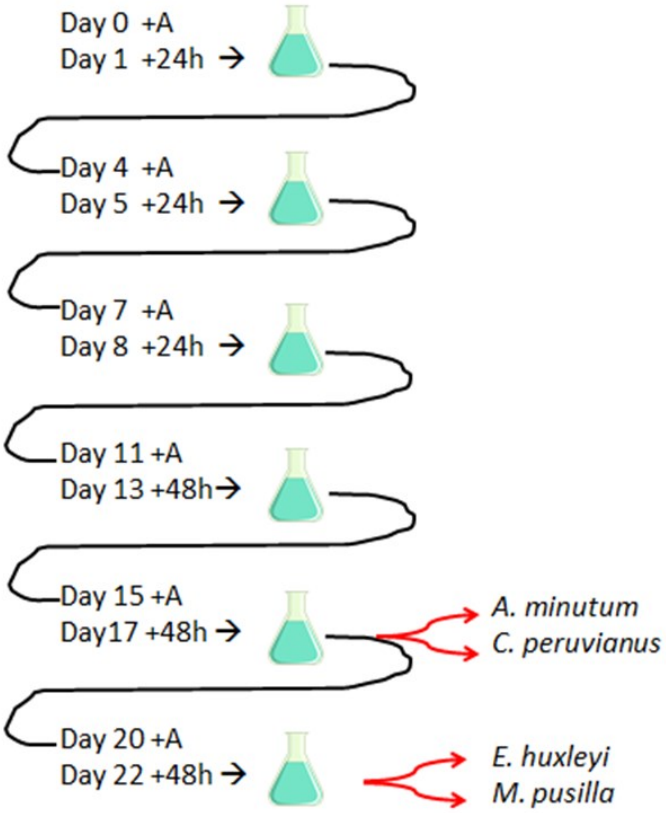

Figure 6: Schematic diagram of antibiotic treatments used to test removal of bacteria from selected phytoplankton strains grown in CM 0 (k/2). A = antibiotic. Black lines indicate period of time until next antibiotic addition. Red arrows indicate last transfer to fresh medium, different depending on the species.

2.2.4. *Experiments V – Growth comparison on Amino acid and Nitrate*

Experiment V was carried out as a preliminary test to examine the ability of algal species to grow on DON as the sole N source and to compare growth rates of the same species grown with DIN only.

Although Aquil* medium gave the best results in terms of growth for some of the species, natural SW was chosen for this experiment as it was suitable for all 4 species.

Nitrate was chosen as the inorganic N source as it is the dominant form of fixed N in natural seawater. A DFAA was chosen as a proxy for the DON pool, being a labile compound derived from major biological cell constituents that account for a substantial fraction of the N flux into and out the DON pool. Concentrations of DFAA are typically low in seawater, resulting in the paradigm that their production and consumption are tightly coupled (Fuhrman, 1987; Keil & Kirchman, 1994; Tappin, Millward, & Fitzsimons, 2010). Assimilated amino acids can be incorporated directly into protein unlike other forms of DON, which require conversion. Arginine was selected as the amino acid source, based on its low C : N ratio relative to other amino acids, additionally, its quantitative importance has been reported by Flynn (1990), and is shown in Table 4.

Table 4: An amino acid utilization ranking for various marine algal species, including *E. huxleyi*. The ranking system is explained in the text; adapted from Flynn (1990).

Amino acid	Utilization	
	Quantitative rank	Qualitative rank
Aspartate	2	7
Glutamate	8	2
Asparagine	12	16
Serine	13	11
Glutamine	18	18
Histidine	6	1
Glycine	4	6
Threonine	10	17
Arginine	**20**	**15**
Taurine	1	3
Alanine	19	8
Tyrosine	3	10
Tryptophan	7	9
Methionine	16	14
Valine	11	5
Phenylalanine	5	13
Isoleucine	9	4
Leucine	14	12
Ornithine	17	20
Lysine	15	19

In his work Flynn added a mixture of 20 L-amino acids to N-deprived cultures of microalgae ranging from picoplankton to microplankton. Intracellular and extracellular amino acids (AAs) concentrations were analysed every 4 hours. The quantitative importance of use for each AA was computed by normalizing original data (100 = maximum use) for each species, and ranking sum across species for each amino acid; higher ranks indicate increasing quantitative importance (i.e., relatively more released/used). Qualitative importance has been computed by ranking amino acid data within species, summing across species for each amino acid and then ranking; higher ranks indicate increasing qualitative importance (i.e., likelihood of release/use).

As shown in Table 4, Flynn reported arginine to be as one of the quickest used by a "typical" population (Flynn, 1990), and was then selected for this experiment as the N-amino acid source.

Four algal species were cultured separately, in duplicate, with nitrate and arginine acting as the sole N source. The N concentration was adjusted to 100 μM in all cultures to enable comparison of growth rates.

3. Methodology

3.1. Chemicals

The reagents purchased for analyses and culture media are shown in Table 5 and were of analytical grade.

Table 5: reagents used for this study, including components of culture media and measurement of arginine concentrations.

CAS number	Chemical	Purity	Supplier
7647-01-0	Hydrochloric acid	Certified grade, 37 % solution in water	Acros Organics
74-79-3	L-Arginine·HCl	≥ 98 %	Sigma-Aldrich
74-79-3	Methanol, CHROMASOLV®, for HPLC	Reagent grade, ≥ 98 %	Sigma-Aldrich
127-09-3	Sodium acetate anhydrous	ReagentPlus®, ≥ 99.0 %	Sigma-Aldrich
643-79-8	*o*-Phthaldialdehyde	98 %	Alfa Aesar,
60-24-2	2-Mercaptoethanol	≥ 99.0 %	Sigma-Aldrich
64-69-7	Iodoacetic acid	≥ 98.0 %	Sigma-Aldrich
1303-96-4	Sodium tetraborate decahydrate	ReagentPlus®, ≥ 99.5 %	Sigma-Aldrich
1310-73-2	Sodium hydroxide solution	50% in H_2O	Sigma-Aldrich
109-99-9	Tetrahydrofuran CHROMASOLV® Plus	≥ 99.9%	Sigma-Aldrich
144-55-8	Sodium hydrogen Carbonate	≥ 99.7 %	Fisher Scientific UK Ltd
7447-40-7	Potassium chloride	99+ %	Acros Organics
7757-82-6	Sodium sulfate (anhydrous)	99+ %	Fisher Scientific UK Ltd
7758-02-3	Potassium bromide	≥ 99 %	Fisher Scientific UK Ltd
10043-35-3	Boric acid	99.8 %	Fisher Scientific UK Ltd
7791-18-6	Magnesium chloride hexahydrate	≥ 99% and ≤ 101%	Fisher Scientific UK Ltd

10035-04-8	Calcium chloride dihydrate	99+ %	Acros Organics
6381-92-6	Ethylenediaminetetraacetic acid disodium salt dihydrate	99+ %	Acros Organics
10026-24-1	Cobalt(II) sulfate heptahydrate	99+ %	Acros Organics
10101-68-5	Manganese(II) sulfate tetrahydrate	≥99 %	Fisher Scientific UK Ltd
10049-21-5	Sodium posphate, monobasic monohydrate	99+ %	Acros Organics
10025-70-4	Strontium chloride hexahydrate	99+ %	Acros Organics
7631-99-4	Sodium ntrate	≥ 99.0 %	Sigma-Aldrich
13517-24-3	Sodium metasilicate nonahydrate	≥ 98 %	Sigma-Aldrich
10102-40-6	Sodium molybdate dihydrate	≥ 99.0 %	Sigma-Aldrich
10025-77-1	Iron (III) chloride hexahydrate	≥ 99 %	Sigma-Aldrich
7446-20-0	Zinc sulfate heptahydrate	≥ 99. 0%	Sigma-Aldrich
67-03-8	Thiamine hydrochloride	≥ 99 %	Sigma-Aldrich
58-85-5	Biotin	≥ 99 %	Sigma-Aldrich
68-19-9	Vitamin B12	≥ 98 %	Sigma-Aldrich
7681-49-4	Sodium fluoride	≥ 99 %	Sigma-Aldrich
10025-70-4	Strontium chloride hexahydrate	99 %	Sigma-Aldrich
10049-21-5	Sodium phosphate monohydrate	≥ 98 %	Sigma-Aldrich
7791-20-0	Nickel (II) chloride hexahydrate	ReagentPlus®	Sigma-Aldrich

3.2. General laboratory preparartion

All glass- and plasticware was soaked in 2% Neutracon™ solution for at least 24 hours, rinsed (x 3) with high purity water (HPW; 18.2 MΩ cm^{-1}), soaked in 10 % hydrochloric acid for a further 24 hours, then rinsed again (x 3) with HPW. The cleaned items were stored in closed containers or within clean, plastic self-sealing bags.

GF/F filters were pre-combusted at 450 °C for 5 hours to remove residual organic matter.

3.3. Analysis of arginine

Arginine (ARG) concentrations in algal cultures were measured by reversed-phase HPLC with fluorimetric detection. ARG was derivatized, pre-column, with *o-phthaldialdehyde* (OPA) and *2-mercaptoethanol* (2-ME) as described in Tappin et al. (2007)

3.3.1. *Preparation of calibration solutions*

Two mobile phase solutions were used: (A) 100 % Methanol and (B) 0.05 M Sodium Acetate (NaAc) plus 5 % v/v Tetrahydrofuran (THF). The latter was prepared as follows: 2.05 g of NaAc was dissolved in 475 mL of HPW and 1.45 mL of 10 % v/v Acetic acid added to adjust the solution to pH 5.70. A 25 mL aliquot of THF was then added to this solution.

Standard solutions of ARG were prepared by dissolving its L-enantiomer, under sterile conditions, in both HPW and filtered-seawater (from coastal station L4 in the Western English Channel). Four calibration solutions of ARG were prepared according to its average, reported concentration in seawater (1 to 20 µM).

3.3.2. *Derivatisation*

The derivatization procedure required 3 reagents: 2-Iodoacetic acid (IAc), Disodium tetraborate (NaTB; $Na_2B_4O_7 \cdot 10H_20$) and OPA/2-ME which were prepared as follows:

I. <u>IAc (IAc in 0.1 M NaTB at pH 10.5):</u> a solution of 0.1 M disodium tetraborate (NaTB) at pH 10.5 was prepared by dissolving 0.95 g of NaTB in 26 mL of HPW, then adding 170 µL of 17.8 M sodium hydroxide (NaOH). Iodoacetic acid (IAc; 0.1487 g) was then dissolved in this solution. The pH was monitored using a portable CamLab Seven2Go™ S2 pH/mV meter.

II. <u>NaTB (0.1 M NaTB at pH 11.5):</u> 0.95 g of NaTB was dissolved in 26 mL of HPW and the pH adjusted to 11.5 through addition of 270 µL of NaOH (17.8 M).

III. OPA/2-ME: NaTB (0.95 g) was dissolved in 26 mL of HPW and 40 µL of NaOH added to reach pH 9.5. To 22.73 mL of this solution was added 123 mg of OPA; this reagent was dissolved with the addition of 2.27 mL MeOH.

Aliquots (1.25 mL) of the prepared OPA solution were stored at -20 ºC and used, along with 5 µL of 2-ME, as required.

To 200 µL of each ARG standard in plastic vials were added 20 µL of (I) and 150 µL of (II); the vials were then shaken and left to stand for 1 min. A 20 µL aliquot of OPA/2-ME solution was then added and the vial shaken and left to stand for 30-60 seconds. A 20 µL aliquot of this derivatized sample was then manually injected through a Rheodyne injection valve into a 50 µL injection loop using a 500 µL syringe prewashed with methanol.

3.3.3. *HPLC*

The HPLC system comprised 2 PU-1580 pumps (JASCO), a rheodyne injection valve connected to the analytical column Gemini-NX 5u C18 11A (Phenomenex), which was preceded by a guard column. The column was encased in an oven and connected to a FP-2020 Plus fluorescence detector (JASCO). Data were recorded using CHROMNav software. The temperature of the column was maintained at 40 ºC and a gradient elution programme was used (Table 6).

Table 6: Gradient elution program used for amino acid HPLC analysis

Time (min)	0	25	36	42	46	51
MeOH (%)	5	35	60	65	100	5
NH_4^+ $CH_3CO_2^-$ (0.05 M) + 5 % THF	95	65	40	35	0	95

Arginine was detected by fluorescence after pre-column derivatization with OPA and 2-ME in buffer solution. The fluorescent derivative was detected using excitation and

emission wavelengths of 332 and 457 nm, respectively (Tappin, Millward & Fitzsimons, 2007).

Mobile phase solutions were degassed by vacuum filtration through 0.2 µm nylon membranes every two days during analysis. In addition, a clean-up of the pump valves was performed using a syringe on each day of use, to remove any air bubbles from the HPLC system. A baseline check was made where mobile phase was passed through the column without sample.

The calibration range for ARG was 1 to 20 µM, and a blank of HPW or seawater, achieving linear calibration curves with R^2 of 0.9992 (Figure 7).

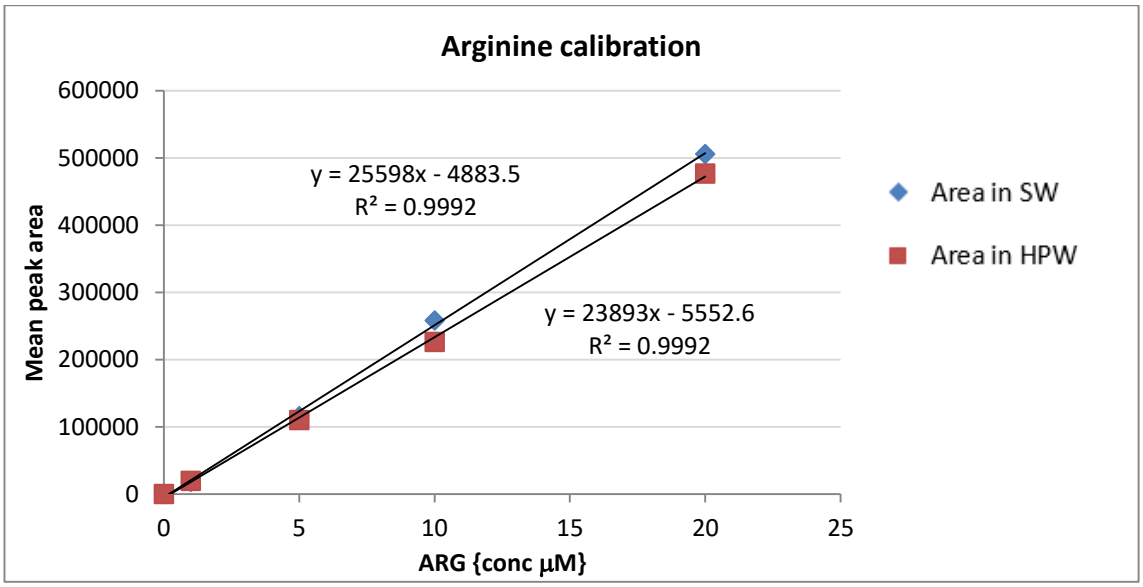

Figure 7: Calibration for L-Arginine measurements by HPLC. Linear regression revealed no significance difference between SW and HPW measurements (e.g. n = 3).

3.4. Phytoplankton batch cultures

Two kinds of algal cultures can be defined: 1) continuous cultures, where cultures are maintained at a chosen point on the growth curve by the regulated addition of fresh culture medium. In practice, a volume of fresh culture medium is added automatically at a rate proportional to the growth rate of the alga, while an equal volume of culture is removed.

2) Limited volume (*batch*) cultures. Here nutrient resources are finite. When the resources present in the culture medium are abundant, growth occurs according to a sigmoid curve, but once the resources have been exhausted, the cultures die unless the medium is partially replenished.

Batch cultures were chosen for this study as they were preferable for ease of manipulation and the volume of media required, while various manipulations were also possible.

Non-axenic batch monocultures of *Emiliania huxleyi* CCMP 1516 (Haptophyta, Cocolithophores), *Micromonas pusilla* RCC 834 (Chlorophyta), *Alexandrium minutum* RCC 1490 (Dinophyta) and *Chaetoceros peruvianus* RCC 2023 (Heterokontophyta, diatoms) were maintained in a Panasonic MLR-352 incubator at the Station Biologique de Roscoff. To ensure optimal growth conditions, irradiance was maintained at ~200 μE m^{-2} s^{-1}, via 3 installed Fluorescent lamps (40 W), with the temperature set at 20 ºC with 14 : 10 h light : dark photoperiod. Although the experimental temperature was 15 ºC, the first period of incubation was used as an acclimation to the new growth medium prepared for the experiment, as it varied from the one used to maintain the algae at the Roscoff Culture Collection. This acclimation period consisted of at least three generations of "sub-culturing" which was achieved by inoculation of a few cells from a culture batch into sterile ThermoFisher polystyrene 30mL culture flasks with filter cap, with new sterile medium at regular intervals.

For artificial medium experiments, polystyrene EasYFlasks of 25 mL growth area with filter cap were filled, up to 20 mL, with previously enriched media and spiked with exponentially growing cells. Incubations continued until the stationary phase was reached.

For Experiment V, cleaned 2 L Nalgene polycarbonate bottles containing growth medium were inoculated with a volume of exponentially growing stock culture (the actual volume was species-dependent) and incubated for 7-15 days depending on the desired cell density. Cell densities were calculated to avoid modification of the chemistry of the medium and,

by extension, the nutritional physiology of the algae. This was calculated both assuming an average reported biomass and using the actual measured biomass from biovolume (see refs per biovolume to µmol C cell^{-1} conversion) for each species, so that the bicarbonate (HCO_3^-) concentration in the medium did not vary by more than 10% of the initial concentration. The calculation is presented in Table 8 and assumes an average HCO_3^- concentration of 2.38 and 2.35 mM in Aquil* medium and natural seawater, respectively (Table 7).

Table 7: Carbonate concentration of both the artificial medium and natural SW, and percentage of C per liter not to be exceeded with phytoplankton biomass.
[a] Dyrssen & Wedborg (1974)

	$NaHCO_3$ (mM)	**10 % (g C L^{-1})**
Aquil*	2.38	0.0145
natural SW [a]	2.35	0.0143

Table 8: Target cell densities for each cultured species based on reference and measured biovolume values. The maximum number of cells achievable is highlighted and estimated from g C L^{-1} so as not to exceed a 10 % decrease in the carbonate concentration (see Table 7) of both the artificial medium and natural SW.

Species	**Measured max pg C cell^{-1}**	**g C L^{-1}**	**Reference max pg C cell^{-1}**	**g C L^{-1}**	**max cells mL^{-1}**	**Reference**
Chaetoceros sp	426	0.0469	112	0.0123	**110,000**	Kumar, M., et al. (2009)
E. huxleyi	23.84	0.0033	21.7	0.0030	**140,000**	Verity et al. (1992)
Alexandrium minutum	1,358	0.0095	2,000	0.0140	**7,000**	Flynn et al. (1996)
Micromonas pusilla	0.415	0.0021	2.36	0.0118	**5,000,000**	Graff et al. (2012)

As shown in Table 8 only *Chaetoceros* sp. exceeded the 10% threshold for measured values (in red) and is likely to change the carbonate concentration if reaching the concentration of 1 x 10^8 cell L^{-1}.

3.5. Preparation of culture medium

The experimental culture medium (CM) comprised a seawater `base' (natural or artificial), enriched with elements essential for growth (i.e. macronutrients, trace metals, chelators and vitamins). Different CM were tested and are listed in Table 9 below.

Table 9: culture media list and details

Culture medium	Recipe	Sterilization
0	modified k/2	SW heated to 100 °C Filtered nutrients stocks
1	ESAW	Autoclaved AW Autoclaved nutrients stocks
2	50% ESAW +50% k/2	
3	Aquil*	Autoclaved AW Autoclaved nutrients stocks
4	10% k/2 + 90% Aquil*	
5	Aquil*	SW heated to 100 °C Filtered nutrients stocks

3.5.1. Natural seawater culture medium

Natural seawater (SW) and Aquil* media were compared as culture media using the modified k/2 recipe.

3.5.1.1. Culture medium 0 – modified k/2

Aliquots of seawater were collected in 20 L carboys at the Astan sampling Station (3° 56' 15 W, 48° 46' 40 N) and aged in the dark for more than 5 months before use. Salinity was ~35, prior to filtration through 0.45 µm WHATMAN glass fibre membranes fitted with a prefilter (1.0 µm pore size) on the top, into polycarbonate bottles to reduce trace metal contamination and alteration of organic molecules inherent with autoclaving. Polycarbonate bottles were then placed in the autoclave and heated to 100 °C for 10 minutes and left for 24 hours under sterile conditions to ensure equilibration of gases (e.g.

CO_2). Although this heating process does not completely sterilize the seawater it kills all eukaryotes and most bacteria (Jutson, Pipe, & Tomas, 2016), and was used to avoid undesired changes in the chemistry of the water.

Concentrated nutrient stock solutions were sterile-filtered (0.2 µm) and added to the seawater to reach the final concentrations shown in Table 10.

Table 10: k/2 medium composition used in Exp. II and III. Trace metals and vitamin concentrations were based on k/2 recipe diluted half strength and modified by Ian Probert (Houdan, Probert, Zatylny, Véron, & Villard, 2006), http://roscoff-culture-collection.org/sites/default/files/MediaRecipesPDF/K2-Ian.pdf), while nutrients were adjusted for the experiment to match the Redfield ratio.

Component		Concentrations (M)
Nutrients	$N\text{-}NO_3^-$/N-Arg	$100 \cdot 10^{-6}$
	$NaH_2PO_4 \cdot 2H_2O$	$6.25 \cdot 10^{-6}$
	$NaSiO_3 \cdot 9H_2O$	$9.37 \cdot 10^{-5}$
Vitamins	Vitamin B_{12}	$1.48 \cdot 10^{-9}$
	Biotin	$4.09 \cdot 10^{-9}$
	Thiamine-HCl	$2.96 \cdot 10^{-7}$
Trace metals I	$Na_2EDTA \cdot 2H_2O$	$5.00 \cdot 10^{-5}$
	$CuSO_4 \cdot 5H_2O$	$5.00 \cdot 10^{-9}$
	$ZnSO_4 \cdot 7H_2O$	$3.90 \cdot 10^{-8}$
	$CoSO_4 \cdot 7H_2O$	$2.50 \cdot 10^{-8}$
	$MnCl_2 \cdot 4H_2O$	$0.45 \cdot 10^{-6}$
	$Na_2MoO_4 \cdot 2H_2O$	$1.50 \cdot 10^{-8}$
	H_2SeO_3	$5.00 \cdot 10^{-9}$
	$NiCl_2 \cdot 6H_2O$	$3.14 \cdot 10^{-9}$
Trace metals II	$Na_2EDTA \cdot 2H_2O$	$5.85 \cdot 10^{-6}$
	$FeCl_3 \cdot 6H_2O$	$5.85 \cdot 10^{-6}$

The final pH of the medium was checked and adjusted to ~8.2 by addition of sterile-filtered NaOH (0.2 M). A final filtration step through a 0.2 µm membrane was performed to maximise bacterial removal.

3.5.2. Artificial seawater culture medium

Artificial or synthetic seawater (AW) consists of "basal seawater" made by dissolving reagent grade salts into HPW and enrichment solutions. The major advantage of AW is

its being entirely defined from the chemical point of view, and that nutrient concentrations can be controlled.

In the present study AW recipes were tested for algal growth using two of the more successful artificial seawater media that have been developed, ESAW and Aquil* media.

3.5.2.1. Culture medium 1 – ESAW

ESAW is an enriched artificial seawater medium designed for coastal and open ocean phytoplankton; it was selected as it had been previously tested for some of the targeted species (Harrison et al., 1980; Santomauro, Sun, Brümmer, & Bill, 2016; Sutton, Varela, Brzezinski, & Beucher, 2013). The original recipe was modified by Berges *et al*. (2001) to include borate only in the salt solution (i.e. not in the trace metal stock), an inorganic phosphate in place of glycerophosphate, silicate stock solution prepared at half-strength without acidification to facilitate dissolution and three trace elements nickel, molybdenum and selenium. The iron is added, solely as chloride (to remove ammonium), from a separate stock with equimolar EDTA.

This recipe was used in Exp. I and II and prepared by dissolving "basal seawater" anhydrous salts and hydrated salts into separate solutions (Table 9). The two solutions were then sterilized in an autoclave at 120 °C for 20 minutes, left overnight for gas exchange and then aseptically combined. Enrichment solutions were also sterilized in an autoclave, and added to reach the final concentrations specified in Table 11. Vitamins and trace metals were added according to the original recipe, while nutrient concentrations were adjusted to study cultures with nitrogen limitation, closer to what is found in the seawater. Phosphate and silica were adjusted to achieve a Redfield ratio of C:Si:N:P = 106:15:16:1 (Brzezinski, 1985; Redfield, 1934).

Table 11: composition of ESAW medium used for Exp. I and II. Nutrient concentrations were adjusted for the experiment, while vitamins and trace metal amount were used according to the original recipe.

Component		Concentrations (M)
Salts (Anhydrous)	NaCl	$3.63 \cdot 10^{-1}$
	Na_2SO_4	$2.50 \cdot 10^{-2}$
	KCl	$8.03 \cdot 10^{-3}$
	$NaHCO_3$	$2.07 \cdot 10^{-3}$
	KBr	$7.25 \cdot 10^{-4}$
	H_3BO_3	$3.72 \cdot 10^{-4}$
	NaF	$6.67 \cdot 10^{-5}$
Salts (Hydrated)	$MgCl_2 \cdot 6H_2O$	$4.71 \cdot 10^{-2}$
	$CaCl_2 \cdot 2H_2O$	$9.14 \cdot 10^{-3}$
	$SrCl_2 \cdot 6H_2O$	$8.18 \cdot 10^{-5}$
Nutrients	$NaNO_3$	$100 \cdot 10^{-6}$
	$NaH_2PO_4 \cdot 2H_2O$	$6.25 \cdot 10^{-6}$
	$NaSiO_3 \cdot 9H_2O$	$9.37 \cdot 10^{-5}$
Vitamins	Vitamin B_{12}	$1.48 \cdot 10^{-9}$
	Biotin	$4.09 \cdot 10^{-9}$
	Thiamine-HCl	$2.96 \cdot 10^{-7}$
Trace metals I	$Na_2EDTA \cdot 2H_2O$	$8.30 \cdot 10^{-6}$
	$ZnSO_4 \cdot 7H_2O$	$2.54 \cdot 10^{-7}$
	$CoSO_4 \cdot 7H_2O$	$5.69 \cdot 10^{-8}$
	$MnSO_4 \cdot 4H_2O$	$2.42 \cdot 10^{-6}$
	$Na_2MoO_4 \cdot 2H_2O$	$6.12 \cdot 10^{-9}$
	Na_2SeO_3	$1.00 \cdot 10^{-9}$
	$NiCl_2 \cdot 6H_2O$	$6.27 \cdot 10^{-9}$
Trace metals II	$Na_2EDTA \cdot 2H_2O$	$6.56 \cdot 10^{-6}$
	$FeCl_3 \cdot 6H_2O$	$6.55 \cdot 10^{-6}$

This final medium was also sterile-filtered (0.2 μm) prior to addition of cell inocula.

The salinity of the prepared medium was 35 and the pH was 8.2 ±0.08.

In Exp. II the CM 1 (ESAW) was mixed with CM 0 (k/2) in order to help algal growth with the addition of natural SW contained in the latter. This third medium will be called CM 2 hereafter.

3.5.2.2. Culture medium 3 – Aquil*

The second synthetic seawater tested was Aquil*, a more recent version of the original Aquil* medium (Morel et al., 1979; Price et al., 1989), modifications to which are discussed by Sunda *et al*. (2005). Two additional modifications were made to this method: 1) the stock solutions, for the Aquil* culturing media, were prepared according to Price *et al*. (1979), and 2) the solutions were not chelexed, as trace metal analysis was not part

of this study. “Basal seawater” was prepared by dissolving salts into separate solutions (Table 10).

Table 12: Composition of Aquil* “basal seawater used for Exp. III

Component		Concentrations (M)
Salts (Anhydrous)	NaCl	$4.20 \cdot 10^{-1}$
	Na_2SO_4	$2.88 \cdot 10^{-2}$
	KCl	$9.39 \cdot 10^{-3}$
	$NaHCO_3$	$2.38 \cdot 10^{-3}$
	KBr	$8.40 \cdot 10^{-4}$
	H_3BO_3	$4.85 \cdot 10^{-5}$
	NaF	$7.15 \cdot 10^{-5}$
Salts (Hydrated)	$MgCl_2 \cdot 6H_2O$	$5.46 \cdot 10^{-2}$
	$CaCl_2 \cdot 2H_2O$	$1.05 \cdot 10^{-2}$
	$SrCl_2 \cdot 6H_2O$	$6.38 \cdot 10^{-5}$
Nutrients	$NaNO_3$	$100 \cdot 10^{-6}$
	$NaH_2PO_4 \cdot 2H_2O$	$6.25 \cdot 10^{-6}$
	$NaSiO_3 \cdot 9H_2O$	$9.37 \cdot 10^{-5}$
Vitamins	Vitamin B_{12}	$1.48 \cdot 10^{-9}$
	Biotin	$4.09 \cdot 10^{-9}$
	Thiamine-HCl	$2.96 \cdot 10^{-7}$
Trace metals I	$Na_2EDTA \cdot 2H_2O$	$5.00 \cdot 10^{-6}$
	$ZnSO_4 \cdot 7H_2O$	$4.00 \cdot 10^{-9}$
	$CoSO_4 \cdot 7H_2O$	$2.50 \cdot 10^{-9}$
	$MnSO_4 \cdot 4H_2O$	$2.30 \cdot 10^{-8}$
	$Na_2MoO_4 \cdot 2H_2O$	$1.00 \cdot 10^{-7}$
	Na_2SeO_3	$1.00 \cdot 10^{-8}$
	$NiCl_2 \cdot 6H_2O$	$3.14 \cdot 10^{-9}$
Trace metals II	$Na_2EDTA \cdot 2H_2O$	$5.00 \cdot 10^{-6}$
	$FeCl_3 \cdot 6H_2O$	$4.51 \cdot 10^{-7}$

Sterilization and enrichments were performed as described for ESAW. In Exp. III algae were inoculated both into Aquil* (CM3) and a mixed medium composed of 10 % natural seawater and 90% synthetic seawater based on the Aquil* recipe, and called CM4 hereafter. This was done to boost algal growth by adding a small amount of natural seawater which may contain important chemicals lacking in the synthetic one, without adding significant N.

The salinity of the prepared medium was 35 (measured with an optic refractometer) and at the pH was 8.2 ±0.06.

3.6. Antibiotic treatment – bacterial removal

In order to investigate if phytoplankton species could directly take up organic nitrogen, axenic cultures were prepared. To remove bacteria from cultures, algal cells were first gently washed by vacuum filtration to remove part of the bacterial biomass and then different antibiotic mixtures were applied.

Treatment with different percentages of antibiotic solution was carried out for 24 or 48 hours, whereupon a very small number of cells were sub-cultured in fresh sterile medium. This new culture was left to grow for at least 3 days verifying a good cell status, post-treatment, with an inverted microscope. The presence of bacteria was monitored using a BD Accuri™ C6 Cytometer equipped with a blue and a red laser, 2 light scatter detectors, and 4 fluorescence detectors with optical filters optimized for the detection of fluorochromes. In order to discriminate heterotrophic bacteria from autotrophs, samples were firstly fixed with 0.1 % glutaraldehyde (final concentration) and stained with the blue-light-excited nucleic acid dye SYBR Green I (SBR I) which is normally added to a final concentration of $1x10^{-4}$ of the commercial solution. Samples were left staining for 15 minutes and analysed for 1 minute with a flow rate of ~65 µL min^{-1} and setting a threshold of 1000 events on DNA side scatter.

Further antibiotic inoculations were made following the steps detailed above, to achieve the lowest possible concentration of bacteria.

3.6.1. Antibiotic treatment of microphytoplankton – *A. minutum* anc *C. Peruvianus*

Alexandrium minutum and *C. peruvianus* cells obtained from the culture collection were left to grow dense (> 1,000 cell mL^{-1}) in the original CM 0 (k/2 + Si only for *C. peruvianus*) before starting the treatment.

Both cells species were gravity-filtered with nylon membranes of 11 µm pore size, previously UV sterilised, and resuspended into sterile fresh medium under aseptic conditions; this partially removes bacteria to ensure that their biomass is not too high for the antibiotic mixture to be effective. Cells were then treated using a method based on Droop (1967) and adapted according to Guillard (2005), but using a modern antibiotic mix suggested by S. Slocombe (SAMS - Scottish Association for Marine Science, UK, *pers. comm*.).

The antibiotic mixture was prepared by dissolving a number of antibiotics (Melford Laboratories Ltd.) into HPW, to the following final concentrations:

- Cefotaxime (500 mg L^{-1})
- Carbenicillin (500 mg L^{-1})
- Kanamycin (200 mg L^{-1})
- Augmentin™ – Amoxicillin sodium salt/Potassium clavulanate (200 mg L^{-1})

The final antibiotic solution was filter-sterilised and stored frozen for less than one month at -20 °C until use. A sterile 24-well plate was then used to inoculate 2 mL of medium and a dilution series of antibiotic solution as shown in Table 11.

Table 13: Dilution series for antibiotic treatment of *A. minutum* and *C. peruvianus*

Well	**1**	**2**	**3**	**4**	**5**	**6**
Medium (k/2)	2 mL	2 mL	2 mL	2 mL	2 mL	2 mL
Antibiotic mix	0 (0%)	10 µL (0.5%)	20 µL (1%)	100 µL (5%)	150 µL (7.5%)	200 µL (10%)
Algal culture	200 µL	200 µL	200 µL	200 µL	200 µL	200 µL

Plates were then incubated at optimum growth temperature and light in a culture cabinet. A daily check under optic microscope was made to ensure algal resistance to the antibiotic. If algae were observed to be growing every 72 hours, a drop was placed into a sterile flask with fresh medium and checked for bacteria by flow cytometry as previously described.

3.6.2. Antibiotic treatment of nano- and picophytoplankton – *E. huxleyi* and *M. pusilla*

Emiliania huxleyi and *M. pusilla* cells obtained from the culture collection were left to grow dense in the original CM 0 (k/2 medium) before starting the treatment. *E. huxleyi* was gravity filtered using UV-sterilised 3 µm polycarbonate membranes, taking care not to leave cells dry for long. The cells were resuspended into sterile fresh medium under aseptic conditions. *M. pusilla* was not filtered due to its small cell size.

In addition to the antibiotic method for microphytoplankton, described above, another antibiotic was tested for both picoplankton species. A Penicillin-Streptomycin-Neomycin (PNS) Antibiotic Mixture was used following Cottrel and Suttle (1993) with modifications; there was no addition of sucrose prior to antibiotic treatment, as bacteria seemed to be already actively growing, and antibiotics were added as a mixture solution and not singularly in series. A sterile 24-well plate was used to inoculate 2 mL of medium and two different concentrations of PNS (Table 12).

Table 14: dilution series for PNS treatment of *E. huxleyi* and *M. pusilla*

Well	**1**	**2**	**3**
Medium (k/2)	2mL	2mL	2mL
Antibiotic mix	0 (0%)	10µL (0.5%)	20µL (1%)
Algal culture	200µL	200µL	200µL

Plates were incubated at optimum growth temperature and light in a culture cabinet. A daily check under optic microscope was made to ensure algae resistance to the antibiotic. If algae were seen to be growing every 72 hours, then a drop was placed into a sterile flask with fresh medium and checked for bacteria using flow cytometry as previously described.

3.7. Determination of algal growth

In *batch* cultures algal growth usually follows a sigmoid curve which consists of four stages (Figure 8):

- *Lag* phase; during which cells adapts to the new environment, there is no increase in cells' number. Its duration is variable, depending on the size of the inoculum and on the physiological conditions of cells.
- *Exponential* phase; in which there is a rapid cell growth in a logarithmic pattern, represented by the curve portion with higher slope.
- *Stationary* phase; growth rate decreases, as a result of nutrient depletion. The number of cells remains almost constant and the phase may last a few weeks.
- *Decline* phase; at this stage the nutrients are almost exhausted, and the cells begin to die, they lyse, and their total number decreases progressively.

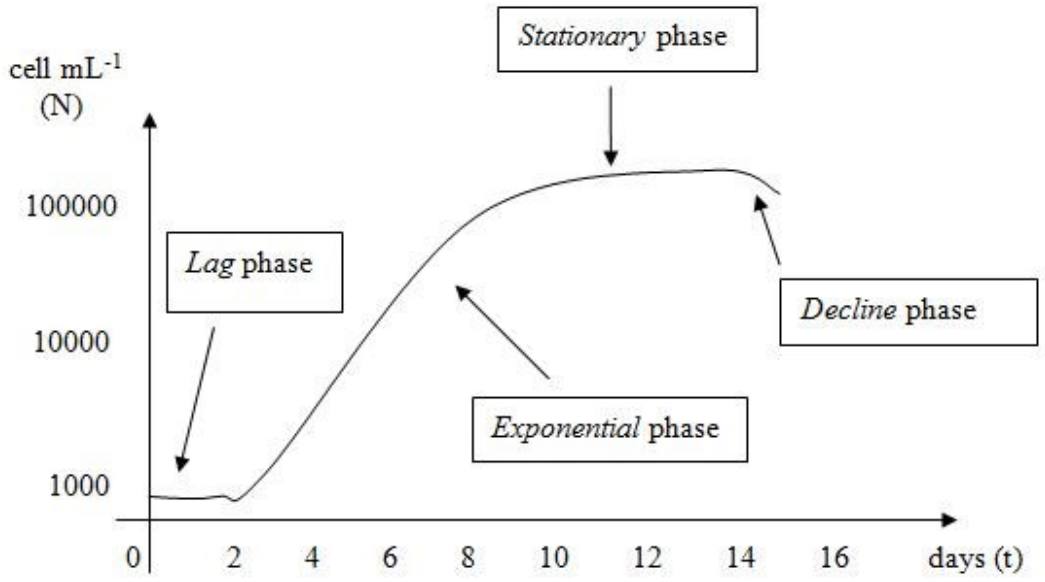

Figure 8: Algal growth curve expected under *batch* conditions

The estimation of population increase, μ, was calculated according to Equation 1.

$$\mu = \frac{ln(N_2 - N_1)}{t_2 - t_1} \qquad (1)$$

Where N represents cells mL^{-1} and t represents the time interval (usually days).

Approximately every two days, cultures were gently but well-mixed and both bacteria and algae enumerated to create growth curves.

3.7.1. *Cell counting with light microscope*

The aim was to tally all of the cells in a known volume of the cultured material when they were settled into one plane. When immobilization was necessary, two or three drops of Lugol's iodine solution were added to facilitate observation. Large phytoplankton species, like *A. minutum* and *C. peruvianus*, were counted under a light microscope, Nikon Eclipse e100, using a glass Segwick-Rafter Counting slide. The chamber was rectangular (50 x 20 mm), divided into 1000 squares of 1 µL each and 1 mm depth, giving a total volume of 1.0 mL (Figure 9). It was suitable for species above 10 µm.

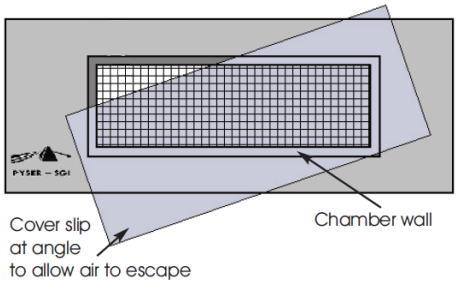

Figure 9: An example of a Sedgewick-Rafter Counting slide. The cover glass must be placed diagonally and the chamber filled in the left open space with 1 mL of sample. The cover glass slides into position to seal the chamber.

For densities higher than 10^4 cells mL^{-1}, cells in a sufficient number of squares were counted, and the average number of cells in the chamber was calculated using Equation 2.

$$Cells\ mL^{-1} = \frac{N \cdot 1000}{n} \qquad (2)$$

Where N represents the total number of counted cells and *n* the number of squared observed.

3.7.2. *Enumerating cells by flow cytometry*

Light microscope counting was not possible for the picoplankton species *E. huxleyi* and *M. pusilla*, due to size constraints so their growth was followed using flow cytometry. This technique allowed the measurement of specific features of cells that flow within a liquid mean, called a *sheath.* Each cell individually met a light source which was shed (*scattered*), obtaining information on size, shape and internal structure. Moreover if cells possessed primary (e.g. chlorophyll *a* or phycoerythrin) or secondary fluorochromes (e.g. stained DNA with SYBR I), the excitation spectrum of which were consistent with light source wavelength, they shed fluorescence which indicated quantity of fluorochromes. Combining scatter and fluorescence data it was possible to discriminate between phytoplankton groups and estimate the number of selected type of cells (Fig. 10) passed through the sheath at a known flow rate (~65 µL min^{-1}).

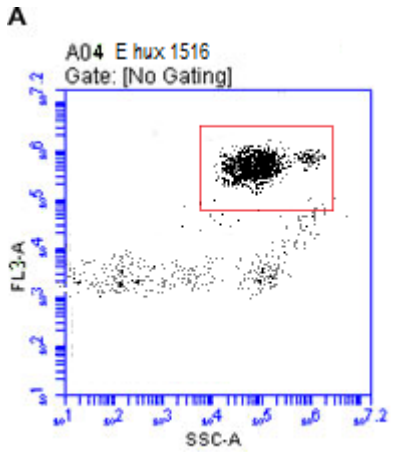

Figure 10: *E. huxleyi* (within the red box) enumeration plot example, defined by Chlorophyll *a* fluorescence (FL3-A) and side scatter (SSC-A). Other dots representing debris and prokaryotes.

The enumeration of cells was performed using a BD Accuri™ C6 Cytometer set for Chl *a* fluorescence side scatter, on in vivo samples analysed with the same settings as per bacteria enumeration (see section 3.6).

3.8. Nutrients and biomass quantification

3.8.1. *Dissolved inorganic nutrients*

In order to assess whether uptake of the main macronutrients occurred under different growth conditions, concentrations of dissolved inorganic nitrate, phosphate and silica were measured at the beginning and end of the final set of culture experiments. A budget for total nitrogen was also calculated using DON concentrations obtained from culture medium sampling at the same time as cell collection.

For Experiment V, 100 mL of each culture were sampled on Day 0 and the final day for measurement of inorganic nutrients, filtered on pre-combusted WHATMAN GF/F glass fiber filters, and stored in previously cleaned sampling bottles at -20 °C until analysis.

The analysis was performed at the Station Biologique de Roscoff (SBR), within 2 months of collection, and followed the national protocol within the SOMLIT (SOMLIT Service d'Observation en Milieu LITtoral) framework used by the CNRS based on Aminot and Kérouel (2004), employing an auto-analyser AXFLOW SEAL AA3 AAHR. The automated determination of nitrate and nitrite was based on the cadmium reduction method. The concentration range was 0-200 µM, or 0-1000 µM with automatic dilution, and the detection limit was 0.05 µM. The determination of phosphate was performed at 820 nm with a linear range from 0-50 µM and a detection limit of 0.003-0.006 µM.

Silica measurements were made within a linear range from 0-200 µM and a detection limit of 0.05 µM.

Ammonium measurements were made only on the day of cell collection, by sampling and filtering the same amount of culture and following the protocol of Koroleff (1969). The assay was based on the Berthelot reaction (1859). In an alkaline medium (pH 8-11.5), dissolved ammonia reacts with hypochlorite to form monochloramine. This compound, forms indophenol blue in the presence of phenol and an oxidizing medium. At 20 °C, the

reaction catalyzed by the nitroprusside ion then developed within 6 hours. The absorption of the coloured complex was measured at 630 nm.

3.8.2. *Biovolume estimation*

The most commonly used traditional biomass estimate for microalgae is cell biovolume, which is calculated from microscopically measured linear dimensions. Calculating phytoplankton carbon from biovolume, rather than from particulate organic carbon, eliminates the error due to detrital particulate matter contained in particulate organic carbon (Mullin, Sloan, & Eppley, 1966). A set of geometric shapes and mathematical equations for calculating algal biovolume of more than 850 pelagic and benthic marine and freshwater microalgal genera was reported by Hillebrand *et al*. (1999).

The calculation of the total biovolume of phytoplankton in a sample requires knowledge of the abundance of the species and an average volume of individual cells. The shape of individual taxa is approximated to that of a solid or a composition of solids, for which it is possible to identify volume formulae. The measures necessary to calculate the volume of the cells were obtained under upright Nikon Eclipse N*i* microscope with SPOT imaging software.

3.8.3. *Particulate organic carbon and nitrogen analysis*

Particulate organic carbon (POC) and nitrogen (PON) concentration measurements allowed quantification of the particulate organic material, which represents the total living matter or that originating from living matter. Furthermore, the POC : PON and POC : chlorophyll *a* ratios are used to characterize the quality (origin, composition, age or age of degradation) of the particulate organic matter. POC and PON were determined by combustion of particulate material recovered by filtration. The combustion of organic material produces volatile oxides, CO_2, CO (in case of incomplete combustion) and NOx, which were then converted into CO_2 and N_2. These compounds were separated by gas chromatography and quantified by Thermal Conductivity Detector detection (TCD). The

main analytical biases were related to material degradation (in particular with wet atmosphere or during homogenisation with water) and contamination by the particulate material (e.g. dust), dissolved or even volatile (ammonia, ammonium chloride), as well as inorganic carbon. In order to minimise biases, the glass apparatus used in the filtration and storage of filters acid-washed then combusted in a muffle furnace for 4 h at 450 °C. Subsamples for Particulate Total Carbon (PTC) and POC PON were taken in replicate. For each culture at the end of the last experiment, 100 to 200 mL (depending on the density) were filtered for POC and PTC collection, using WHATMAN GF/F glass fibre filters of 25mm diameter, and applying a pressure < 15 mm Hg to promote filtration while avoiding disruption of cells and release of material. Filters were then put into pill boxes (slightly opened) and dried overnight in an oven at 55 °C, then stored closed in a desiccator until analyses. In order to discriminate between particulate organic and inorganic carbon, which might be consistent for coccolithophores for example, a decarbonation step was necessary. Samples for POC measurement were acid-treated by placing fuming HCl in the dessicator with the pill boxes opened, and left for about 4 hours under vacuum.

For the analyses all filters were folded with flat ended forceps and placed into a FlashEA® 1112 Organic Elemental Analyzer with autosampler at SBR. Nicotinamide was used as a standard and results were corrected with blank values, where only seawater medium was filtered.

3.9. Chlorophyll *a*

Chlorophyll *a* (Chl *a*) is indicative of phytoplankton biomass in the marine environment; it constitutes 1-2% of the organic matter dry weight of algae. The content of organic matter can also be estimated from Chl *a* using conversion factors. The POC : Chl *a* ratio varies between species, depending on the different physiological and environmental conditions; in marine environments this ratio is in the range 23-79. Sometimes a

significant fraction of autotrophic pigments, in deep oceanic or highly trophic waters, are represented by degradation products of chlorophyll, resulting from senescent cells, debris and faecal material, and they are generically termed "pheopigments" (Pheo *a*).

Both Chl *a* and Pheo were detected by fluorescence, following Strickland and Parsons (1972), and based on the property that chlorophyll pigments emit red fluorescence when excited by blue or ultraviolet light. The fluorimeter must be equipped with a blue lamp, a blue excitation filter (420 - 450 nm) and a red emission filter (> 665 nm). The fluorescence of the sample was measured before and after acidification to take into account accessories pigments and pheopigments. Concentrations of Chl *a* were expressed in $\mu g\ L^{-1}$, and the required analytical accuracy is +/- 15 %.

For Experiment V 50 - 150 mL (depending on the density) were collected for each culture at the end of the growth cycle, using Whatman GF / F filters and applying pressure not exceeding 15 mm Hg. Filters were folded, wrapped in aluminium foil and stored at -20 °C until analyses.

Chl *a* was extracted into a 90 % acetone solution and acidified with HCl (0.3 M), both of which were prepared using reagent grade solutions and HPW. Each filter was folded into a centrifuge tube and 5 mL of 90 % acetone added before the mixture was ground thoroughly with a glass rod. Tubes were placed overnight in a refrigerator (4 °C), in a rack covered with foil to protect samples from light shock. The samples were subsequently centrifuged for 5 min at 3000 rpm to complete the extraction from the filter, and the supernatant transferred to a measuring tube and analysed with a Turner Designs 10-AU fluorometer calibrated with 1 mg Chl *a* from *Anacystis nidulans* (ref C-6144 Sigma-Aldrich). This first reading corresponded to F_0, then 20 µL of 0.3 HCl mL^{-1} of acetone extract was added. When the signal was stable (1-5 min after the addition of acid) the fluorescence F_a was measured.

The Chl *a* and pheophytin *a* (Pheo *a*) concentrations were calculated according to Holm-Hansen *et al*. (1965) as shown in Equations 3 and 4, respectively.

$$Chl\ a\ =\ K_x \cdot \left(\frac{F_0}{F_a}\right)_{max} \cdot \left(\frac{(F_0 - F_a)}{\left(\frac{F_0}{F_a}\right)_{max} - 1}\right) \cdot \left(\frac{V_{ext}}{V_{filt}}\right) \quad (3)$$

Where K_x= fluorimetric calibration constant; F_0=fluorescence before acidification; F_a=fluorescence after acidification; V_{ext}= volume of acetone extract [L]; V_{filt}= volume of sample filtered [L]; $(F_o/F_a)_{max}$= acidification ratio of pure Chl *a* for the specific instrument.

$$Pheo\ a\ =\ K_x \cdot \frac{\left(\frac{F_0}{F_a}\right)_{max}}{\left(\frac{F_0}{F_a}\right)_{max} - 1} \cdot \left(\frac{F_0}{F_a}\right)_{max} \cdot (F_0 - F_a) \cdot \left(\frac{V_{ext}}{V_{filt}}\right) \quad (4)$$

Where K_x= fluorimetric calibration constant; F_0=fluorescence before acidification; F_a=fluorescence after acidification; V_{ext}= volume of acetone extract [L]; V_{filt}= volume of sample filtered [L]; $(F_o/F_a)_{max}$= acidification ratio of pure Chl *a* for the specific instrument.

4. Results

4.1. Phytoplankton growth in artificial medium

In Exp. I aliquots of the RCC algal strains (*E. huxleyi*, *Synechococcus* sp, *C. peruvianus* and *A. minutum*) were inoculated in CM 1 (ESAW) prepared with autoclaved ESAW artificial water enriched with autoclaved nutrients stock solution. The 14 days of growth was monitored using flow cytometry for all the species to test feasibility, with the cyanobacterium *Synechococcus* sp. RCC 744 initially chosen for the experiment and tested in place of *M. pusilla* (Figure 11).

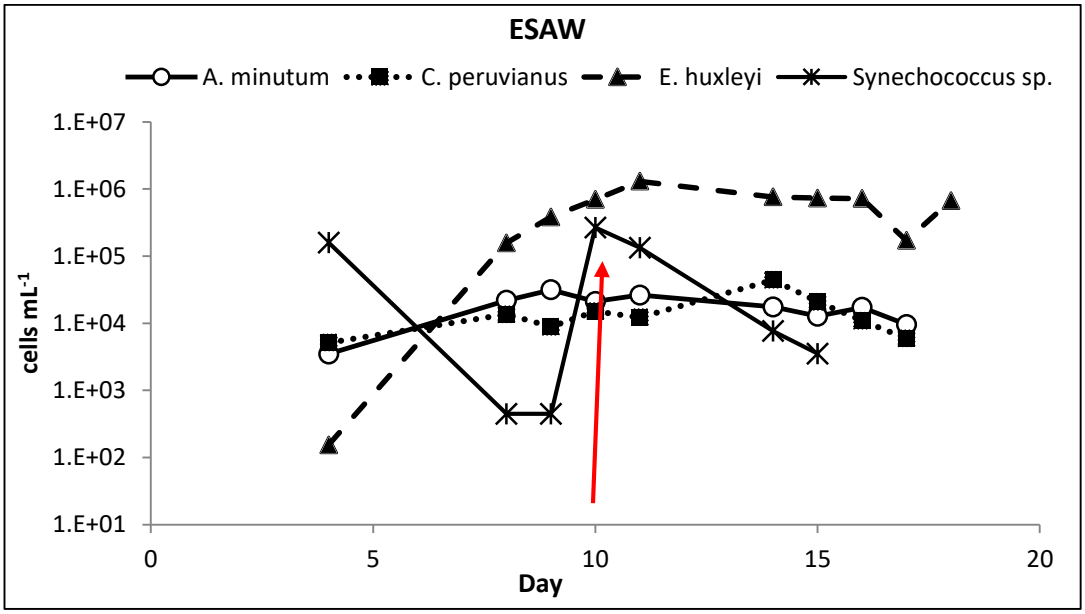

Figure 11: ESAW growth test using selected algal species. Red arrow indicating the second inoculum for *Synechococcus sp.*

Although *E. huxleyi* grew best in the medium, the flow cytometry and microscopy observation revealed two different populations; some cells were coccolith-bearing while others were naked, indications that growth conditions were not optimised for this strain. A second inoculum of *Synechococcus* sp was made on day 10 to test a possible recovery, but the species biomass continued to decline. *Synechococcus* sp was subsequently replaced by *M. pusilla*. Both *C. peruvianus* and *A. minutum* did not show significant

growth, which may have been related to the flow cytometry technique not being a reliable counting method for heavy diatoms that do not easily remain in suspension, or large motile dinoflagellates. When inspected under a microscope, *A. minutum* cells were deformed compared with those in the original RCC culture, but appeared to be actively swimming; *C. peruvianus* produced auxospores, which is usually an indication of cellular stress.

In Exp. II cell growth was compared using CM 0 (k/2), CM 1 (ESAW) and the mixed medium CM 2 (1 : 1 k/2 : ESAW), as culture media. Cell enumeration was performed by light microscope for *C. peruvianus* and *A. minutum*, and by flow cytometry for *M. pusilla* and *E. huxleyi*.

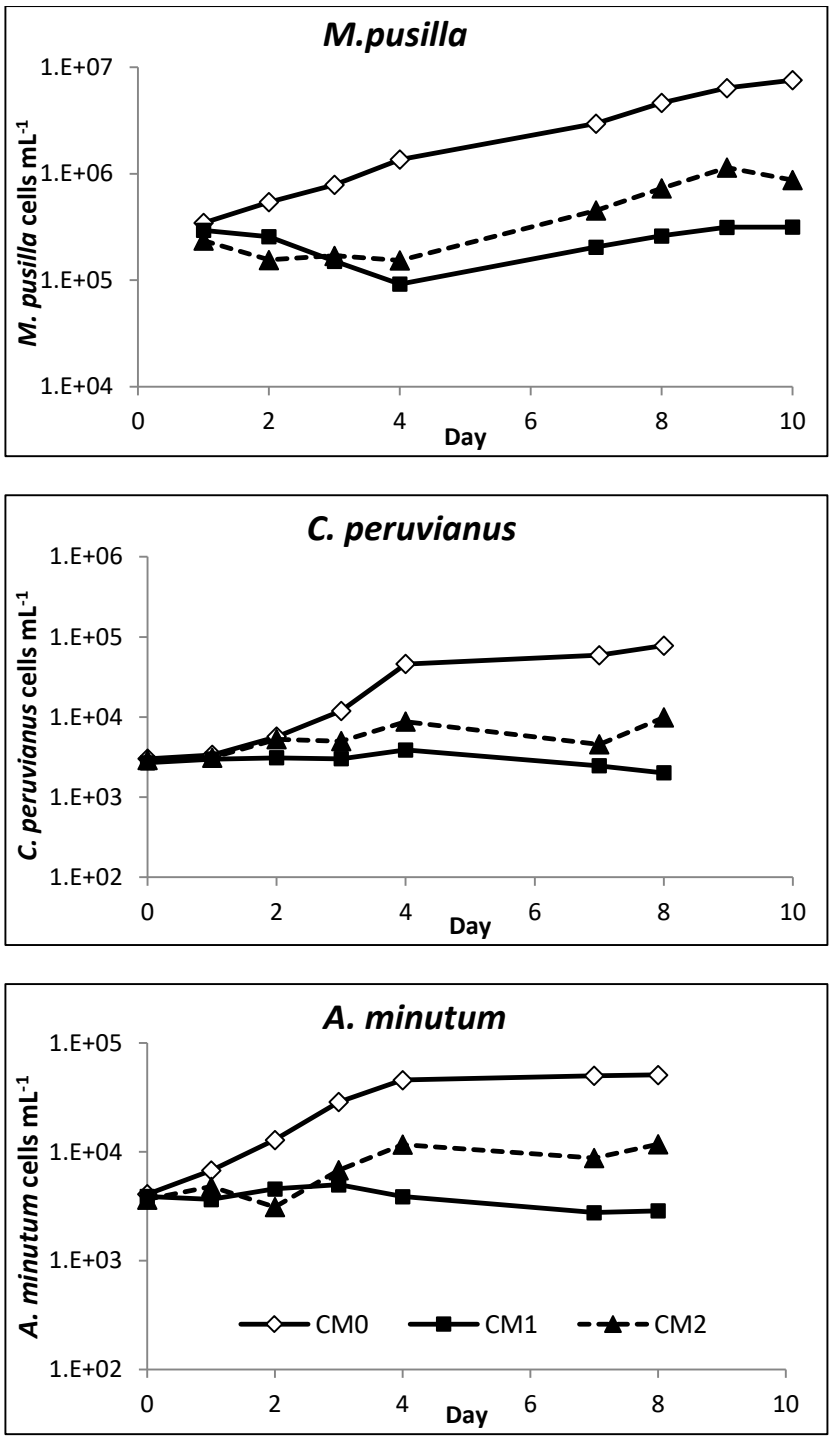

Figure 12: growth comparison of monoalgal strains in a number of culture media.

The ESAW (CM1) medium appeared to inhibit the growth of all species as indicated in Figure 12. Where k/2 was added to ESAW (CM2), growth was enhanced for all strains, although an exponential phase was apparent only for *M. pusilla*, which overall had a low growth rate (Table 15) with respect to reported values for the species, which were 0.32 and 0.72 day $^{-1}$, respectively (Maat, Crawfurd, Timmermans, & Brussaard, 2014), most

likely because the initial inoculum has already reached steady-state (more than 10^5 cells·mL $^{-1}$).

Table 15: Growth rate (day^{-1}) estimations for Experiment 2. These were calculated only where possible according to Equation 1.

Medium	*M. pusilla*	*A. minutum*	*C. peruvianus*
CM0 (k/2)	0.35	0.73	0.87
CM1 (ESAW)	0.27		
CM2 (k/2+ESAW)	0.40	0.66	

As indicated in Table 13, *C. peruvianus* did not grow in the artificial medium (CM1 and CM2), but the growth rates for both *M. pusilla* and *A. minutum* were comparable in k/2 and the mixed medium CM2.

For experiment II it was also possible to choose from among a large number of available *E. huxleyi* strains (Figure 13). *E. huxleyi* RCC 911 and RCC 1220 strains were isolated in the Pacific Ocean and have been widely used for culture studies; RCC 1268 was isolated in the English Channel and was chosen as characteristic of the ecosystem of interest; CCMP 1516 was the first coccolithophore reference genome to be sequenced and was chosen for its inability to form flagellated cells.

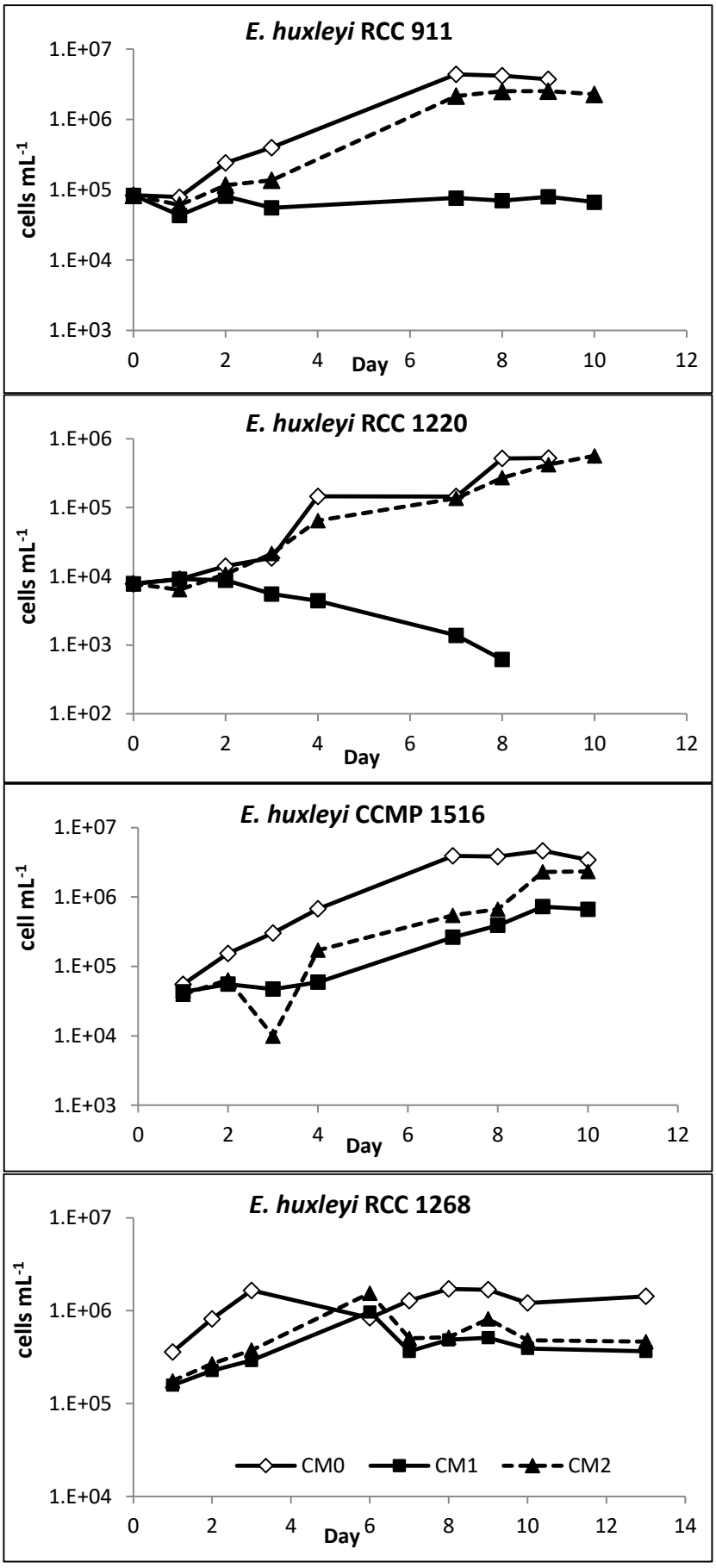

Figure 13: Growth comparison of *E. huxleyi* strains monoalgal cultures with different tested media.

Growth of all *E. huxleyi* strains tested was inhibited in ESAW medium, with lower growth rates also observed in the mixed medium compared to that based on natural SW CM 0 (Table 16); CCMP 1516 gave the best growth, though with a lower abundance compared to CM 0.

Table 16: growth rates of *E. huxleyi* strains tested in CM0, CM1 and the mixed media CM2 (see Appendix for details). Calculation of growth rate was not possible in all cases.

	CM0 (k/2)	**CM1 (ESAW)**	**CM2 (k/2+ESAW)**
CCMP 1516	0.71	0.50	0.52
RCC 1268	0.76	0.36	0.43
RCC 1220	0.46		0.54
RCC 911	0.67		0.69

RCC 911 and RCC 1220 exhibited similar growth in CM0 and CM2, but light microscope observations revealed a majority of non-coccolith forming cells for these strains (Figure 14A). The RCC 1268 culture was almost totally comprised of flagellate haploids cells, indicating that possible stressors were occurring. *E. huxleyi* CCMP 1516 was chosen for subsequent experiments as the growth rate of 0.5 day^{-1} was comparable to reported values (Daniels, Sheward, & Poulton, 2014) and cells were coccolith–forming (Figure 14B).

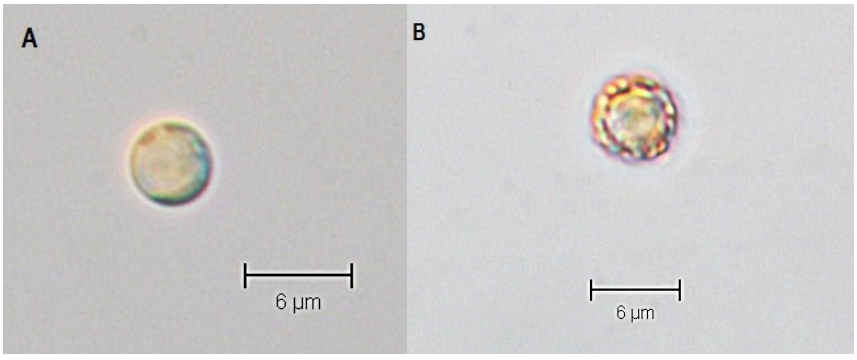

Figure 14: *E. huxleyi* A) RCC 1220 strain with no coccoliths and B) CCMP 1516 strain surrounded by coccoliths, cultured with CM1.

For Exp. III Aquil* recipe was tested; cells growing in the mixed CM2 (k/2+ESAW) were spiked in CM3 (Aquil*) and in the mixed CM4 (10% k/2 + 90% Aquil*). Growth was monitored by light microscopy for *A. minutum* and *C. peruvianus*, and by flow cytometry for *M. pusilla* and *E. huxleyi* (Figure 15).

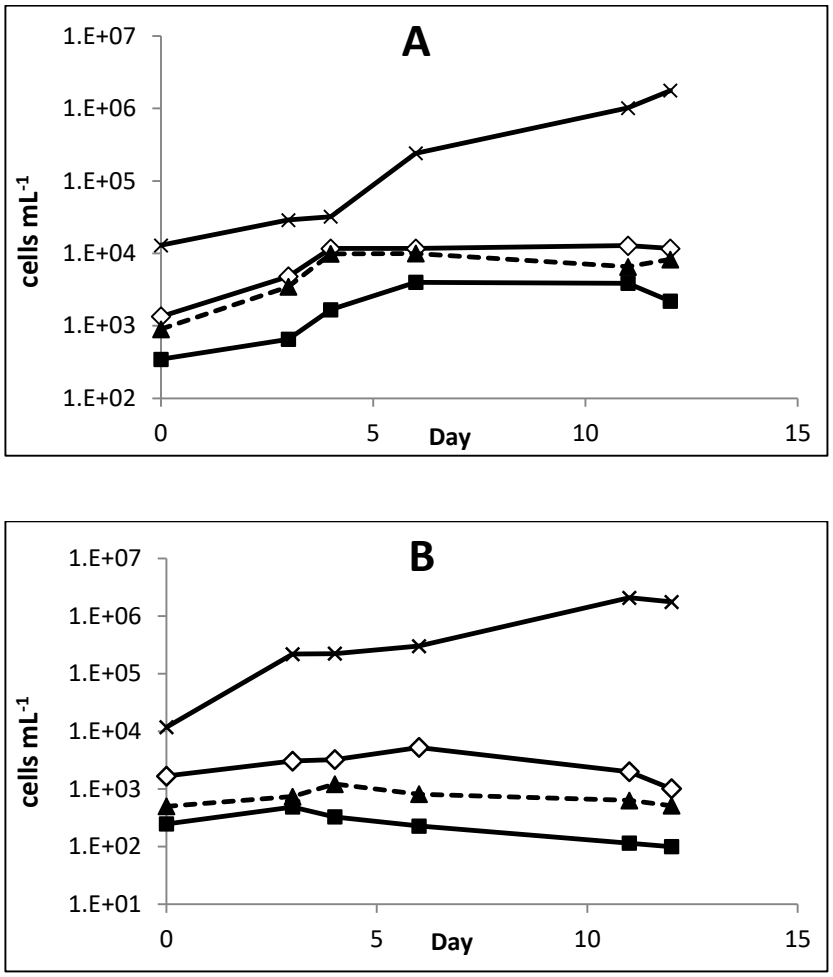

Figure 15: Growth comparison of monoalgal cultures in A) CM3 (Aquil*) B) CM4 (10% k/2, 90% Aquil*); ×, *M. pusilla*; ◊, *A. minutum*; ▲, *E. huxleyi* CCMP 1516; ■, *C. peruvianus*.

Growth in the CM 3 medium was comparable to the CM 0 for *M. pusilla*, though the rate was lower than the minimum mean value for the species (Table 17).

All the other cultivated species were able to grow if 10 % of CM 0 was added to the mixture, although rates were all lower than in the k/2 medium.

Table 17: growth rates comparison of selected species between mixed CM4, CM3 and CM0.

Medium	*A. minutum*	*C. peruvianus*	*E. huxleyi 1516*	*M. pusilla*
CM 0 (k/2)	0.73	0.87	0.71	0.35
CM 3 (Aquil*)				0.26
CM 4 (10% k/2 + 90% Aquil*)	0.54	0.60	0.60	0.50

With both the ESAW and Aquil* recipes, cells of the dinoflagellate, *A. minutum*, were deformed and *C. peruvianus* was producing auxospores (Fig. 16). These physiological effects were thought most likely due to the absence of one or more elements in the water. As a result, natural seawater was used for subsequent experiments.

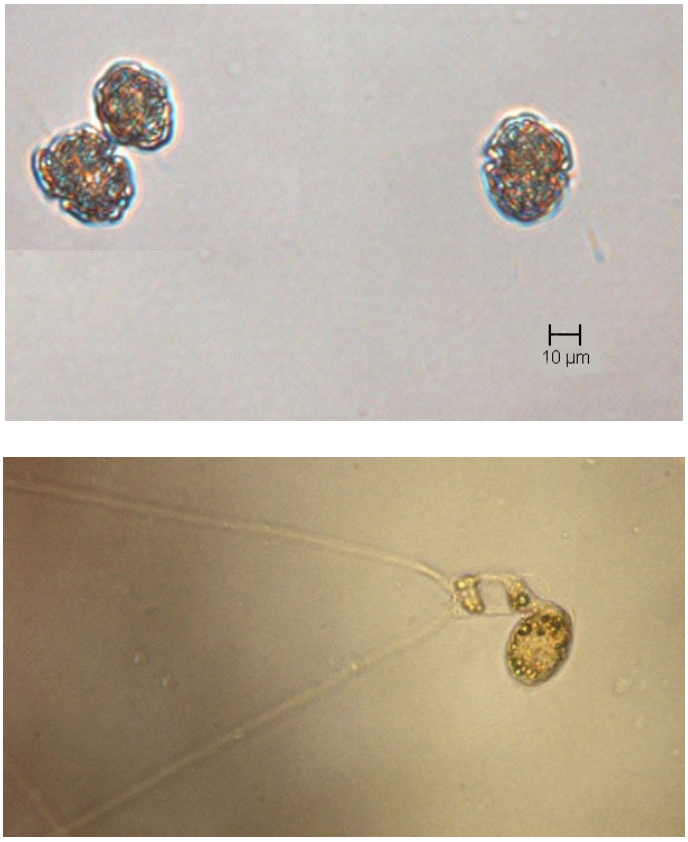

Figure 16: deformation of *A. minutum* and auxosporilation of *C. peruvianus* cultured with artificial media.

4.2. Axenic culturing

All species were treated with antibiotic for more than a month to remove bacteria; micro-phytoplankton experiments were of shorter duration as pre-filtration steps largely removed significant bacterial biomass compared to smaller species, like *E. huxleyi*, as prokaryotes can live attached to coccoliths, or *M. pusilla* which is not much bigger than bacteria.

None of the strains was sensitive to specific antibiotic or concentration treatments, although *M. pusilla* cells were not actively moving when incubated with PNS antibiotic, even if growing. As shown in Figure 17, with both antibiotic mixtures neither higher (Figure 17A) nor lower (Figure 17B) concentrations were completely effective to, and no particular sensitivity was apparent for higher concentrations.

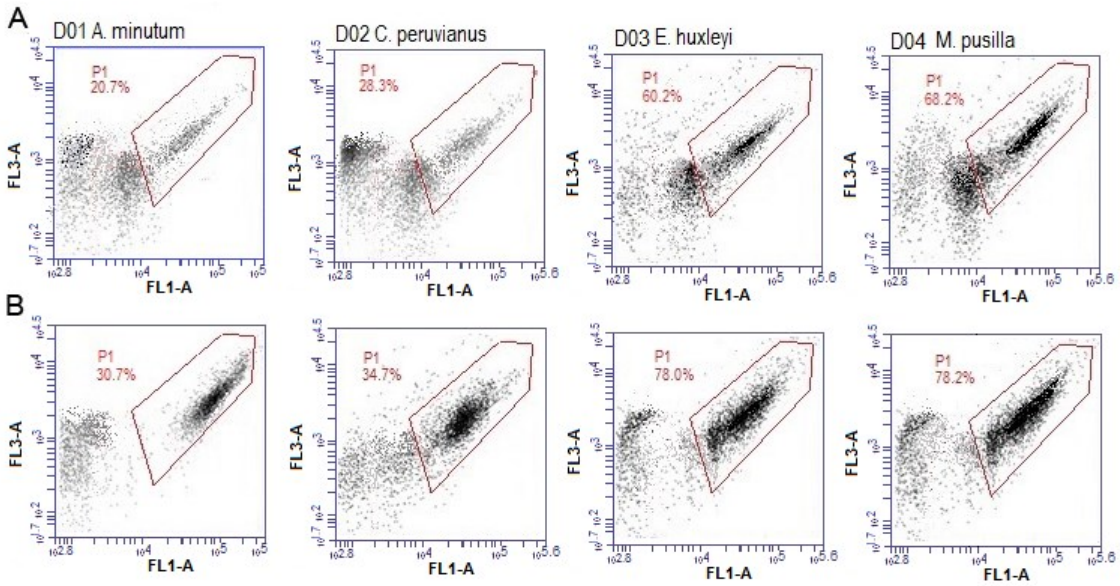

Figure 17: Flow cytometric distributions of bacterial cells during antibiotic treatment with: A) higher concentration; 7.5 % for *A. minutum* and *C. peruvianus*, and 1 % for *E. huxleyi* and *M. pusilla* and B) lower concentration of antibiotic; 5 % for *A. minutum* and *C. peruvianus*, and 0.5 % for *E. huxleyi* and *M. pusilla* concentrations for four phytoplankton species. Samples were stained with SYBR® Green I and visualized on FL3-A vs FL1-A density plots on the BD Accuri C6. A standard gate (P1) was applied to each sample to exclude debris and background.

Higher bacterial removal was achieved in microphytoplankton samples using the 7.5 % concentration of antibiotic solution in antibiotic incubation lasting 24 hours and with 72 hours of recovery between each antibiotic addition (n = 5).

For picophytoplankton species the highest bacterial removal was achieved using the 1 % concentration of PNS antibiotic solution in n = 6 antibiotic incubation lasting 24 hours and with 72 hours of recovery in fresh medium between each antibiotic addition.

As shown in Figure 18, higher concentrations of antibiotics removed most of the bacterial cells.

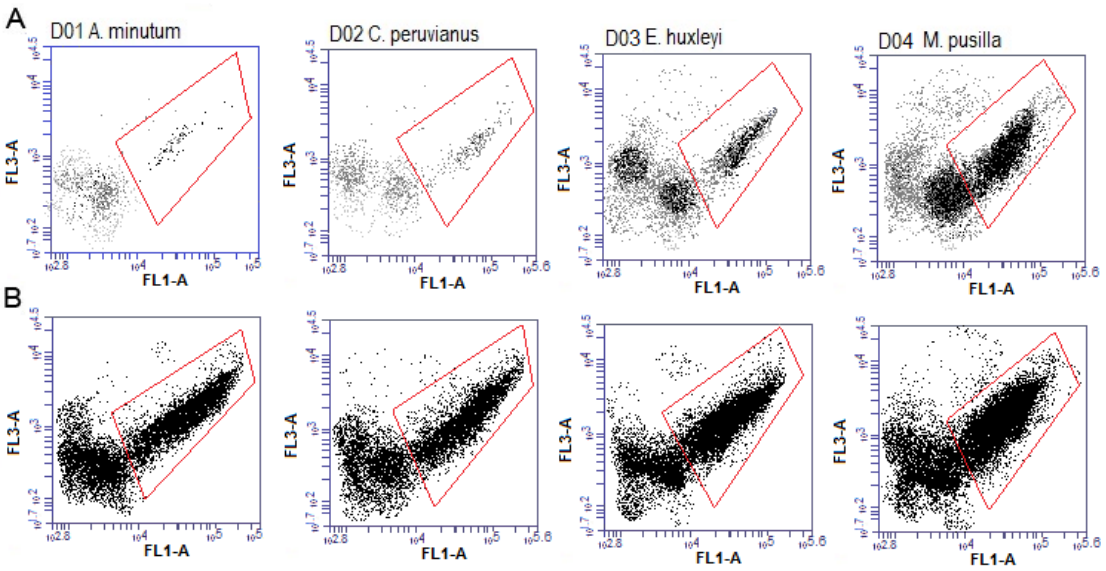

Figure 18: flow cytometric distributions of bacterial cells during antibiotic treatment with A) higher antibiotic concentrations; 7.5% for *A. minutum* and *C. peruvianus*, and 1 % for *E. huxleyi* and *M. pusilla* and B) control cultures with no antibiotic added and sub-cultured in the same way as the treated ones. Samples were stained with SYBR® Green I and visualized on FL3-A vs FL1-A density plots on the BD Accuri C6. A standard gate (P1) was applied to each sample to exclude debris and background.

The generation times of the treated cultures and the controls were not significantly different ($P > 0.005$, ANOVA) in the 2 weeks following the treatment. Direct observation by epifluorescence microscopy indicated that bacteria were absent only in *A. minutum*, while *C. peruvianus* still contained a few bacteria cells and *E. huxleyi* and *M. pusilla* were not axenic and required further treatment.

4.3. Phytoplankton growth comparison with ARG or NO_3^- as sole N source

4.3.1. *Emiliania huxleyi*

The selected *E. huxleyi* strain (CCMP 1516) was grown in duplicate cultures containing NO_3^-, denominated afterword as NO_3^- cultures, and with arginine, denominated as ARG cultures, as the sole N-source, for a period of 7 days. Incubations were stopped as soon as the targeted maximum cell density was reached (< 140,000 cell mL^{-1}). As demonstrated in Figure 19, *E. huxleyi* growth was rapid and continuous throughout the incubation period with no differences between N sources and each culture reaching a similar abundance yield.

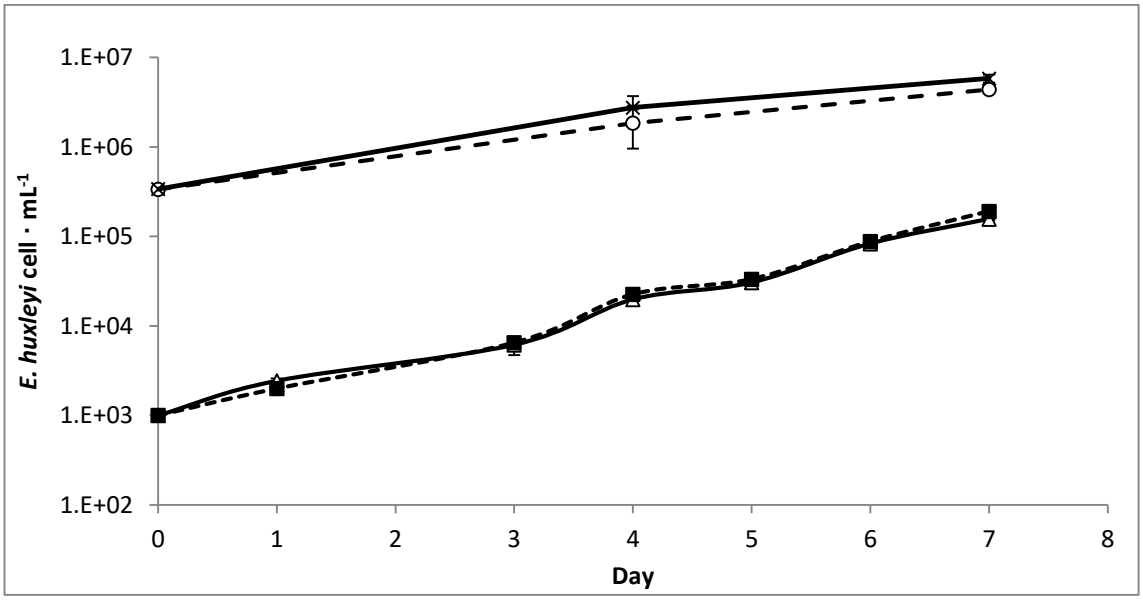

Figure 19: growth of *E. huxleyi* cultures containing NO_3^- (Δ) and Arg (■), and bacteria enumeration. with NO_3^- (○) and ARG (×). Note that the data points represent the average of duplicate samples counted in triplicate (n=6).

The percentage of bacterial biomass was estimated as an average of 20 fg C $cell^{-1}$ (Lee & Fuhrman, 1987), and was quantified on harvesting day as constituting 5.24 % of the total estimated organic C. Growth parameters (Table 18) with both N sources were within the reported range for cultured *E. huxleyi* (Daniels, Sheward & Poulton, 2014), but overall

revealed a slightly faster growth rate within the ARG cultures, although not significantly different to NO_3^- cultures.

Table 18: *E. huxleyi* and bacteria growth parameters; μ = growth rate, t_d = doubling time, k = number of divisions per day. Calculations were based on Andersen (2005).

	NO_3^- cultures		**ARG cultures**	
	E. huxleyi	**bacteria**	***E. huxleyi***	**bacteria**
μ	0.706	0.393	0.757	0.526
t_d	0.982	1.763	0.916	1.317
k	1.018	0.567	1.092	0.758

It can be also noted how growth rates of bacteria and *E. huxleyi* diverge less within the ARG cultures.

Concentrations of NO_3^- and ARG were quantified on day 0 and on harvesting day, while NH_4^+ was measured only at the end of the experiment.

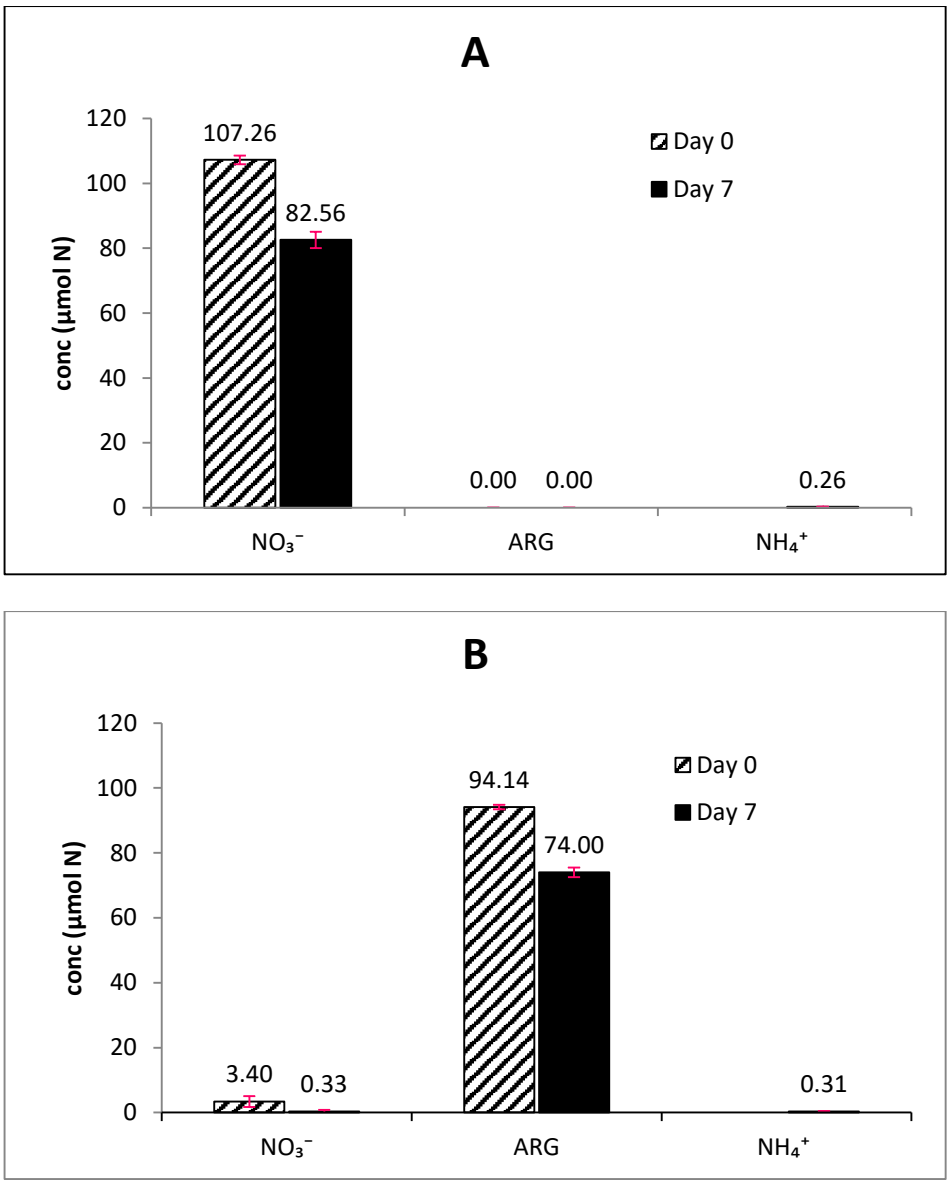

Figure 20: Concentrations of dissolved nutrients measured on Days 0 and 7 of in cultures of *E. huxleyi* containing A) NO_3^- and B) ARG as the sole nitrogen source. NO_3^- and ARG were analysed at the beginning and end of the incubation, while NH_4^+ was quantified on last day only. Values represent the average of duplicate samples counted in duplicate (n=4).

As shown in Figure 20A, cultures containing NO_3^- as the N-source consumed 23.3 % of the nitrate during the incubation. A small amount of NH_4^+ was measured on day 7, probably due to bacterial conversion of NO_3^-. The ARG cultures (Figure 20B) contained low NO_3^- concentrations, probably originating from the residual SW concentration, although aged, and was almost entirely consumed by the end of the experiment. Total N consumption was 23.2 µM of N in ARG cultures, 86.7% of which was accounted for by

ARG uptake, and 24.7 µM of N in NO_3^- cultures. In ARG cultures, concentrations of NH_4^+ on Day 7 were similar to the NO_3^- cultures.

For both cultures, consumption of the supplied N source was approximately 20 %, reflected in similar *E. huxleyi* abundance and growth, and indicating that ARG was the main source of N taken up in the ARG cultures. The initial, small concentration of NO_3^- in ARG cultures may have been assimilated by algal cells but could not account for the reported cell N-content (Daniels, Sheward & Poulton, 2014), based on the number of cells measured on Day 7 (Table 19).

Table 19: N-NO_3^- demand estimation for *E. huxleyi* cultures enriched with ARG. The theoretical density is calculated by adding the density of the culture on Day 0.

NO_3^- [µmol L^{-1}] on Day 0	3.401
N quota [µmol $cell^{-1}$]	1.00×10^{-7}
Final density (cells L^{-1})	1.90×10^{8}
Theoretical density per NO_3^- [µmol L^{-1}] on Day 0	3.50×10^{7}

As shown in Table 19, the theoretical *E. huxleyi* density, calculated from the density at Day 0, if uptake was based only on the initial NO_3^- [µmol L^{-1}] concentration, would have been no more than 3.5×10^7 cells L^{-1}, while the actual measured density was more than five times higher (1.9×10^8 cells L^{-1}), indicating that *E. huxleyi* must have used ARG for growth. The same evaluation was possible for the ARG demand (Table 20), according to the reported mean N and C quota for *E. huxleyi* (Daniels, Sheward & Poulton, 2014) and bacteria (Hoch, Fogel, & Kirchman, 1992).

Table 20: ARG demand estimation for *E. huxleyi* cultures enriched with Arg. Calculation were made based on reference N and C quota and using the total density difference between the final day and day 0 of the experiment ($\Delta n = n_{end} - n_{start}$).

		Bacteria	*E. huxleyi*
ARG consumed	µmol N L^{-1}	20.1	
	µmol C L^{-1}	30.2	
Theoretical cellular quota	µmol N	1.00 $x10^{-8}$	1.00 $x10^{-7}$
	µmol C	1.67 $x10^{-9}$	9.19 $x10^{-7}$
ARG uptake	µmol N L^{-1}	54.9	18.9
	µmol C L^{-1}	9.15	174.5
Total ARG demand	µmol N L^{-1}	73.8	
	µmol C L^{-1}	183.6	
Theoretical density per N-ARG consumed	cells L^{-1}	2.01 $x10^{9}$	2.01 $x10^{8}$
Density on last day	cells L^{-1}	5.83 $x10^{9}$	1.91 $x10^{8}$

Stated the consumed ARG concentration of 20.1 µmol N L^{-1} and that the reference cellular N quota is 1 $x10^{-8}$ and 1 $x10^{-7}$ µmol $cell^{-1}$ for bacteria and *E. huxleyi* respectively, we would expect a theoretical final density of 2.01 x 10^{9} and 2.01 x 10^{8} cell L^{-1} of bacteria and *E. huxleyi* respectively. Experimentally we obtained a comparable abundance for *E. huxleyi* while doubled abundance of bacteria compare to the theoretical estimate. Furthermore, based on the theoretical N and C quota we found a greater relative reliance on N-ARG by bacteria and a greater C-ARG uptake by *E. huxleyi*. The total ARG demand estimated is higher for both N and C than the actual ARG consumed, indicating a possible further uptake of IN by *E. huxleyi* converted by bacteria, and a greater C supply from ARG which could be resulted in C respiration. It was not possible then to infer if *E. huxleyi* grew solely by direct uptake of ARG or through uptake of NH_4^+ after bacterial mineralisation of ARG, also demonstrated by the large difference between the ARG consumption measured (20 µmol N L^{-1}) and that estimated from N quotas and density difference between end and start of the experiment (73.8 µmol N L^{-1}).

In order to constrain the N budget of the cultures, organic N and C analyses were performed at the end of the incubations to obtain cellular N and C quotas (Table 21).

Table 21: PON and POC quantified on harvesting day and related to biomass estimation by biovolume.

E. huxleyi	**NO_3^-**	**ARG**
PON [µmol N $cell^{-1}$]	7.99×10^{-8}	7.12×10^{-8}
POC [µmol C $cell^{-1}$]	4.0×10^{-3}	3.6×10^{-3}
C : N ratio (atomic)	6.21	6.25
Biovolume [µmol C $cell^{-1}$]	1.0×10^{-6}	9.2×10^{-7}
% algal biomass on last day	95.6	94.7
% bacterial biomass on last day	4.4	5.2

Both POC and PON were slightly higher in NO_3^- cultures, as was C : N ratio, although not significantly. Since the standard elemental stoichiometry is generally assumed to be 106 C: 16 N: 1 P (Redfield 1958), cells in good nutritional status should have a C : N ratio close to 6.6, similar to what found in both NO_3^- and ARG *E. huxleyi* cultures of this experiment, indicating that bot N sources were at optimal concentrations. An estimation of cell C content, using biovolume data, was made using the theoretical equation reported for protist plankton (Menden-Deuer and Lessard, 2000), resulting in a consistently higher C per cell content, indicating a possible loss of OC during filtration of cultures and CHN measurement. The percentage of algal biomass, based on biovolume data, resulted predominant above bacteria.

Chlorophyll *a* was analysed by fluorescence at the end of the experiment. The ARG cultures contained Chl *a* concentrations around 0.096 pg $cell^{-1}$, and this was 0.156 pg $cell^{-1}$ in NO_3^- cultures. Although values were not significantly different ($P > 0.005$, ANOVA), they seemed to reflect a lower energy requirement derived from photosynthesis in cells incubated with ARG as the sole N source. This is probably due to the fact that amino acids are directly incorporated in proteins, requiring less energy (Antia, Harrison and Oliveira, 1991).

4.3.2. *Micromonas pusilla*

M. pusilla was incubated in duplicate under identical conditions to *E. huxleyi*, for a period of 15 days. For NO_3^- cultures, the incubations were stopped once the targeted maximum cell density (< 5,000,000 cell mL^{-1}) had been reached, as pH variation of 0.5 – 0.8 units around the ideal value of 8.2 was measured, probably due to the high cell density. ARG cultures were at pH 8.2 ± 0.08 throughout. As shown in Figure 21, *M. pusilla* growth was rapid and continuous throughout the incubation period for both NO_3^- and ARG cultures, although the latter had a lower yield and growth rate.

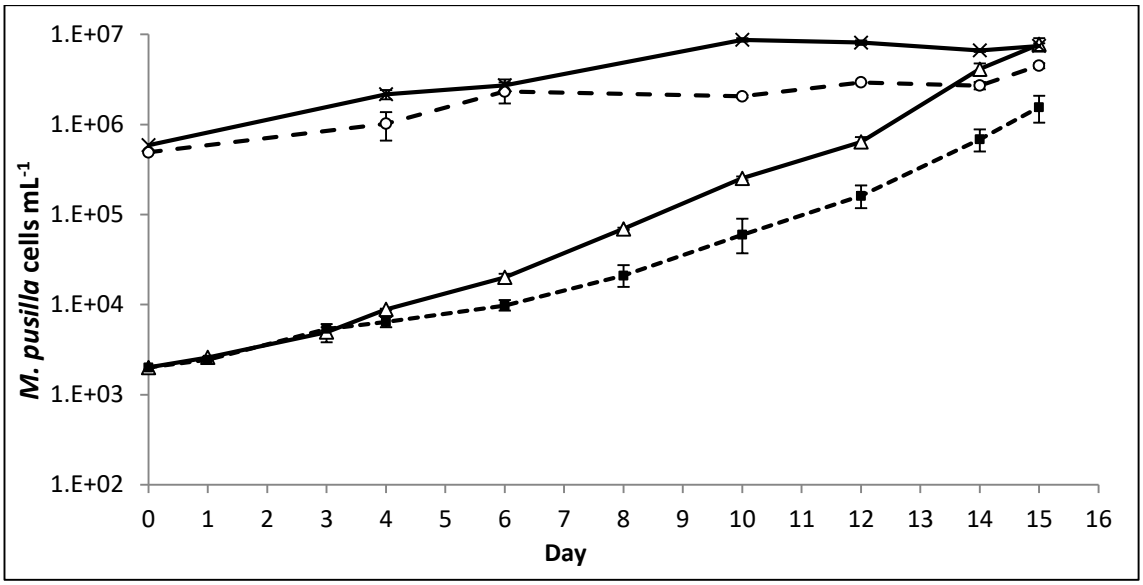

Figure 21. Growth of *M. pusilla* in cultures containing NO_3^- (Δ) and ARG (■), and bacterial enumeration: NO_3^- (○) and ARG (×). The data points represent the average of duplicate samples counted in triplicate (n=6).

M. pusilla grew most rapidly and achieved the highest yield on NO_3^-, but also grew on ARG. *M. pusilla* growth rates were lower, overall, than reported in culture studies, considering mean values of 0.72 ± 0.08 day^{-1} (Maat *et al.*, 2014). Bacterial abundance was high during the entire experiment and in ARG cultures was estimated to decrease from 82 to 18 % of the total estimated organic C on Days 10 and 14, respectively.

Although all growth parameters confirmed slower growth when *M. pusilla* was cultured with ARG only (Table 22), the cultures did show a consistent increase in abundance. The difference between bacterial and *Micromonas* growth is much more evident with NO_3^- cultures, with a divergence of 0.7 day^{-1} divisions per day in NO_3^- cultures and only 0.34 day^{-1} divisions per day in ARG cultures. This divergence is clearly more evident than what observed for *E. huxleyi*, revealing a more similar growth behaviour between bacteria and *M. pusilla*.

Table 22: *M. pusilla* and bacteria growth parameters; μ - growth rate, t_d = doubling time, k = number of divisions per day. For calculation details see Andersen (2005).

	NO_3^- cultures		**ARG cultures**	
	M. pusilla	**bacteria**	***M. pusilla***	**bacteria**
μ	0.66	0.183	0.558	0.325
t_d	1.048	3.785	1.241	2.135
k	0.954	0.264	0.80	0.468

Nutrients consumption is presented in Figures 22; total N consumption was higher in ARG cultures with 95.3 μmoles of N taken up against 71.6 in NO_3^- cultures. This was also related to the higher density of *M. pusilla* reached in the former cultures (7 x 10^9 cells L^{-1} compared with 1.5 x 10^9 cells L^{-1} in ARG cultures), where in addition a higher NH_4^+ concentration, with respect to NO_3^- cultures and *E. huxleyi* experiments, was also measured on Day 14.

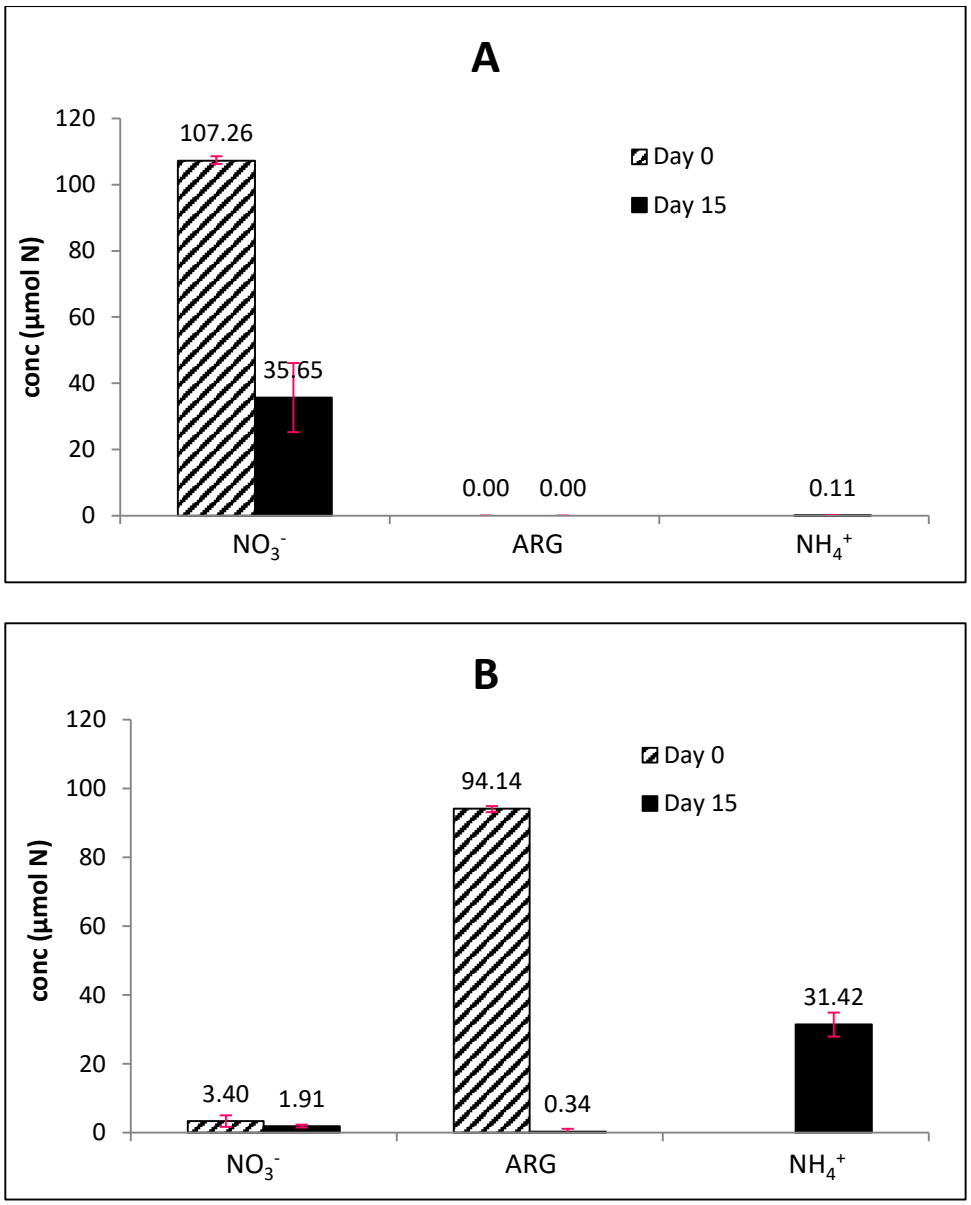

Figure 22: Dissolved nutrient concentrations on day 0 and 14 of *M. pusilla* incubations with A) NO_3^- and B) ARG. NO_3^- and ARG were analysed at the beginning and end of the incubation, while NH_4^+ was quantified on last day only. Values represent the average of duplicate samples counted in duplicate (n=4).

When cultured with NO_3^- *M. pusilla* took up less N (71.6 µmoles of N) but reached a higher density. On the contrary when incubated with ARG the uptake of N was consistently higher (95.3 µmoles of N) but with a smaller final abundance (1.5 x 10^9 cells L^{-1} compared with 7 x 10^9 cells L^{-1} in NO_3^- cultures). Moreover ARG cultures presented a higher concentration of both bacteria (7.4 x 10^9 cells L^{-1} compared with 4.5 x 10^9 cells L^{-1} in NO_3^- cultures), and NH_4^+ indicating a possible larger uptake requirement due to the bacterial population.

As discussed for *E. huxleyi*, it was possible to exclude a sole subsistence of *M. pusilla* on NO_3^- within the ARG cultures, based on the initial trace concentration of the former (Table 23), according to the reported N quota for this species (Maat *et al.*, 2014).

Table 23: N- NO_3^- demand estimation for *M. pusilla* cultures enriched with ARG. The theoretical density is calculated by adding the density of the culture on Day 0.

NO_3^- [µmol N L^{-1}] on Day 0	3.401
N quota [µmol $cell^{-1}$]	1.48 x 10^{-8}
Final density (cells L^{-1})	1.55 x10^9
Theoretical density per NO_3^- [µmol L^{-1}] on Day 0	2.31 x10^8

The number of *M. pusilla* cells obtained (1.5 x10^9 cell L^{-1}) was considerably higher (2.31 x10^8) than the theoretical density estimated from the cellular N quota and the NO_3^- concentration on Day 0, indicating that growth of *M. pusilla* was not based only on the initial NO_3^- concentration. A similar evaluation was performed for ARG concentration, based on the reported N quota for *M. pusilla* (Maat *et al.*, 2014) and bacteria (Hoch et al., 1992) (Table 24).

Table 24: ARG demand estimation for *M. pusilla* cultures enriched with ARG. Calculation were made based on reference N and C quota and using the total density difference between the final day and day 0 of the experiment ($\Delta n = n_{end} - n_{start}$).

		Bacteria	*M. pusilla*
ARG consumed	µmol N L^{-1}	93.8	
	µmol C L^{-1}	140.7	
Theoretical cellular quota	µmol N	1.00 x10^{-8}	1.48 x10^{-6}
	µmol C	1.67 x10^{-9}	3.83 x10^{-8}
ARG uptake	µmol N L^{-1}	68.5	22.9
	µmol C L^{-1}	11.4	59.4
Total ARG demand	µmol N L^{-1}	91.4	
	µmol C L^{-1}	70.8	
Theoretical density per N-ARG consumed	cells L^{-1}	9.38 x10^9	6.56 x10^9
Density on last day	cells L^{-1}	7.44 x10^9	1.551 x10^9

The final bacterial density of 7.4 x10^9 cells L^{-1} was comparable to that estimated by N-ARG demand (9.38 ·10^9 cell L^{-1}). As such, it could be concluded that the bacterial population grew exclusively on ARG. On the contrary, the theoretical yield of *M. pusilla* (6.55 x 10^9 cell L^{-1}) for the estimated N-ARG demand was considerably higher than the density actually obtained (1.55 x 10^9 cell L^{-1}), which presumes that the cells assimilated IN forms like NH_4^+, produced from ARG mineralisation.

The ARG uptake, estimated from density difference between end and start of the experiment and the theoretical N and C quotas, revealed a greater N uptake by bacteria, but a greater C uptake by *M. pusilla.* Overall the total uptake was equal to the N-ARG consumption measured but the C-ARG demand was half of what actually consumed. Considered the strong ARG consumption in ARG cultures this can indicate a possible competition between *M. pusilla* and bacteria for what concerns OC and ON respectively. Moreover, even though ON turnover by bacteria can occur in a few hours (Gruber, 2008), this does not explain why both cultures grew at a comparable rate for the first days of the incubations.

PON and POC were quantified on the day of harvesting and compared to C biomass estimated from biovolume measurements in order to constrain the estimates of N demand for each culture (Table 25).

Table 25: PON and POC quantified on harvesting day of *M. pusilla* cultures and related to biomass estimation by biovolume.

M. pusilla	**NO_3^-**	**ARG**
PON [µmol N $cell^{-1}$]	4.60 x10^{-9}	1.60 x10^{-8}
POC [µmol C $cell^{-1}$]	1.59 x10^{-4}	4.90 x10^{-4}
C : N ratio (atomic)	4.2	3.7
Biovolume [µmol C $cell^{-1}$]	2.25 x10^{-8}	3.19 x10^{-8}
% algal biomass on last day	96.60	82.24
% bacterial biomass on last day	3.39	17.76

As shown in Table 25, PON and POC per cell were higher in ARG cultures, although they consumed consistently more N than NO_3^- cultures. C:N ratio was also in those latter,

leading to the conclusion that ARG uptake can be less efficient for N assimilation in *M. pusilla*.

Both C biomass measurements indicated that the ARG cultures had a higher C content but the percentage of bacterial biomass was also higher than in NO_3^- cultures. As seen for *E. huxleyi* the C content per cell calculated from biovolume measurements resulted double than that measured by CHN, indicating either a possible loss of OC during filtration or that the theoretical equation reported for protist plankton by Menden-Deuer and Lessard, (2000) is not a suitable method for biomass estimation for *M. pusilla*.

Chl *a* content was 9.59 fg cell $^{-1}$ in ARG cultures and 8.88 fg cell $^{-1}$ for NO_3^- cultures. Values were not significantly different ($P > 0.005$, ANOVA) indicating equal energy requirements from photosynthesis with both N sources.

4.3.3. *Alexandrium minutum*

Alexandrium minutum was incubated in duplicate with both IN and ON for a period of 11 days, and harvested pH revealed an increase to 9.0, and a target cell density (≥ 7,000 cell mL^{-1}) was exceeded. As shown in Figure 23, *A. minutum* growth of both NO_3^- and ARG cultures, was less rapid than that of both *E. huxleyi* and *M. pusilla* due to a higher volume and biomass of dinoflagellates. There was no significant difference ($P > 0.005$, ANOVA) in growth between the two treatments throughout the incubation period, although ARG cultures had a slightly lower growth rate (Figure 23).

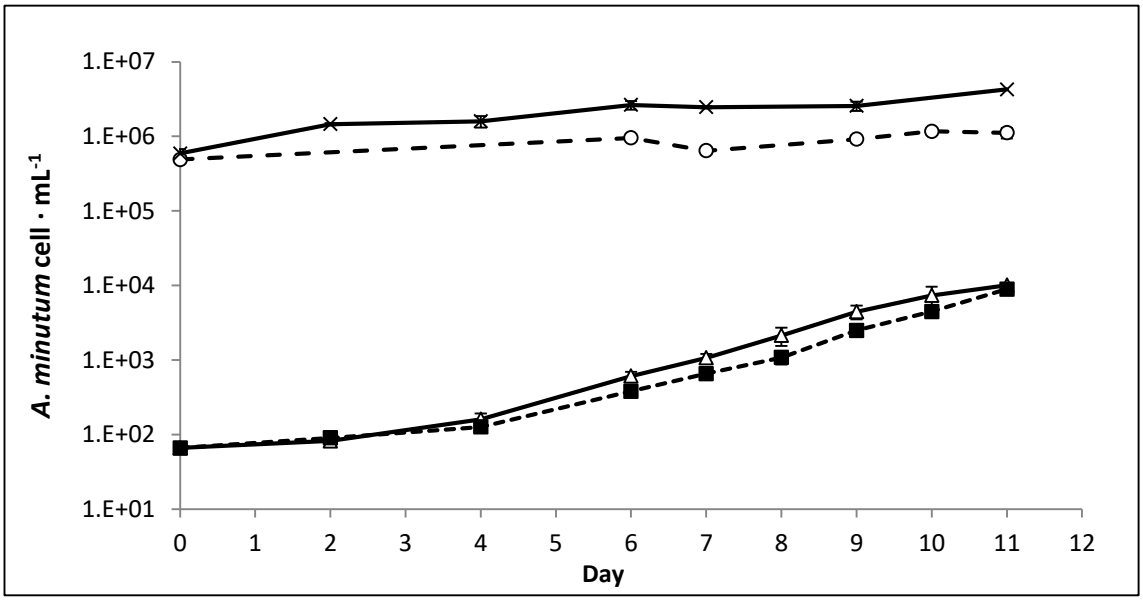

Figure 23: growth of *A. minutum* cultures with NO_3^- (Δ) and Arg (■), and bacteria enumeration. with NO_3^- (○) and Arg (×). The data points represent the average of duplicate samples counted in triplicate (n=6).

Growth rates were of 0.59 day^{-1} (SD=0.03) and 0.63 day^{-1} (SD=0.02), for ARG and NO_3^- cultures respectively (Table 26). All growth parameters confirmed a slightly slower growth rate where *A. minutum* was incubated with ARG, although there was no significant difference measured with NO_3^- cultures, and the rates corresponded to the ranges reported (Béchemin, Grzebik, Hachame, Hummert, & Maestrini, 1999; Maguer, L'Helguen, Madec, Labry, & Le Corre, 2007).

Table 26: *A. minutum* and bacteria growth parameters; μ - growth rate, t_d - doubling time, k - number of divisions per day. For calculation details see reference Andersen (2005).

	NO_3^- cultures		**ARG cultures**	
	A. minutum	**bacteria**	***A. minutum***	**bacteria**
μ	0.633	0.111	0.594	0.250
t_d	1.094	6.256	1.167	2.775
k	0.914	0.160	0.857	0.360

On the contrary table 26 shows a consistently greater duplication time for bacteria cultured with NO_3^- , and growth was in fact much faster with ARG. Although bacteria and *Alexandrium* growth rates diverge less in ARG culture, this is less evident than for *M. pusilla* cultures, probably due to the very different physiology between dinoflagellates and bacteria.

Although bacteria abundance was high during the entire experiment, in ARG cultures bacterial biomass was estimated to be only 5 % of the total estimated organic C on Day 7, decreasing to 1 % by Day 11.

Dissolved nutrient data revealed a total uptake of 97.6 μmol N in NO_3^- cultures and of 61 μmol N in ARG cultures, this is probably due to a final smaller density of these latter. Both cultures presented a comparable trace concentration of NH_4^+ at the end of the experiment (Figure 24A and B), demonstrating a similar growth of *A. minutum* and bacteria with the two N substrates.

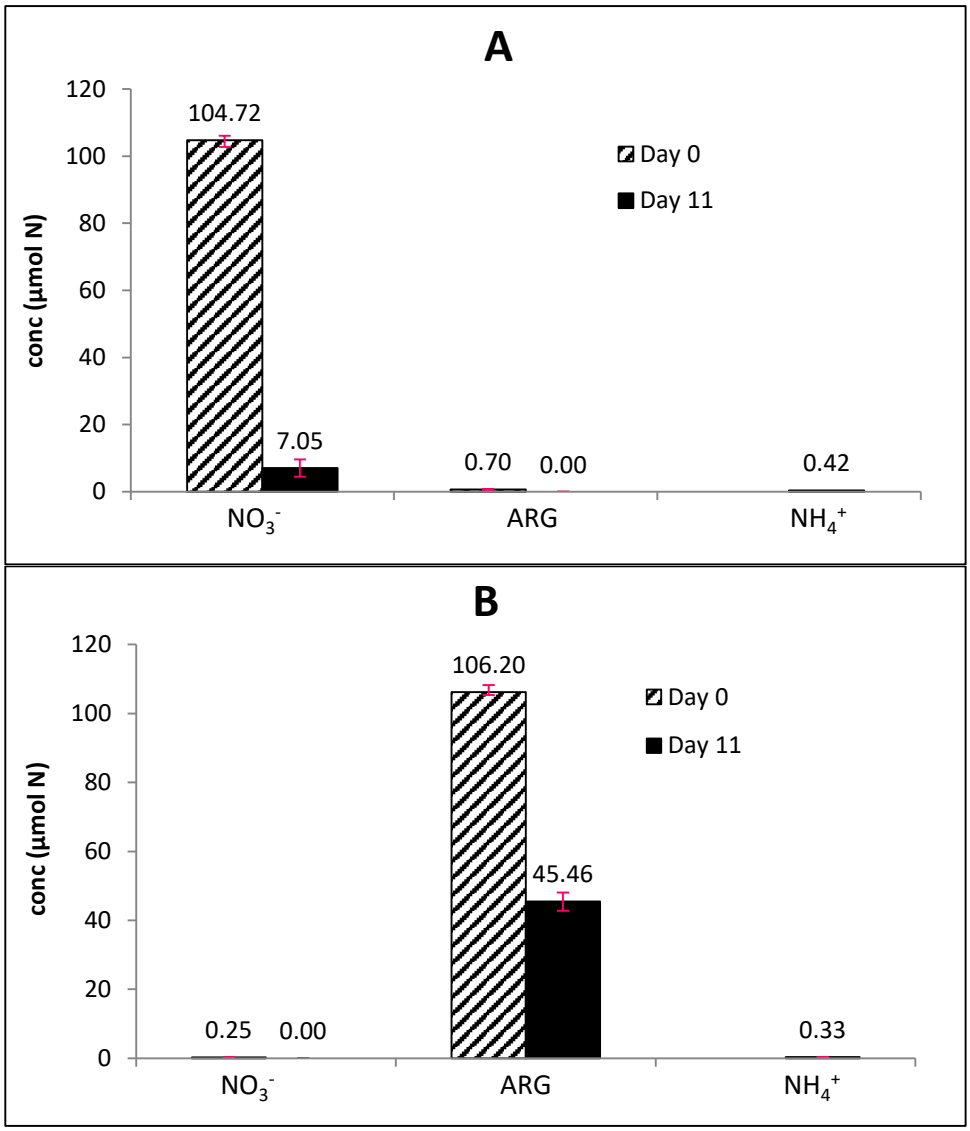

Figure 24: dissolved nutrients concentration on day 0 and 11 of *A. minutum* experiments with A) NO_3^- and B) ARG. NO_3^- and ARG were analysed at the beginning and end of the incubation, while NH_4^+ was quantified on last day only. Values represent the average of duplicate samples counted in duplicate (n=4).

The initial small concentration of NO_3^- in ARG cultures was assimilated but it would not have been enough to obtain the cell density as shown in Table 27.

Table 27: N- NO_3^- demand estimation for *A. minutum* cultures enriched with ARG. The theoretical density is calculated by adding the density of the culture on Day 0.

NO_3^- [µmol N L^{-1}] on Day 0	0.245
N quota [µmol $cell^{-1}$]	5.1×10^{-6}
Final density (cells L^{-1})	8.89×10^6
Theoretical density per NO_3^- [µmol L^{-1}] Day 0	1.14×10^5

As shown in Table 27, the theoretical *A. minutum* density, if uptake were based only on the initial NO_3^- [µmol L^{-1}] concentration, would have been no more than 1.14 x10^5 cells L^{-1}, while the actual measured density was almost two hundred times higher (8.9 x10^6 cells L^{-1}) based on the reported N quota (Béchemin *et al*., 1999), indicating that the NO_3^- within the culture was not sufficient to support this cell density. In order to confirm that the growth was supported by ARG, an equal evaluation for both *A. minutum* and bacteria (Hoch, Fogel & Kirchman, 1992) N quota was carried out (Table 28).

Table 28: ARG demand estimation for *A. minutum* cultures enriched with ARG. Calculation were made based on reference N and C quota and using the total density difference between the final day and day 0 of the experiment ($\Delta n = n_{end} - n_{start}$).

		Bacteria	*A. minutum*
ARG consumed	µmol N L^{-1}	60.7	
	µmol C L^{-1}	91.1	
Theoretical cellular quota	µmol N	1.00 x 10^{-8}	5.10 x 10^{-6}
	µmol C	1.67 x10^{-9}	4.91 x10^{-5}
ARG uptake	µmol N L^{-1}	36.8	44.9
	µmol C L^{-1}	6.1	433.5
Total ARG demand	µmol N L^{-1}	81.8	
	µmol C L^{-1}	439.6	
Theoretical density per N-ARG consumed	cells L^{-1}	6.07 x10^9	1.19 x10^7
Density on last day	cells L^{-1}	4.27 x10^9	8.89 x10^6

Stated the consumed ARG concentration of 60.7 µmol N L^{-1} and that the reference cellular N quota is 1.0 x 10^{-8} and 5.1 x10^{-6} µmol $cell^{-1}$ for bacteria and *A. minutum* respectively, we would expect a theoretical final density of 6.07 x 10^9 and 1.19 x 10^7 cell L^{-1} of bacteria and *A. minutum* respectively. Both bacteria and *A. minutum* grown with ARG were in the same abundance range of the theoretical, indicating that ARG uptake and assimilation by *A. minutum* was supposedly possible. The total N-ARG uptake estimated from density differences and the reported N quotas revealed a greater N uptake than what measured.

This could be a bias due to the reported N quotas for *A. minutum*, as the PON measured at the end of this experiment, assuming that bacterial biomass was not relevant for the analyses, gave a lower N quota of 4.54 x10^{-6} µmol cell^{-1} for *A. minutum*, which would to lead to a total N-ARG uptake of 76.8 µmol N L^{-1}.

In order to constrain the N budget, organic N and C were measured at the end of incubation (Table 29).

Table 29: PON and POC quantified on harvesting day of *M. pusilla* cultures and related to biomass estimation by biovolume.

A. muntum	**NO_3^-**	**ARG**
PON [µmol N cell^{-1}]	8.25 x 10^{-6}	4.54 x 10^{-6}
POC [µmol C cell^{-1}]	3.38 x 10^{-1}	3.66 x 10^{-1}
C : N ratio (atomic)	5.1	10.2
Biovolume [µmol C cell^{-1}]	4.90 x10^{-5}	7.76 x10^{-5}
% algal biomass on last day	99.7	98.4
% bacterial biomass on last day	0.23	1.60

ARG cultures assimilated 26 µmoles of N less than NO_3^- cultures, and this also resulted in a lower cell density (1.2 x 10^6 cell L^{-1}) and a lower PON per cell, indicating a possible equal assimilation rate.

In contrast, OC levels were slightly higher in the ARG cultures, revealing a greater propensity for ON to increase algal biomass, as bacterial biomass was estimated to be only 1 % of the total OC. This is also demonstrated by the double C:N ratio found in ARG cultures, revealing N-limitation at the end of the experiment for these cultures. Although the C content per cell estimated from biovolume resulted higher then the measured POC, as per previous species, the difference between NO_3^- and ARG cultures is comparable to the POC measurement. The percentage of bacterial biomass, estimated from biovolume measurements, was low for both ARG and NO_3^- cultures of *A. minutum*.

Chl *a* was measured in ARG cultures at a concentration of 3.47 pg cell^{-1} (SD=1.04) and 7.12 pg cell^{-1} (SD=1.28) in NO_3^- cultures. As already shown for *E. huxleyi*, cells of

A. minutum incubated with ARG had a lower Chl *a* concentration, indicating a possible less energy requirement from photosynthesis.

4.3.4. *Chaetoceros peruvianus*

During incubation of *C. peruvianus* the target maximum cell density, estimated as 110,000 cell mL^{-1}, was too high as pH started to vary from the initial and ideal value of 8.2 ±0.08 above 6000 cell mL^{-1}. On harvesting day the pH was 8.46 ± 0.05 for NO_3^- cultures and 8.53 ± 0.02 for ARG cultures, indicating a possible deviation of the carbonate equilibrium due to cell density. An estimation of the target maximum cell density, related to the *genus* in general, can be less adequate for species where biomass variance is high (Béchemin *et al*., 1999; Li *et al*., 2017).

As shown in Figure 25, the incubation was stopped after 8 days for NO_3^- cultures and at Day 12 for those incubated with ARG.

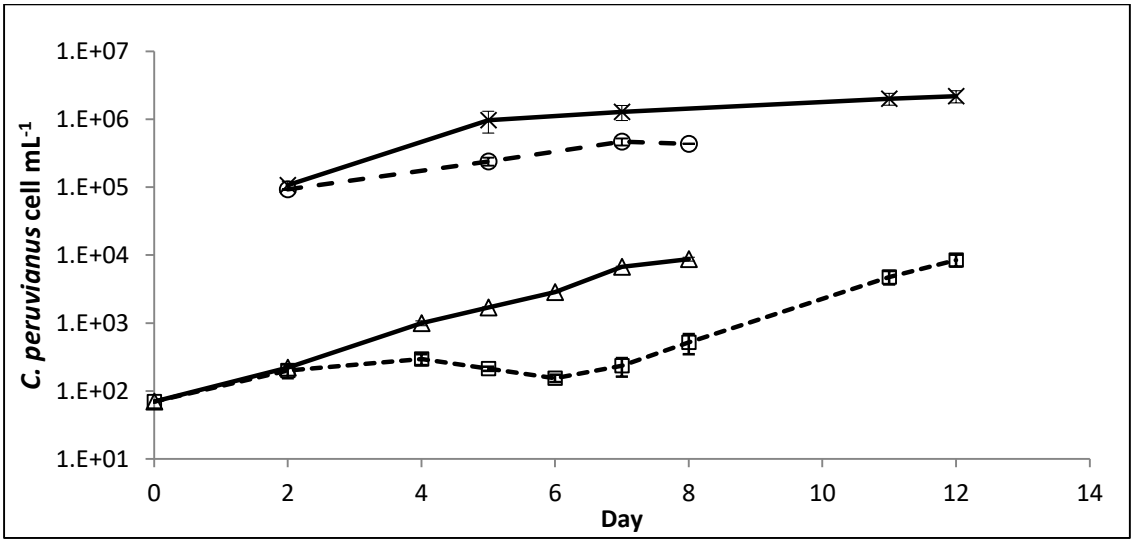

Figure 25: Growth of *C. peruvianus* cultures containing NO_3^- (Δ) and Arg (□), and bacteria enumeration in NO_3^- (○) and Arg (×) cultures. The data points represent the average of duplicate samples counted in triplicate (n=6). Max variation on day 12 was approximately 2000 cells between replicates.

C. peruvianus grown with NO_3^- showed continuous growth throughout the incubation period, which was stopped just before the onset of stationary phase. The ARG cultures

did not enter exponential growth until Day 7, but reached the same abundance as NO_3^- cultures after a further 5 days. Culture replicate A, enriched with ARG, reached a final density of 7.3 x 10^6 cell L^{-1} of *C. peruvianus* and 1.8 x 10^9 cell L^{-1} of bacteria, while replicate B reached 9.7 x 10^6 cell L^{-1} of *C. peruvianus* and 2.5 x 10^9 cell L^{-1} of bacteria. Bacterial abundance was higher in ARG cultures during the entire experiment, but decreased from 25 to 1.8 % of total organic carbon at Days 6 and 11, respectively. Parameters and rates of exponential growth differed from Days 2 to 7, for NO_3^- cultures, and from Days 7 to 11 for ARG cultures (Table 30).

Table 30: *C. peruvianus* and bacteria growth parameters of cultures during exponential phase; μ - growth rate, t_d - doubling time, k - number of divisions per day. For calculation details see Andersen (2005).

	NO_3^- cultures		**ARG cultures**	
	C. peruvianus	**bacteria**	***C. peruvianus***	**bacteria**
μ	0.684	0.323	0.756	0.496
t_d	1.013	2.147	0.917	1.396
k	0.987	0.466	1.091	0.716

Although the exponential growth rate was higher in ARG cultures, for both *C. peruvianus* and bacteria, the difference with NO_3^- cultures was not significant ($P > 0.005$, ANOVA) , and in the range of previous culture studies for the selected *genus* (Lomas & Glibert, 2000; Sarthou et al., 2005). Growth parameters revealed consistently less divisions per day (*k* day^{-1}) by bacteria when cultured with NO_3^- instead of ARG, while the diatom growth rate diverge less between the two N sources.

Dissolved NO_3^- and ARG were analysed at the beginning and end of the incubations, while NH_4^+ was quantified on the last day only. These data were significantly different ($P < 0.001$, ANOVA) in culture replicates where ARG was the N source, and are shown in Figure 26.

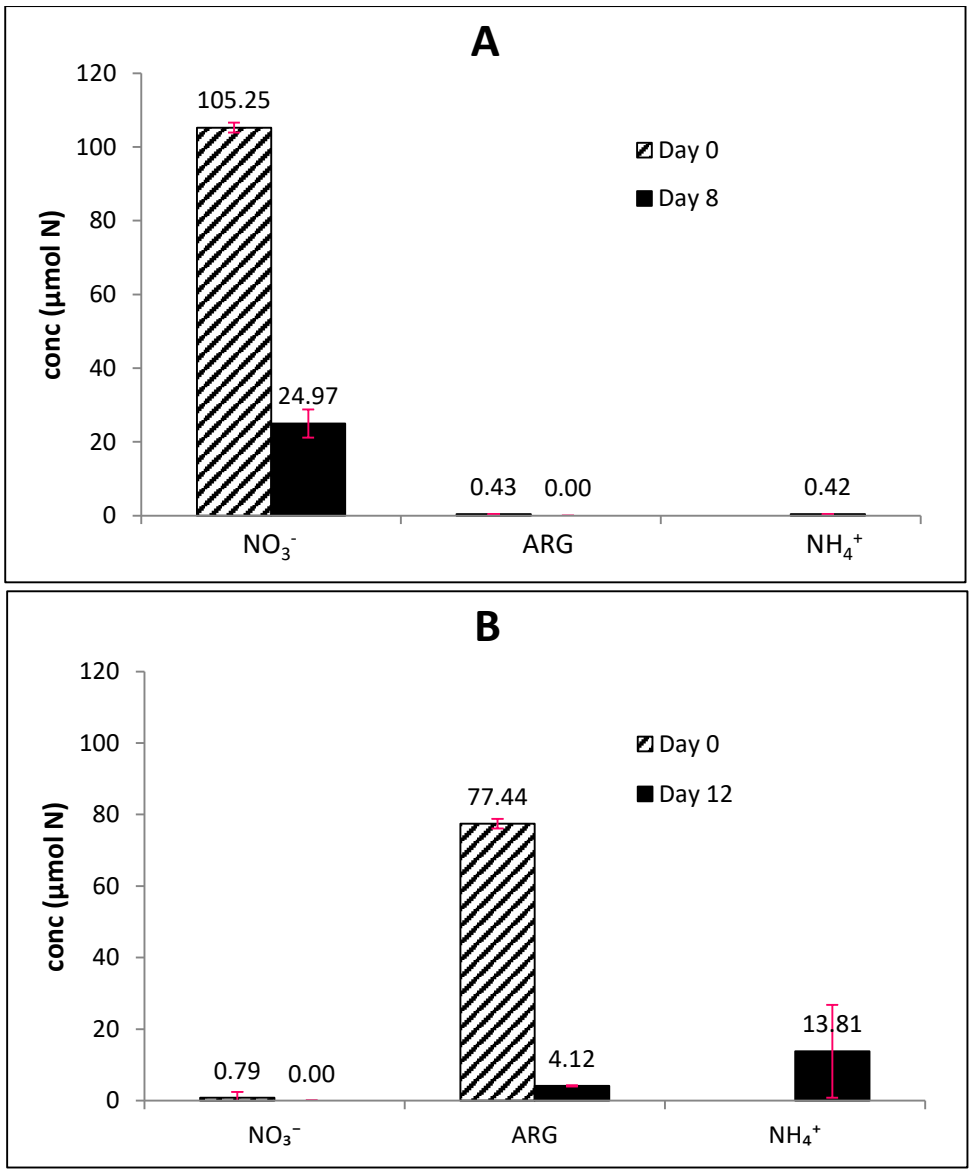

Figure 26: Dissolved concentrations of nitrogen substrates in *C. peruvianus* experiments: A) NO_3^- on Days 0 and 8; B) ARG on Days 0 and 12. Note that for ARG cultures, average NH_4^+ concentrations in culture replicates A and B is presented with standard deviation revealing the high differences between the two replicates.

In the NO_3^- cultures, 80 µmoles of N of the total NO_3^- was consumed (76%) and a small amount of NH_4^+ was detected at the end of the experiment, considered negligible. ARG cultures of *C. peruvianus* contained only 0.79 µM of NO_3^- at start of the experiment, and assimilated 73.3 µmoles of N from dissolved ARG (98%). Higher concentration of NH_4^+ (27 µmoles of N) was measured on Day 12 only in replicate B of the ARG cultures of *C. peruvianus*, where both the diatom and bacteria had a higher final density.

Cultures of *C. peruvianus* enriched with ARG contained 0.787 µM of NO_3^- at Day 0, which could not sustain the measured density (Table 31), based on an N quota of 7.8 $x10^{-6}$ µmol $cell^{-1}$. The average N quota for *C. peruvianus* was computed based on PON analyses of the cultures as this *genus* can have a highly variable volume. The final culture density was calculated as the average of duplicates.

Table 31: N-NO_3^- demand estimation for *C. peruvianus* cultures enriched with ARG. The theoretical density is calculated by adding the density of the culture on Day 0.

NO_3^- [µmol N L^{-1}] on Day 0	0.787
N quota [µmol $cell^{-1}$]	7.78 $x10^{-6}$
Density (cells L^{-1}) on Day 12	8.48 $x10^6$
Theoretical density per NO_3^- [µmol L^{-1}] Day 0	1.71 $x10^5$

An equal estimation was made, considering the N-ARG demand of both bacteria (Hoch et al., 1992) and *C. peruvianus* (Table 32). For this replicate densities and N concentrations were averaged (n = 2) and N quotas per cell were computed by PON analyses, rather than literature estimation.

Table 32: ARG demand estimation for *A. minutum* cultures enriched with ARG. Calculation were made based on reference N and C quota and using the total density difference between the final day and day 0 of the experiment ($\Delta n = n_{end} - n_{start}$).

		Bacteria	*C.*
ARG consumed	µmol N L^{-1}	73.3	
	µmol C L^{-1}	109.9	
Theorical cellular quota	µmol N $cell^-$	1.00 $x10^-$	7.78 x 10^{-6}
	µmol C $cell^{-1}$	1.67 $x10^-$	3.8 $x10^{-5}$
ARG uptake	µmol N L^{-1}	20.8	65.4
	µmol C L^{-1}	3.5	319.6
Total ARG demand	µmol N L^{-1}	86.2	
	µmol C L^{-1}	323.1	
Theoretical density per N-ARG	cells L^{-1}	7.33 $x10^9$	9.42 $x10^6$
Density on last day	cells L^{-1}	2.19 $x10^9$	8.48 $x10^6$

The obtained density of *C. peruvianus* was comparable to the theoretical estimated, indicating that growth for the species could have been sustained by ARG. In contrast the actual bacterial biomass was four times less than the theoretical density for the amount of ARG consumed, possibly indicating that the reported N quota for bacteria (Hoch *et al*., 1992) was not suitable.

The ARG uptake estimated from density differences and the reported N and C quotas revealed a greater N and C uptake by *C. peruvianus* than by bacteria. Overall the total N-ARG estimated demand was comparable to the actual N-ARG consumed, while the C-ARG supply was consistently higher than the dissolved C-ARG consumed.This probably indicates that the C supply from ARG was not sufficient.The ON and C quotas per cell were calculated with elemental analyses performed at the end of the incubations (Table 33). The measured POC was then compared with that inferred from biovolume according to Menden-Deuer and Lessard (2000).

Table 33: PON and POC quantified on harvesting day of *M. pusilla* cultures and related to biomass estimation by biovolume.

C.peruvianus	**NO_3^-**	**ARG**
PON [µmol N cell^{-1}]	5.80 x10^{-6}	7.78 x10^{-6}
POC [µmol C cell^{-1}]	2.06 x10^{-1}	2.71 x10^{-1}
C : N ratio (atomic)	4.43	4.36
Biovolume [µmol C cell^{-1}]	3.17 x10^{-5}	3.80 x10^{-5}
% algal biomass on last day	99.7	98.2
% bacterial biomass on last day	0.26	1.81

ARG cultures consumed 7.8 µmol N less than NO_3^- cultures, but measured PON per cell was higher, indicating more efficient N assimilation. On the other hand POC (measured via biovolume and CHN) and C:N were similar with the two N sources, indicating a less efficient C assimilation from ARG. Bacterial biomass estimated was very low at end of the experiment, indicating a predominance of the diatom.

The Chl *a* concentration was 8.7 and 7.7 pg cell $^{-1}$ in ARG and NO_3^- cultures, respectively. Values of Chl *a* concentration were not significantly different ($P > 0.005$, ANOVA) between the two N sources.

5. Discussion

The ability of algal species to exploit ON sources has been previously demonstrated (Farrell et al., 2013; Moneta et al., 2014; M R Mulholland & Lee, 2009; Yuan et al., 2012) and it is clear that some components of the DON pool in natural waters can serve as direct sources of N nutrition for phytoplankton and bacteria. These findings have implications for marine ecosystem function and health, since climate change scenarios predict variable riverine inputs to coastal areas, altered N: P ratios, and changes in the inorganic to organic balance of the nutrient pools.

The aims of this study were to examine the extent to which marine phytoplankton developed when only DON was available, using monoalgal cultures (i.e. algae in the presence of bacteria), and how growth rates on DIN and DON compared for the same species. By choosing ecologically relevant algal species this work was intended to clarify if the availability of labile components of DON, like amino acids or oligopeptides, may be important in determining not only algal biomass, but also species composition.

5.1. Testing artificial media

Experiment I, II and III were performed to identify the best culture medium (CM listed below, Table 34) for the selected species.

Table 34: list of culture media (CM) used in Exp. I, II and III

CM	Recipe	Sterilization
0	modified k/2	SW heated to 100 °C Filtered nutrients stocks
1	ESAW	Autoclaved AW Autoclaved nutrients stocks
2	50% ESAW +50% k/2	
3	Aquil*	Autoclaved AW Autoclaved nutrients stocks
4	10% k/2 + 90% Aquil*	
5	Aquil*	SW heated to 100 °C Filtered nutrients stocks

With Exp. I it appeared clear that CM 1 (ESAW), prepared with autoclaved AW and autoclaved stock solutions, was not ideal for all species; while *Synechococcus* sp. clearly did not grow, *E. huxleyi* grew strongly but half of the population were not coccolith-bearing; *C. peruvianus* cultures presented auxospores and *A. minutum* cells were often deformed. Moreover, in this experiment, flow cytometry proved not be feasible for enumeration of both diatoms and dinoflagellates as the sinking process and large cells interfered with the analyses.

In Exp. II, CM1 (ESAW) had the lowest growth for all the species, while with the natural SW-based CM0 (k/2) they all grew well, and growth in the mixed CM3 (k/2+ESAW) reached a medium density between CM1 and CM0. This clearly demonstrated how the addition of non-autoclaved natural SW and non-autoclaved stock solutions enhanced the growth of all the species tested. Three of the four *E. huxleyi* strains tested in this experiment were inhibited by CM1 (ESAW) and all of them presented stressed cells in the mixed CM3 (Aquil*), even though growth was similar to that in CM0 (k/2). Cultured Pacific strains (RCC 911 and 1220) mostly contained “naked” cells, which is a frequent event in *E. huxleyi* cultures (Paasche, 2002), and these are thought to be mutants. The strain from the English Channel (RCC 1268) consisted of flagellate haploids

cells instead which are known to have different nutrition physiology with respect to coccolith bearing cells (Klaveness, 1972). Although this last *E. huxleyi* strain was initially considered, the more cosmopolitan CCMP 1516 strain was chosen for further experiments as it grew best in the artificial media tested.

Exp. III confirmed the lack of some fundamental components in CM3, based on the Aquil* recipe, which in general gave poor results, as *M. pusilla* was the only species reaching an accepted cell density in both CM3 and the mixed CM4 (10% k/2+ 90% Aquil*).

Previous studies have demonstrated how environmental stressing factors can lead to biological changes in phytoplankton cells; low trace metal concentrations will limit the growth rate of the organism principally through impairment of many biochemical functions (Morel, Milligan, & Saito, 2003). For example, iron and manganese play essential metabolic functions in photosynthetic electron transport and detoxification of reactive oxygen species, copper contributes to formation of plastocyanin and ferrous oxidase, zinc and cadmium are linked to the functioning of carbonic anhydrase and alkaline phosphatase. The precipitation of the relatively high concentration of trace metals, due to medium preparation and sterilization, can result in adsorption of other elements, reducing their availability (Andersen, 2005). Sterilization of the trace elements stock solution through autoclaving at 120 ºC may have caused precipitation and speciation of some components, like iron or zinc. The iron and zinc requirement of *E. huxleyi* is lower than in coastal diatoms, like for other oceanic coccolithophorids (Larry E Brand, 1991; Muggli & Harrison, 1997; Sunda & Huntsman, 1995a, 1995b). This can explain why, in Exp. I, *E. huxleyi* was the only species which grew.

Among the two tested recipes, Aquil* was the more oligotrophic, with less risk of precipitation during the sterilization process and so was preferred, although filter sterilization of enrichment stock solutions may be used in order to avoid it.

5.2. Axenic culture preparation

Experiment IV was performed to obtain axenic cultures of the selected species, and the approach based on Droop (1967) was selected as convenient procedure involving minimal manipulation. Washing algal cells by gentle filtration is a key step that removes large amounts of bacteria associated with large diatoms and dinoflagellates, but is not so efficient with small flagellates or coccolithophores. The lethality of the antibiotic treatment is an intensity-time relationship, the intensity being the concentration of antibiotics and the time being the period of exposure before transfer to antibiotic-free medium. Both antibiotic mixtures used were effective and not toxic to the algae; *C. peruvianus* and *A. minutum* were both resistant to the Slocombe mixture and exhibited healthy growth. The PNS mixture was not toxic to *E. huxleyi* or *M. pusilla*. Although the latter was not actively moving during treatment, it was able to recover this ability after several transfers to fresh medium. During the antibiotic treatments, determination of the sensitivity of algae was achieved for simplicity with inspections of eventual growth inhibition and cell status under light microscope. The method (modified from Droop 1967) recommends examination of sterile transfer into fresh medium over several weeks, but this examination was done only over two weeks due to time constraints. Incubation with the antibiotic up to 48 hours and a transfer period into antibiotic-free medium after 72 hours proved to be effective.

The treatment removed bacteria in *A. minutum* cultures; further treatment would be required in *C. peruvianus*, *E. huxleyi* and *M. pusilla* cultures to obtain axenic cultures. For this latter species, addition of peptone or sucrose before treatment is recommended for further studies to stimulate growth of bacteria, making them susceptible to antibiotics like Penicillin (Cottrell & Suttle, 1993). Examination of algal biomass should be monitored over several weeks by in vivo fluorescence, along with bacterial biomass by

epifluorescence or flow cytometry. This experiment produced axenic cultures of *A. minutum* only, which were not used for subsequent experiments for comparison.

5.3. Phytoplankton growth comparison with ARG or NO_3^- as sole N source

To establish the capacity for phytoplankton to take up DON, growth rates of selected species in culture systems were examined in Exp. V. Although the methods used cannot unequivocally distinguish between phytoplankton and bacterial processes, the results show that growth varied among cultured algae preconditioned with the two nitrogen sources. All the species reached similar density when cultured with the amino acid ARG and NO_3^- as the only N source, indicating that DON can address ecosystem biodiversity and functioning, and it is possible then, to accept the hypothesis tested in this work, as that algal species that can directly access oligopeptides gain an advantage over competitors at low levels of DIN, even though further co-culturing experiments of different phytoplankton species in the same batch can offer a more holistic view on the species-specific interactions against ON direct uptake.

Two species, *A. minutum* and *C. peruvianus*, presented an initial lag phase, characteristic of a cell that is adjusting its physiological functioning to the environment, with the latter more prominent. This lag phase could suggest an initial bacterial degradation of the dissolved ARG leading to the release of IN, for example NH_4^+, which would be subsequently exploited by algae. This though cannot be true for *A. minutum* as: (i) the same slow growth phase was observed in NO_3^- cultures, (ii) only a trace concentration of NH_4^+ was measured in ARG culture at the end of the experiment, with similar concentrations in the NO_3^- cultures and (iii) N-demand estimates, based on the consumed N-ARG moles, correlated with the final cell density. All of the above indicate that the species did not develop on IN produced from ARG mineralisation but on the ON substrate. Despite a higher POC content per cell, *A. minutum* cultured with ARG had a significantly lower concentration of Chl *a,* suggesting a lower energy requirement from

photosynthesis when ARG was the only N source, also confirmed by the higher C : N ratio.

C. peruvianus had a higher growth rate when cultured with ARG, which started only after 6 days of incubation; N-demand estimates confirmed the obtained algal density but not the bacterial one, indicating that final abundance of *C. peruvianus* could be sustained on ARG as estimated, but that bacteria should have reached a higher density if utilising ARG only. This is the first study on this particular species of *Chaetoceros* that collates growth rates on different sources of N, so comparisons are difficult. There was residual NH_4^+ only in one replicate of *C. peruvianus* cultured with ARG. This flask had a higher abundance of bacteria which probably could release more NH_4^+. When resources are plentiful, also larger phytoplankton, like *C. peruvianus*, may grow faster than their smaller relatives, allowed by an increase in the effective surface-to-volume ratio, due to changes in cell shape and the presence of vacuole, or the accumulation of non-limiting substrates to increase cell size and optimize nutrient uptake.

On a global scale any excess in the C supply favoured by the ARG assimilation, here experimented with both with *A. minutum* and *C. peruvianus* will potentially increase the C biomass of those larger phytoplankton species with a subsequent increase in the C:N ratio of grazer as well. Moreover larger phytoplankton are mostly grazed by metazoan herbivores with longer generation times (order of weeks/months) than that of phytoplankton (order of hours/days) (Marañón et al., 2009), and thanks to this growth response time lag are able to form blooms until nutrients are exhausted. Although it is unlikely that a bloom of *A. minutum* could be sustained only by DFAAs, these could enhance toxin content as ARG has been shown to be a precursor for saxitoxins (Anderson et al., 2012). Further studies are needed to investigate this correlation.

Growth of *E. huxleyi* was fast and continuous with both NO_3^- and ARG, and equal moles of N were consumed in NO_3^- and ARG cultures, confirming the ability of the

coccolithophore to take up the DFAA. As the cosmopolitan blooming species *E. huxleyi*, can have an impact on C and S cycling and, hence, global climate, will reach the same abundance and growth rate with ARG as with NO_3^-, there would be possible excess of C from the assimilation of the amino acid, this will have potential consequences on the local, and also global CO_2 sequestration in the ocean.

Both POC and PON were lower in ARG cultures indicating that ARG assimilation can be less effective for biomass formation of *E. huxleyi*. Although high nitrogen nutrient concentrations (25 μmoles of ARG) were used in these experiments, they raise the possibility that *E. huxleyi* could use organic nitrogen when IN is low, or that produced by microzooplankton organisms, some of which are known to excrete purines, in nitrate-poor parts of the ocean. Palenik and Koke (1995) reported that several clones of *E. huxleyi*, when grown under nitrogen limitation, develop a specific surface-bound protein of unknown function.

M. pusilla presented a significantly slower growth and lower final density ($P < 0.005$, ANOVA) when incubated with ARG. Overall N consumption was higher in ARG cultures, indicating less efficient assimilation of ON for this species. The high concentration of NH_4^+ in ARG cultures of *M. pusilla* at the end of the experiment suggested bacterial conversion of ARG, and possibly that this algal species could benefit indirectly. Despite the slower growth, both POC and PON were higher in ARG cultures indicating that any released NH_4^+ was more effective than NO_3^- for N and C assimilation. It can be inferred that both substrates were taken up simultaneously. A concomitant uptake of several chemical forms was previously documented in the picoflagellate *Micromonas pusill*a by Cochlan and Harrison (1991).

Growth of smaller size fraction of phytoplankton, like *E. huxleyi* and *M. pusilla* was rapid and continuous with ARG, and although reaching slower growth rates sometimes with respect to NO_3^-, some sort of competition for both ON and OC will take

place against bacteria when DIN concentrations are lower than those of DON. The potential interaction between phytoplankton and bacteria (here experimented with *M. pusilla* and *C. peruvianus*) to potentially release NH_4^+ as a consequences of the ARG mineralisation, can act as a blooming trigger for other phytoplankton species. In particular, as smaller species (like *M. pusilla*) are at an advantage to remain within the euphotic zone, relevant in strongly stratified water columns, any NH_4^+ release will enhance blooming forming species in this first layer of the summary water column.

In oligotrophic gyres DON can act as an important N source especially with the predicted increase in stratification occurring in these regions, which will reduce DIN supply for phytoplankton. These changes can cause an important shift in the primary producers composition which needs to be monitored, considering the possible impact on the marine trophic web that will follow primary producers.

6. Conclusions

This study has shown that *E. huxleyi*, *A. minutum*, *M. pusilla* and *C. peruvianus* can grow on organic N, either by direct or indirect uptake, and develop comparable biomasses to species using inorganic N.

A. minutum grew in the presence of ARG along with the cosmopolitan *E. huxleyi*; N-demand estimates, based on the molar concentration of N-ARG consumed, correlated with the final cell density, indicating that the species did not develop on inorganic N produced from ARG mineralisation, but directly on the ON substrate. Since *A. minimum* has been linked to harmful algal blooms, and *E. huxleyi* contributes significantly to oceanic $CaCO_3$ deposition, their ability to utilise DON has environmental consequences in addition to the oceanic N-budget. Both *C. peruvianus* and *M. pusilla* cultures contained dissolved ammonium at the end of the experimental period, indicating potential indirect use by the algae of organic N converted to inorganic N by bacteria. The potential interaction between phytoplankton and bacteria (here experimented with *M. pusilla* and *C. peruvianus*) to potentially release NH_4^+ as a consequence of the ARG mineralisation, can act as a blooming trigger for other phytoplankton species. Further assessments are needed to investigate the importance of bacteria in regulating DON turnover, with the establishment of axenic cultures using the method tested in this study.

In conclusion any anthropogenic increase in labile forms of DON, like ARG, can alter the biomass of the smaller phytoplankton size fraction (like *E. huxleyi* and *M. pusilla*), which is relatively stable over time due to the grazing control, with consequences on the marine trophic net and also global CO_2 sequestration in the ocean.. Moreover any excess in the C supply favoured by the ARG assimilation, here experimented with both with *A. minutum* and *C. peruvianus* will potentially increase the C biomass of those larger phytoplankton species with a subsequent increase in the C:N ratio of grazer as well.

7. Appendix I. Experiments list and details

Experiment	Aims	Species	Culture media	Monitoring
I	Testing ESAW recipe	*E. huxleyi* *Synechoccous* sp. *C. peruvianus* *A. minutum*	CM 1	Flow cytometry
II	Testing mixed media Testing *E. Huxleyi* strains	*M. pusilla* *C. peruvianus* *A. minutum* *E. huxleyi* RCC 911 *E. huxleyi* RCC 1220 *E. huxleyi* RCC 1268 *E. huxleyi* CCMP 1516	CM 0 CM 1 CM 2	Flow cytometry and light microscopy
III	Testing Aquil* recipe	*E. huxleyi* *M. pusilla* *C. peruvianus* *A. minutum*	CM 3 CM 4	Flow cytometry and light microscopy
IV	Preparing axenic cultures	*E. huxleyi* *M. pusilla* *C. peruvianus* *A. minutum*	CM 0	Flow cytometry and light microscopy
V	Testing growth on ARG	*E. huxleyi* *M. pusilla* *C. peruvianus* *A. minutum*	CM 5	Flow cytometry and light microscopy

8. References

Admiraal, W., Peletier, H., & Laane, R. W. P. M. (1986). Nitrogen metabolism of marine planktonic diatoms; excretion, assimilation and cellular pools of free amino acids in seven species with different cell size. *Journal of Experimental Marine Biology and Ecology*, *98*(3), 241–263.

Aluwihare, L. I., & Meador, T. (2008). Chemical composition of marine dissolved organic nitrogen. San Diego, CA, USA: Academic Press.

Amato, A., Dell'Aquila, G., Musacchia, F., Annunziata, R., Ugarte, A., Maillet, N., … Ferrante, M. I. (2017). Marine diatoms change their gene expression profile when exposed to microscale turbulence under nutrient replete conditions. *Scientific Reports*, *7*(1), 3826.

Amin, S. A., Parker, M. S., & Armbrust, E. V. (2012). Interactions between diatoms and bacteria. *Microbiology and Molecular Biology Reviews*, *76*(3), 667–684.

Aminot, A., & Kérouel, R. (2004). *Hydrologie des écosystèmes marins: paramètres et analyses*. Editions Quae.

Andersen, R. A. (2005). *Algal culturing techniques*. Academic press.

Anderson, D. M., Alpermann, T. J., Cembella, A. D., Collos, Y., Masseret, E., & Montresor, M. (2012). The globally distributed genus Alexandrium: multifaceted roles in marine ecosystems and impacts on human health. *Harmful Algae*, *14*, 10–35.

Antia, N. J., Harrison, P. J., & Oliveira, L. (1991). The role of dissolved organic nitrogen in phytoplankton nutrition, cell biology and ecology. *Phycologia*, *30*(1), 1–89.

Arnold, H. E., Kerrison, P., & Steinke, M. (2013). Interacting effects of ocean acidification and warming on growth and DMS-production in the haptophyte coccolithophore Emiliania huxleyi. *Global Change Biology*, *19*(4), 1007–1016.

Bates, N. R., & Hansell, D. A. (1999). A high resolution study of surface layer hydrographic and biogeochemical properties between Chesapeake Bay and Bermuda. *Marine Chemistry*, *67*(1), 1–16.

Béchemin, C., Grzebik, D., Hachame, F., Hummert, C., & Maestrini, S. Y. (1999). Effect of different nitrogen/phosphorus nutrient ratios on the toxin content in Alexandrium minutum. *Aquat Microb Ecol*, *20*, 157–165.

Beman, J. M., Arrigo, K. R., & Matson, P. A. (2005). Agricultural runoff fuels large phytoplankton blooms in vulnerable areas of the ocean. *Nature*, *434*(7030), 211–214.

Benner, R., Biddanda, B., Black, B., & McCarthy, M. (1997). Abundance, size distribution, and stable carbon and nitrogen isotopic compositions of marine organic matter isolated by tangential-flow ultrafiltration. *Marine Chemistry*, *57*(3), 243–263.

Benner, R., & Kaiser, K. (2003). Abundance of amino sugars and peptidoglycan in marine particulate and dissolved organic matter. *Limnology and Oceanography*, *48*(1), 118.

Berg, G. M., Glibert, P. M., Jørgensen, N. O. G., Balode, M., & Purina, I. (2001). Variability in inorganic and organic nitrogen uptake associated with riverine nutrient input in the Gulf of Riga, Baltic Sea. *Estuaries*, *24*(2), 204–214.

Berg, G. M., Repeta, D. J., & Laroche, J. (2002). Dissolved organic nitrogen hydrolysis rates in axenic cultures of Aureococcus anophagefferens (Pelagophyceae): comparison with heterotrophic bacteria. *Applied and Environmental Microbiology*, *68*(1), 401–404.

Berges, J. A., Franklin, D. G., & Harrison, P. J. (2001). Evolution of an artificial seawater medium: improvements in enriched seawater, artificial water over the last two decades. *Journal of Phycology*, *37*, 1138–1145.

Berman, T., & Bronk, D. A. (2003). Dissolved organic nitrogen: a dynamic participant in aquatic ecosystems. *Aquatic Microbial Ecology*, *31*(3), 279–305.

Berman, T., & Chava, S. (1999). Algal growth on organic compounds as nitrogen sources. *Journal of Plankton Research*, *21*(8), 1423–1437.

Berthelot, M. (1859). Violet d'aniline. *Rep Chim App*, *1*(284), 688.

Braarud, T. (1963). Reproduction in the marine coccolithophorid Coccolithus huxleyi in culture. *Pubblicazioni Della Stazione Zoologica Di Napoli*, *33*, 110–116.

Brand, L. E. (1991). Minimum iron requirements of marine phytoplankton and the implications for the biogeochemical control of new production. *Limnology and Oceanography*, *36*(8), 1756–1771.

Brand, L. E., & Guillard, R. R. L. (1981). The effects of continuous light and light intensity on the reproduction rates of twenty-two species of marine phytoplankton. *Journal of Experimental Marine Biology and Ecology*, *50*(2), 119–132.

Bratbak, G., Jacobsen, A., & Heldal, M. (1998). Viral lysis of Phaeocystis pouchetii and bacterial secondary production. *Aquatic Microbial Ecology*, *16*(1), 11–16.

Bronk, D. A. (2002). Dynamics of DON. In D. A. Hansell & C. A. Carlson (Eds.), *Biogeochemistry of marine dissolved organic matter* (Vol. 384, pp. 153–247). Academic Press.

Bronk, D. A., & Ward, B. B. (2000). Magnitude of dissolved organic nitrogen release relative to gross nitrogen uptake in marine systems. *Limnology and Oceanography*, *45*(8), 1879–1883.

Brzezinski, M. A. (1985). The Si: C: N ratio of marine diatoms: interspecific varability and the effect of some environmental variables. *Journal of Phycology*, *21*(3), 347–357.

Butler, E. I., Knox, S., & Liddicoat, M. I. (1979). The relationship between inorganic and organic nutrients in sea water. *Journal of the Marine Biological Association of the United Kingdom*, *59*(1), 239–250.

Carr, N. G., & Whitton, B. A. (1973). *The biology of blue-green algae* (Vol. 9). Univ of California Press.

Cavender-Bares, K. K., Karl, D. M., & Chisholm, S. W. (2001). Nutrient gradients in the western North Atlantic Ocean: Relationship to microbial community structure and comparison to patterns in the Pacific Ocean. *Deep Sea Research Part I: Oceanographic Research Papers*, *48*(11), 2373–2395.

Cho, B. C., Park, M. G., Shim, J. H., & Azam, F. (1996). Significance of bacteria in urea dynamics in coastal surface waters. *Marine Ecology Progress Series. Oldendorf*, *142*(1), 19–26.

Cochlan, W. P., & Harrison, P. J. (1991). Kinetics of nitrogen (nitrate, ammonium and

urea)uptake by the picoflagellate Micromonas pusilla (Prasinophyceae). *J. Exp. Mar. Biol. Ecol.*, *153*, 129–141.

Cochlan, W. P., Herndon, J., & Kudela, R. M. (2008). Inorganic and organic nitrogen uptake by the toxigenic diatom Pseudo-nitzschia australis (Bacillariophyceae). *Harmful Algae*, *8*, 111–118.

Cottrell, M. T., & Suttle, C. A. (1993). Production of axenic cultures of Micromonas pusilla (PRASINOPHYCEAE) using antibiotics. *Journal of Phycology*, *29*(3), 385–387.

Curtis-Jackson, P. K., Massé, G., Gledhill, M., & Fitzsimons, M. F. (2009). Characterisation of low molecular weight dissolved organic nitrogen by liquid chromatography-electrospray ionisation-mass spectrometry. *Limnology and Oceanography: Methods*, *7*(1), 52–63.

Daniels, C. J., Sheward, R. M., & Poulton, A. J. (2014). Biogeochemical implications of comparative growth rates of Emiliania huxleyi and Coccolithus species. *Biogeosciences*, *11*(23), 6915–6925.

Davis, A. M., Tink, M., Rohde, K., & Brodie, J. E. (2016). Urea contributions to dissolved “organic”nitrogen losses from intensive, fertilised agriculture. *Agriculture, Ecosystems & Environment*, *223*, 190–196.

Droop, M. R. (1967). A procedure for routine purification of algal cultures with antibiotics. *British Phycological Bulletin*, *3*(2), 295–297. https://doi.org/10.1080/00071616700650171

Falkowski, P. G. (1975). Nitrate uptake in marine phytoplankton: (Nitrate, Chloride)-activated Adenosine Triphosphatase from Skeletonema costatum (Bacillariophyceae). *Journal of Phycology*, *11*(3), 323–326.

Falkowski, P., Scholes, R. J., Boyle, E. E. A., Canadell, J., Canfield, D., Elser, J., … Linder, S. (2000). The global carbon cycle: a test of our knowledge of earth as a system. *Science*, *290*(5490), 291–296.

Farrell, M., Hill, P. W., Farrar, J., DeLuca, T. H., Roberts, P., Kielland, K., … Bardgett, R. D. (2013). Oligopeptides represent a preferred source of organic N uptake: a global phenomenon? *Ecosystems*, *16*(1), 133–145.

Fisher, N. L., & Halsey, K. (2016). Mechanisms that increase the growth efficiency of diatoms in low light. *Photosynthesis Research*, *129*(2), 183–197.

Flynn, K. J. (1990). Composition of intracellular and extracellular pools of amino acids, and amino acid utilization of microalgae of different sizes. *J. Exp. Mar. Biol. Ecol.*, *139*, 151–166.

Flynn, K. J., & Butler, I. (1986). Nitrogen sources for the growth of marine microalgae: role of dissolved free amino acids. *Marine Ecology Progress Series*, *34*, 281–304.

Flynn, K. J., & Wright, C. R. N. (1986). The simultaneous assimilation of ammonium and L-arginine by the marine diatom Phaeodactylum tricornutum Bohlin. *Journal of Experimental Marine Biology and Ecology*, *95*(3), 257–269.

Fuhrman, J. (1987). Close coupling between release and uptake of dissolved free amino acids in seawater studied by an isotope dilution approach. *Mar. Ecol. Prog. Ser*, *37*, 45–52.

Fuhrman, J. (1990). Dissolved free amino acid cycling in an estuarine outflow plume. *Marine Ecology Progress Series MESEDT*, *66*(1/2).

Galloway, J. N., Dentener, F. J., Capone, D. G., Boyer, E. W., Howarth, R. W., Seitzinger, S. P., … Holland, E. A. (2004). Nitrogen cycles: past, present, and future. *Biogeochemistry*, *70*(2), 153–226.

Geider, R. J., Delucia, E. H., Falkowski, P. G., Finzi, A. C., Grime, J. P., Grace, J., … Osborne, B. A. (2001). Primary productivity of planet earth: biological determinants and physical constraints in terrestrial and aquatic habitats. *Global Change Biology*, *7*(8), 849–882.

Gibb, S. W., Mantoura, R. F. C., Liss, P. S., & Barlow, R. G. (1999). Distributions and biogeochemistries of methylamines and ammonium in the Arabian Sea. *Deep Sea Research Part II: Topical Studies in Oceanography*, *46*(3), 593–615.

Gobler, C. J., & Sañudo-Wilhelmy, S. A. (2001). Effects of organic carbon, organic nitrogen, inorganic nutrients, and iron additions on the growth of phytoplankton and bacteria during a brown tide bloom. *Marine Ecology Progress Series*, *209*, 19–34.

Goldman, J. C., McCarthy, J. J., & Peavey, D. G. (1979). Growth rate influence on the

chemical composition of phytoplankton in oceanic waters.

Graham, L. E., Graham, J. M., & Wilcox, L. W. (2009). *Algae* (Second Ed.). Benjamin Cummings.

Graneli, E., & Carlsson, P. (1998). The ecological significance of phagotrophy in photosynthetic flagellates. In: Physiological ecology of harmful algal blooms: proceedings of the NATO Advanced Study Institute on "The Physiological Ecology of Harmful Algal Blooms", held at the Bermuda Biological Station for Research, Bermuda, USA, May 27 - June 6, 1996 / [ed] Don.

Graneli, E., Edler, L., Gedziorowska, D., & Nyman, U. (1985). Influence of humic and fulvic acids on Prorocentrum minimum (Pav.).

Gruber, N. (2008). The marine nitrogen cycle: overview and challenges. In *Nitrogen in the marine environment* (pp. 1–50).

Gruber, N., & Galloway, J. N. (2008). An Earth-system perspective of the global nitrogen cycle. *Nature*, *451*, 293–296.

Guillard, R. R. L. (2005). Purification methods for microalgae. In R. A. Andersen (Ed.), *Algal culturing techniques* (pp. 117–132). Elsevier Academic Press.

Guilloux, L., Rigaut-Jalabert, F., Jouenne, F., Ristori, S., Viprey, M., Not, F., … Simon, N. (2013). An annotated checklist of Marine Phytoplankton taxa at the SOMLIT-Astan time series off Roscoff (Western English Channel, France): data collected from 2000 to 2010. *Cah Biol Mar*, *54*, 247–256.

Halim, Y. (1960). Alexandrium minutum nov. g. nov. sp. dinoflagellé provocant des "eaux rouges." *Vie et Milieu*, *11*(1), 102–105.

Hallegraeff, G. M., Anderson, D. M., Cembella, A. D., Enevoldsen, H. O., & Commission, I. O. (2003). *Manual on harmful marine microalgae*. Unesco.

Happey, C. M. (1970). The effects of stratification on phyto-planktonic diatoms in a small body of water. *The Journal of Ecology*, 635–651.

Harrison, P. J., Waters, R. E., & Taylor, F. J. R. (1980). A broad spectrum artificial seawater medium for coastal and open ocean phytoplankton. *Journal of Phycology*, *16*, 28–35.

Hasle, G. R., Syvertsen, E. E., Steidinger, K. A., Tangen, K., & Tomas, C. R. (1996). *Identifying marine diatoms and dinoflagellates*. Academic Press.

Hillebrand, H., Dürselen, C., Kirschtel, D., Pollingher, U., & Zohary, T. (1999). Biovolume calculation for pelagic and benthic microalgae. *Journal of Phycology*, *35*(2), 403–424.

Hoch, M. P., Fogel, M. L., & Kirchman, D. L. (1992). Isotope fractionation associated with ammonium uptake by a marine bacterium. *Limnology and Oceanography*, *37*(7), 1447–1459. https://doi.org/10.4319/lo.1992.37.7.1447

Holm-Hansen, O., Lorenzen, C. J., Holmes, R. W., & Strickland, J. D. H. (1965). Fluorometric determination of chlorophyll. *Journal Du Conseil*, *30*(1), 3–15.

Hopkinson, C. S., Buffam, I., Hobbie, J., Vallino, J., Perdue, M., Eversmeyer, B., … Moran, M. A. (1998). Terrestrial inputs of organic matter to coastal ecosystems: An intercomparison of chemical characteristics and bioavailability. *Biogeochemistry*, *43*(3), 211–234.

Houdan, A., Probert, I., Zatylny, C., Véron, B., & Villard, C. (2006). Ecology of oceanic coccolithophores. I. Nutritional preferences of the two stages in the life cycle of Coccolithus braarudii and Calcidiscus leptoporus. *Aquatic Microbial Ecology*, *44*(3), 291–301.

Hu, Z., Duan, S., Xu, N., & Mulholland, M. R. (2014). Growth and Nitrogen Uptake Kinetics in Cultured Prorocentrum donghaiense. *Plos One*, *9*(4), e94030.

Jauffrais, T., Jesus, B., Méléder, V., Turpin, V., Arnaldo, D., Rimbault, P., & Jézéquel, V. M. (2016). Physiological and photophysiological responses of the benthic diatom Entomoneis paludosa (Bacillariophyceae) to dissolved inorganic and organic nitrogen in culture. *Marine Biology*, *163*(5), 115.

Jones, R. I. (1994). Mixotrophy in planktonic protists as a spectrum of nutritional strategies. *Marine Microbial Food Webs*, *8*, 87–96.

Jumars, P. A., Penry, D. L., Baross, J. A., Perry, M. J., & Frost, B. W. (1989). Closing the microbial loop: dissolved carbon pathway to heterotrophic bacteria from incomplete ingestion, digestion and absorption in animals. *Deep Sea Research Part A. Oceanographic Research Papers*, *36*(4), 483–495.

Jutson, M. G., Pipe, R. K., & Tomas, C. R. (2016). The Cultivation of Marine Phytoplankton. In M. N. Tsaloglou (Ed.), *Microalgae - Current Research and Application*. Caister Academic Press.

Keil, R. G., & Kirchman, D. L. (1994). Abiotic transformation of labile protein to refractory protein in sea water. *Marine Chemistry*, *45*(3), 187–196.

Kibet, L. C., Bryant, R. B., Buda, A. R., Kleinman, P. J. A., Saporito, L. S., Allen, A. L., … May, E. B. (2016). Persistence and Surface Transport of Urea-Nitrogen: A Rainfall Simulation Study. *Journal of Environmental Quality*, *45*(3), 1062–1070.

Klaveness, D. (1972). Coccolithus huxleyi (Lohm.) Kamptn II. The flagellate cell, aberrant cell types, vegetative propagation and life cycles. *British Phycological Journal*, *7*(3), 309–318.

Koroleff, F. (1969). Direct determination of ammonia in natural waters as indophenol blue. *Int. Con. Explor. Sea, CM C*, *9*.

Lampert, W. (1978). Release of dissolved organic carbon by grazing zooplankton. *Limnology and Oceanography*, *23*(4), 831–834.

Lana, A., Ell, T. G., Simo', R., Vallina, S. M., Ballabrera-Poy, J., Kettle, A. J., & Johnson, J. E. (2011). An updated climatology of surface dimethlysulfide concentrations and emission fluxes in the global ocean. *Global Biogeochemical Cycles*, *25*(1).

LaRoche, J., Nuzzi, R., Waters, R., Wyman, K., Falkowski, P., & Wallace, D. (1997). Brown tide blooms in Long Island's coastal waters linked to interannual variability in groundwater flow. *Global Change Biology*, *3*(5), 397–410.

LeDoux, M., Fremy, J. M., Nezan, E., & Erard, E. (1989). Recent occurrence of paralytic shellfish poisoning(PSP) toxins from the northwestern coasts of France. *Journal of Shellfish Research*, *8*(2), 486.

Lee, S., & Fuhrman, J. A. (1987). Relationships between biovolume and biomass of naturally derived marine bacterioplankton. *Applied and Environmental Microbiology*, *53*(6), 1298–1303.

Maat, D. S., Crawfurd, K. J., Timmermans, K. R., & Brussaard, C. P. D. (2014). Elevated CO2 and phosphate limitation favor Micromonas pusilla through

stimulated growth and reduced viral impact. *Applied and Environmental Microbiology*, *80*(10), 3119–3127.

Maguer, J. F., L'Helguen, S., Madec, C., Labry, C., & Le Corre, P. (2007). Nitrogen uptake and assimilation kinetics in Alexandrium minutum (Dynophyceae): effect of N-limited growth rate on nitrate and ammonium interactions. *Journal of Phycology*, *43*(2), 295–303.

Marañón, E., Steele, J., Thorpe, A., & Turekian, K. (2009). Phytoplankton size structure. *Sciences, Elements of Physical Oceanography: A Derivative of the Encyclopedia of Ocean*, *85*.

Mitamura, O., Nakamoto, N., Ibanez, M. D. S. R., Cavalcante, P. R. S., Neto, J. P. C., & Barbieri, R. (2013). The Significance of Regenerated Nitrogenous Compounds as a Nitrogen Source for Phytoplankton in the Whitewater of the Pre-Amazonian Floodplain in Brazil [論文].

Monbet, P., McKelvie, I. D., & Worsfold, P. J. (2007). A protocol to assess the enzymatic release of dissolved organic phosphorus species in waters under environmentally relevant conditions. *Environmental Science & Technology*, *41*(21), 7479–7485.

Moneta, A., Veuger, B., van Rijswijk, P., Meysman, F., Soetaert, K., & Middelburg, J. J. (2014). Dissolved inorganic and organic nitrogen uptake in the coastal North Sea: A seasonal study. *Estuarine, Coastal and Shelf Science*, *147*, 78–86.

Monteiro, F. M., Bach, L. T., Brownlee, C., Bown, P., Rickaby, R. E. M., Poulton, A. J., … Ridgwell, A. (2016). Why marine phytoplankton calcify. *Science Advances*, *2*.

Montresor, M., Vitale, L., D'Alelio, D., & Ferrante, M. I. (2016). Sex in marine planktonic diatoms: insights and challenges. *Perspectives in Phycology*, *3*(2), 61–75.

Morel, F. M. M., Milligan, A. J., & Saito, M. A. (2003). Marine Bioinorganic Chemistry: The Role of Trace Metals in the Oceanic Cycles of Major Nutrients.

Morel, F. M. M., Rueter, J. G., Anderson, D. M., & Guillard, R. R. L. (1979). Aquil: a chemically defined phytoplankton culture medium for trace metal studies. *Journal*

of Phycology, *15*, 135–141.

Moschonas, G., Gowen, R. J., Stewart, B. N., & Davidson, K. (2015). Nitrogen dynamics in the Irish Sea and adjacent shelf waters: An exploration of dissolved organic nitrogen. *Estuarine, Coastal and Shelf Science*, *164*, 276–287.

Moschonas, G., Gowen, R., Paterson, R. F., Mitchell, E., Stewart, B. M., McNeil, S., … Davidson, K. (2017). Nitrogen dynamics and phytoplankton community structure: the role of organic nutrients. *Biogeochemistry*, *134*(1–2), 125–145.

Muggli, D. L., & Harrison, P. J. (1997). Effects of iron on two oceanic phytoplankters grown in natural NE subarctic Pacific seawater with no artificial chelators present. *Journal of Experimental Marine Biology and Ecology*, *212*(2), 225–237.

Mulholland, M. R., Glibert, P. M., Berg, G. M., Van Heukelem, L., Pantoja, S., & Lee, C. (1998). Extracellular amino acid oxidation by microplankton: A cross-ecosystem comparison. *Aquatic Microbial Ecology*, *15*(2), 141–152.

Mulholland, M. R., & Lee, C. (2009). Peptide hydrolysis and the uptake of dipeptides by phytoplankton. *Limnology and Oceanography*, *54*(3), 856–868.

Mulholland, M. R., Morse, R. E., Boneillo, G. E., Bernhardt, P. W., Filippino, K. C., Procise, L. A., … Hunley, W. S. (2009). Understanding causes and impacts of the dinoflagellate, Cochlodinium polykrikoides, blooms in the Chesapeake Bay. *Estuaries and Coasts*, *32*(4), 734–747.

Mullin, M. M., Sloan, P. R., & Eppley, R. W. (1966). Relationship between carbon content, cell volume, and area in phytoplankton. *Limnology and Oceanography*, *11*(2), 307–311.

Nanninga, H. J., & Tyrrell, T. (1996). Importance of light for the formation of algal blooms by Emiliania huxleyi. *Marine Ecology Progress Series*, 195–203.

Not, F., Latasa, M., Marie, D., Cariou, T., Vaulot, D., & Simon, N. (2004). A single species, Micromonas pusilla (Prasinophyceae), dominates the eukaryotic picoplankton in the Western English Channel. *Applied and Environmental Microbiology*, *70*(7), 4064–4072.

Paasche, E. (2002). A review of the coccolithophorid Emiliania huxleyi (Prymnesiophyceae), with particular reference to growth, coccolith formation, and

calcification-photosynthesis interactions. *Phycologia*, *40*(6), 503–529.

Paerl, H. W., & Tucker, C. S. (1995). Ecology of blue-green algae in aquaculture ponds. *Journal of the World Aquaculture Society*, *26*(2), 109–131.

Palenik, B., & Koke, J. A. (1995). Characterization of a nitrogen-regulated protein identified by cell surface biotinylation of a marine phytoplankton. *Applied and Environmental Microbiology*, *61*(9), 3311–3315.

Pancic, M., Hanse, P. J., Tammilehto, A., & Lundholm, N. (2015). Resilience to temperature and pH changes in a future climate change scenario in six strains of the polar diatom Fragilariopsis cylindrus. *Biogeosciences*, *12*, 4235–4244.

Pegau, W. S., Boss, E., & Martinez, A. (2002). Ocean color observations of eddies during the summer in the Gulf of California. *Geophys. Res. Lett.*, *29*.

Pertola, S., Kuosa, H., & Olsonen, R. (2005). Is the invasion of Prorocentrum minimum (Dinophyceae) related to the nitrogen enrichment of the Baltic Sea? *Harmful Algae*, *4*(3), 481–492.

Pickett-Heaps, J., Schmid, A. M. M., & Edgar, L. A. (1990). The cell biology of diatom valve formation. *Progress in Phycological Research*, *7*, 1–157.

Poulton, A. J., Adey, T. R., Balch, W. M., & Holligan, P. M. (2007). Relating coccolithophore calcification rates to phytoplankton community dynamics: regional differences and implications for carbon export. *Deep Sea Research Part II: Topical Studies in Oceanography*, *54*, 538–557.

Poulton, A. J., Painter, S. C., Young, J. R., Bates, N. R., Balch, W. M., Bowler, B., … Lyczsckowski, E. (2013). The 2008 Emiliania huxleyi bloom along the Patagonian Shelf: Ecology, biogeochemistry, and cellular calcification. *Global Biogeochemical Cycles Cycles*, *27*, 1023–1033.

Price, N. M., Harrison, G. I., Hering, J. G., Hudson, R. J., Nirel, P. M. V, Palenik, B., & Morel, F. M. M. (1989). Preparation and chemistry of the artificial algal culture medium Aquil. *Biological Oceanography*, *6*(5–6), 443–461.

Price, N. M., & Harrison, P. J. (1988). Urea uptake by Sargasso Sea phytoplankton: saturated and in situ uptake rates. *Deep Sea Research Part A. Oceanographic Research Papers*, *35*(9), 1579–1593.

Raven, J. A. (1981). Nutrient transport in microalgae. *Advances in Microbial Physiology*, *21*, 47–226.

Redfield, A. C. (1934). *On the proportions of organic derivatives in sea water and their relation to the composition of plankton*. University Press of Liverpool, UK.

Reynolds, C. S. (2007). Variability in the provision and function of mucilage in phytoplankton: facultative responses to the environment. *Hydrobiologia*, *578*(1), 37–45.

Riley, W. J., Ortiz-Monasterio, I., & Matson, P. A. (2001). Nitrogen leaching and soil nitrate, nitrite, and ammonium levels under irrigated wheat in Northern Mexico. *Nutrient Cycling Agroecosyst.*, *61*, 223–236.

Santomauro, G., Sun, W.-L., Brümmer, F., & Bill, J. (2016). Incorporation of zinc into the coccoliths of the microalga Emiliania huxleyi. *BioMetals*, *29*(2), 225–234.

Schell, D. M. (1974). Uptake and regeneration of free amino acids in marine waters of Southeast Alaska.

Seitzinger, S. P., & Sanders, R. W. (1999). Atmospheric inputs of dissolved organic nitrogen stimulate estuarine bacteria and phytoplankton. *Limnology and Oceanography*, *44*(3), 721–730.

Sellner, K. G., & Nealley, E. W. (1997). Diel fluctuations in dissolved free amino acids and monosaccharides in Chesapeake Bay dinoflagellate blooms. *Marine Chemistry*, *56*(3), 193–200.

Smayda, T. J. (1958). Biogeographical studies of marine phytoplankton. *Oikos*, *9*(2), 158–191.

Spector, D. L. (2012). *Dinoflagellates*. Academic Press.

Strickland, J. D. H., & Parsons, T. R. (1972). A practical handbook of seawater analysis. *Fisheries Research Board of Canada*, 167.

Sunda, W. G., & Huntsman, S. A. (1995a). Cobalt and zinc interreplacement in marine phytoplankton: biological and geochemical implications. *Limnology and Oceanography*, *40*(8), 1404–1417.

Sunda, W. G., & Huntsman, S. A. (1995b). Iron uptake and growth limitation in oceanic

and coastal phytoplankton. *Marine Chemistry*, *50*(1), 189–206.

Sunda, W. G., Price, N. M., & Morel, F. M. M. (2005). Trace metal ion buffers and their use in culture studies. *Algal Culturing Techniques*, 35–63.

Sutton, J. N., Varela, D. E., Brzezinski, M. A., & Beucher, C. P. (2013). Species-dependent silicon isotope fractionation by marine diatoms. *Geochimica et Cosmochimica Acta*, *104*, 300–309.

Svara, J., Weferling, N., & Hofmann, T. (2002). Organic Phosphorus Compounds. In *Ullmann's Encyclopedia of Industrial Chemistry*.

Tanoue, E. (1995). Detection of dissolved protein molecules in oceanic waters. *Marine Chemistry*, *51*(3), 239–252.

Tappin, A. D., Millward, G. E., & Fitzsimons, M. F. (2010). Particle–water interactions of organic nitrogen in turbid estuaries. *Marine Chemistry*, *122*(1), 28–38.

Taylor, A. R., Brownlee, C., & Wheeler, G. (2017). Coccolithophore cell biology: Chalking up progress. *Annual Review of Marine Science*, *9*, 283–310.

Therkildsen, M. S., Isaksen, M. F., & Lomstein, B. A. (1997). Urea production by the marine bacteria Delaya venusta and Pseudomonas stutzeri grown in a minimal medium. *Aquatic Microbial Ecology*, *13*(2), 213–217.

Thomsen, L., & Jähmlich, S. (1998). An in situ experiment to investigate the modification of particulate matter and urea above a benthic sandy silt community in the Baltic Sea. *Hydrobiologia*, *375*, 353–361.

Throndsen, J. (1976). Occurrence and productivity of small marine flagellates. *Norwegian Journal of Botany*, *23*(4).

Tyrrell, T., & Merico, A. (2004). Emiliania huxleyi :bloom observations and the conditions that induce them. In *Coccolithophores* (pp. 75–97). Springer.

Tyrrell, T., & Taylor, A. H. (1996). A modelling study of Emiliania huxleyi in the NE Atlantic. *Journal of Marine Systems*, *9*(1), 83–112.

Werner, D. (1977). *The biology of diatoms* (Vol. 13). Univ of California Press.

Westbroek, P., Brown, C. W., van Bleijswijk, J., Brownlee, C., Brummer, G. J., Conte, M., … Knappertsbusch, M. (1993). A model system approach to biological climate

forcing. The example of Emiliania huxleyi. *Global and Planetary Change*, *8*(1), 27–46.

Wetz, M. S., Cira, E. K., Sterba-Boatwright, B., Montagna, P. A., Palmer, T. A., & Hayes, K. C. (2017). Exceptionally high organic nitrogen concentrations in a semi-arid South Texas estuary susceptible to brown tide blooms. *Estuarine, Coastal and Shelf Science*, *188*, 27–37.

Wheeler, P. A. (1983). Phytoplankton nitrogen metabolism. In E. J. Carpenter & D. G. Capone (Eds.), *Nitrogen in the marine environment* (pp. 309–346). Academic Press.

Wheeler, P., North, B., Littler, M., & Stephens, G. (1977). Uptake of Glycine by natural phytoplankton communities. *Limnology and Oceanography*, *22*(5), 900–910.

Widdicombe, C. E., Eloire, D., Harbour, D., Harris, R. P., & Somerfield, P. J. (2010). Long-term phytoplankton community dynamics in the Western English Channel. *Journal of Plankton Research*, fbp127.

Willén, E. (1991). Planktonic diatoms-an ecological review. *Algological Studies*, *62*, 69–106.

Wong, C. S., Yu, Z., Waser, N. A. D., Whitney, F. A., & Johnson, W. K. (2002). Seasonal changes in the distribution of dissolved organic nitrogen in coastal and open-ocean waters in the North East Pacific: sources and sinks. *Deep Sea Research Part II: Topical Studies in Oceanography*, *49*(24), 5759–5773.

Yuan, X., Glibert, P. M., Xu, J., Liu, H., Chen, M., Liu, H., … Harrison, P. J. (2012). Inorganic and organic nitrogen uptake by phytoplankton and bacteria in Hong Kong waters. *Estuaries and Coasts*, *35*(1), 325–334.

Zehr, P. J., & Ward, B. B. (2002). Nitrogen cycling in the ocean: new perspectives on processes and paradigms. *Applied and Environmental Microbiology*, *68*(3), 1015–1024.

Zhang, G., Shengkang, L., Xiaoyong, S., & Xiurong, H. (2015). Dissolved organic nitrogen bioavailability indicated by amino acids during a diatom to dinoflagellate bloom succession in the Changjiang River estuary and its adjacent shelf. *Marine Chemistry*, *176*, 83–95.

Ziveri, P., de Bernardi, B., Baumann, K.-H., Stoll, H. M., & Mortyn, P. G. (2007). Sinking of coccolith carbonate and potential contribution to organic carbon ballasting in the deep ocean. *Deep Sea Research Part II: Topical Studies in Oceanography*, *54*, 659–675.